

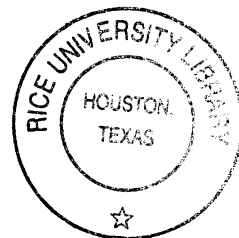
RICE UNIVERSITY

**Response of the Texas Coast to Global Change: Geologic Versus  
Historic Timescales**

By


**Davin Johannes Wallace**


A THESIS SUBMITTED  
IN PARTIAL FULFILLMENT OF THE  
REQUIREMENTS FOR THE DEGREE

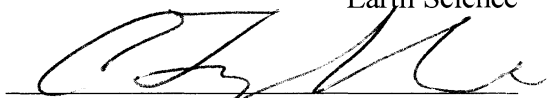



**Doctor of Philosophy**


APPROVED, THESIS COMMITTEE:

  
John B. Anderson, W. Maurice Ewing  
Professor in Oceanography

  
Brandon Dugan, Assistant Professor of  
Earth Science

  
Cin-Ty A. Lee, Associate Professor of  
Earth Science

  
Carrie A. Masiello, Assistant Professor  
of Earth Science

  
Philip Bedient, Herman and George R.  
Brown Professor of  
Civil and Environmental Engineering

Thesis  
Geol.  
2010  
Wallace

HOUSTON, TEXAS  
MAY 2010

92396000

# **ABSTRACT**

Response of the Texas Coast to Global Change: Geologic Versus Historic Timescales

by

Davin Johannes Wallace

The response of coastal systems to global change is currently not well understood. To understand current patterns and predict future trends, we establish a geologic record of coastal change along the Gulf of Mexico coast.

A study examining the natural versus anthropogenic mechanisms of erosion reveals several sand sources and sinks along the upper Texas coast. It appears that hurricane washover and offshore sand deposits are minimal sand sinks, while flood-tidal deltas are areas of significant sand sequestration. Additionally, it appears that damming of rivers has had only a minimal effect on sedimentation along the upper Texas coast. However, hard engineering structures placed on the beach have exacerbated erosion due to trapping sand of that would otherwise be in the longshore transport system.

Coastal sand budgets are derived to put geologic events (such as hurricanes and erosion) into context. Sand budgets often use engineering assumptions to establish sand transport within a coastal system. However, a disconnect typically exists between engineering principles and geologic concepts when quantifying these budgets. Geologic principles are relied upon to calculate a sand budget and evaluate published sediment budgets. This reveals that assuming too shallow a depth of closure can result in ~17% error in the total calculated sediment flux and an error of ~40% of the total longshore transport flux for the upper Texas coast. This suggests that revised approaches are necessary to accurately represent sand transport within the coastal zone.

The long-term probability of hurricane impacts in the western Gulf of Mexico is constructed. For south Texas, an intense hurricane landfall probability of  $\sim .46\%$  is established for the past  $\sim 5,000$  years. Based on published studies, this is similar to the intense hurricane impact probability of  $\sim .39\%$  for the eastern Gulf of Mexico.

Studying the evolution of San Luis Pass provides a unique opportunity to study the response of accelerated sea-level rise and hurricane impacts on the evolution of a natural tidal delta system and adjacent Galveston Island. This study reveals an increased sand flux into San Luis pass tidal delta, and suggests that the erosion along Galveston Island has more than doubled over historic time relative to geologic time.

## **Acknowledgements**

There are so many people one needs to thank for a Ph.D. to be possible. Everyone from scientific colleagues to family members and friends each has had a profound impact on both my life and graduate work.

First and foremost, I would like to thank my advisor, Dr. John Anderson. John taught me to think outside of the box, and helped develop my scientific thinking, research ideas, and writing skills. We spent many long hours together in the field, in the lab, and at Rice. John gave me the perfect amount of freedom to develop scientific ideas, but also support whenever I had questions. His passion and respect for science rubs off on all of his students and colleagues. I truly feel honored to have worked with such a brilliant scientist.

I could also not have completed a Ph.D. without the support of my family. There were many times when I looked to my parents for support, and they have always been there for me since I was a child. My grandparents have always been kind and loving. My brother has helped to keep me grounded, and has always been supportive of my work. My family has kept me focused, driven, and happy over the years. They have always been proud of my accomplishments and have been an inspiration to me.

I am grateful for the help of Dr. Alison Henning, who helped me to develop teaching and course planning skills. Alison is an amazing scientist, educator, and person to work with.

I am also thankful for my committee members, Drs. Carrie Masiello, Brandon Dugan, Cin-Ty Lee, and Philip Bedient for providing helpful and constructive comments for this work.

Many colleagues helped develop research ideas, worked on data, and contributed directly to fieldwork. I would like to thank Dr. Alex Simms, Dr. Antonio Rodriguez, Dr. Julia Wellner, Dr. Kristy Milliken, Dr. Tyler Smith, Rodrigo Fernández, Brad Michalchuk, Robert Weight, Winnie Yu, Nicole Kwan, Christine Gerbode, Emily Chin, Alexandra Kirshner, Rebecca Minzoni, Travis Stollendorf, and Captain Ernie Cisneros.



My graduate work was funded by many sources, all of which were crucial for this research. Funding was provided for by the National Science Foundation, David Worthington research fund, BP, and Chevron.

I am also especially grateful for the Department of Earth Science at Rice University, for their unwavering support and help with any matter. They have provided me with many opportunities, and have been generous and kind my entire time at Rice.

## Table of Contents

<b>Abstract</b> .....	ii
<b>Acknowledgements</b> .....	iv
<b>List of Figures</b> .....	vii
<b>List of Tables</b> .....	ix
<b>Chapter 1</b> -Introduction.....	1
<b>Chapter 2</b> - Natural versus anthropogenic mechanisms of erosion along the upper Texas coast <sup>1</sup> .....	3
<b>Chapter 3</b> - Transgressive ravinement versus depth of closure: A geological perspective from the upper Texas coast <sup>2</sup> .....	28
<b>Chapter 4</b> - Evidence of similar probability of intense hurricane strikes for the Gulf of Mexico over the late Holocene <sup>3</sup> .....	51
<b>Chapter 5</b> - Response of a low-gradient coast to global change: A case study of the Galveston Island and San Luis Pass inlet complex, Texas .....	63
<b>References</b> .....	81
<b>Appendix A</b> <sup>4</sup> .....	90

---

<sup>1</sup> This chapter has been edited, reformatted, and reprinted with permission: Wallace, D.J., Anderson, J.B., and Rodriguez, A.B., 2009, Natural versus anthropogenic mechanisms of erosion along the upper Texas Coast. *in*: Kelley, J.T., Pilkey, O.H., and Cooper, J.A.G., ed., America's Most Vulnerable Coastal Communities: The Geological Society of America Special Paper 460, p. 137-147.

<sup>2</sup> This chapter is a reformatted and reprinted (with permission) version of: Wallace, D.J., Anderson, J.B., and Fernández, R. A., 2010, Transgressive ravinement versus depth of closure: A geological perspective from the upper Texas coast, *Journal of Coastal Research*, (in review).

<sup>3</sup> This chapter has been edited, reformatted, and reprinted with permission: Wallace, D.J., and Anderson, J.B., 2010, Evidence of similar probability of intense hurricane strikes for the Gulf of Mexico over the late Holocene, *Geology*, (in press).

<sup>4</sup> This appendix has been edited, reformatted, and reprinted with permission from the online supplementary information: Wallace, D.J., and Anderson, J.B., 2010, Evidence of similar probability of intense hurricane strikes for the Gulf of Mexico over the late Holocene, *Geology*, (in press).

## **List of Figures**

<b>Figure 2-1</b> – Study area map of the upper Texas coast.....	5
<b>Figure 2-2</b> – Anthropogenic structures along the upper Texas coast.....	6
<b>Figure 2-3</b> – Bolivar Peninsula.....	9
<b>Figure 2-4</b> – Galveston Island.....	10
<b>Figure 2-5</b> – Subsurface geology of the upper Texas coast.....	12
<b>Figure 2-6</b> – Bolivar Roads tidal delta.....	14
<b>Figure 2-7</b> – San Luis Pass tidal delta.....	16
<b>Figure 2-8</b> – Offshore core profiles from the upper Texas coast.....	18
<b>Figure 3-1</b> – Study area map of the upper Texas coast .....	30
<b>Figure 3-2</b> – Core transects from the upper Texas coast .....	31
<b>Figure 3-3</b> – Subsurface geology from Bolivar Peninsula to Follets Island .....	35
<b>Figure 3-4</b> – Offshore core transects used to estimate sand volumes .....	36
<b>Figure 3-5</b> – Lithologic description of cores from Follets Island .....	37
<b>Figure 3-6</b> – Equilibrium profile model .....	39
<b>Figure 3-7</b> – Bathymetry changes in the Brazos delta through time .....	40
<b>Figure 3-8</b> – Revised sand budget .....	44
<b>Figure 4-1</b> – Study area map of the south Texas coast.....	54
<b>Figure 4-2</b> – Grain size and relative storm intensities from cores.....	55
<b>Figure 4-3</b> – Gulf of Mexico intense hurricane landfall probabilities .....	58
<b>Figure 5-1</b> – Study area map of the upper Texas coast.....	66
<b>Figure 5-2</b> – Satellite image of San Luis Pass tidal delta and core locations .....	67
<b>Figure 5-3</b> – San Luis Pass and Galveston Island core descriptions.....	73
<b>Figure 5-4</b> – Evolution of San Luis Pass tidal delta.....	78
<b>Appendix A-1</b> –Hurricane Allen record.....	91
<b>Appendix A-2</b> – Intense hurricane landfall probability comparison.....	93
<b>Appendix A-3</b> – Texas paleoclimate study compilation.....	94

<b>Appendix A-4 – Grain-size shell error analysis.....</b>	<b>95</b>
--	-----------

## **List of Tables**

<b>Table 5-1</b> – San Luis Pass tidal delta radiocarbon results.....	71
<b>Appendix A-Table 1</b> – Laguna Madre radiocarbon results.....	92

## CHAPTER 1

### 1.0 Introduction

Barrier islands are complex systems, and their evolution through time is generally poorly understood. The Texas coast stretches roughly 400 kilometers, and contains progradational, aggradational, and transgressive barrier island types. The upper Texas coast is one of the most developed sections of the Gulf of Mexico region, so understanding its evolution becomes particularly germane. To understand observed changes over historic time, we must first put these changes into context by examining the geologic record. Over the late Holocene, the upper Texas coast responded to climate, hurricane, eustatic, oceanographic, and sediment supply variations. To undertake a study of this nature, both local and regional evolution patterns along the Texas coast are focused upon. Some forcing mechanisms, such as hurricanes and sand transport, affect the Texas barriers similarly. Therefore, to fully understand barrier island evolution, it is necessary to understand the effect certain of forcing mechanisms at different spatial and temporal scales.

In this study, a comprehensive analysis is provided of the response of the barrier island systems along the upper Texas coast to various forcing mechanisms over the late Holocene compared to historic time. In Chapter 2, the different coastal processes and erosion mechanisms are introduced, and recently observed changes are compared with natural processes. To put geologic data into historic context, a detailed sand budget for the upper Texas coast is quantified in Chapter 3. In Chapter 4 the rate of intense hurricane impacts for the Gulf of Mexico over the late Holocene is documented. Additionally, this chapter discusses the effect of climate variations on the probability of intense hurricane impacts for the Gulf of Mexico in the past. In Chapter 5, San Luis Pass, a natural tidal delta adjacent to Galveston Island, is examined.

This feature is an ideal laboratory for measuring the long-term and historical effects of hurricane impacts and accelerated sea-level rise on Galveston Island because it is the ultimate repository for sand eroded from the island.

Over the late Holocene, coastal change appears to have been quite dramatic despite a relatively constant rate of hurricane impacts. An acceleration in the rate of relative sea-level rise, however, likely would have dramatic consequences for the Texas coast.

## CHAPTER 2

### Natural versus anthropogenic mechanisms of erosion along the upper Texas coast<sup>1</sup>

#### 2.0 Abstract

Galveston Island and Bolivar Peninsula have experienced a well-documented history of shoreline and bay shoreline change ranging from +3.63 m/yr to -1.95 m/yr. By integrating core, light detection and ranging (LIDAR), and coastal change data, we develop a sand budget that attempts to quantify long-term sand sources (e.g., fluvial sand cannibalization through transgression) and sinks (washover fans, offshore sand bodies, and flood-tidal deltas). These results are then considered in light of anthropogenic influences (e.g., beach-nourishment projects, coastal engineering structures, and dredging operations) in an attempt to relate natural versus human influence on coastal change. Our findings suggest that hurricane washover (Galveston Island = 0.4 m/100 yr; Bolivar Peninsula varies from 0.154 m/100 yr to 0.095 m/100 yr) and offshore sand deposits are minimal long-term sand sinks. Flood-tidal deltas, however, appear to be major locations for natural sand sequestration. We also conclude that damming of rivers has had minimal impact on the upper Texas coast, although hard structures, such as the Galveston seawall and its groins, have exacerbated erosion along a shoreline that is currently sand starved. The impact of hard structures has mainly been one of trapping sand in locations where that sand would not have naturally accreted. Sand supply is minimal, so understanding and developing a better sand budget for the Texas coast are vital to sustainability.

---

<sup>1</sup> This chapter has been edited, reformatted, and reprinted with permission: Wallace, D.J., Anderson, J.B., and Rodriguez, A.B., 2009, Natural versus anthropogenic mechanisms of erosion along the upper Texas Coast. *in*: Kelley, J.T., Pilkey, O.H., and Cooper, J.A.G., ed., America's Most Vulnerable Coastal Communities: The Geological Society of America Special Paper 460, p. 137-147.



## 2.1 Introduction

Like most coastal areas, the Texas coast is experiencing rapid population growth and development. The largest populated areas are concentrated in the upper Texas coast on Bolivar Peninsula and Galveston Island (Fig. 2-1). Currently, natural shoreline change rates in the area vary from +3.63 m/yr to -1.95 m/yr (Gibeaut et al., 2006). Residents want to nourish beaches, and calls for government assistance in combating beach erosion typically include claims that humans caused the problem. Millions of dollars have already been spent by the state of Texas to combat coastal erosion. Unfortunately, most of this money has been spent on relatively small beach nourishment projects lasting only a few years or even months. These projects involve trucking sand excavated from sand pits, including sand pits on the barriers, onto the beach. Although Section 61.013 of the Texas Open Beaches Act forbids placing "...any obstruction, barrier, or restraint that will interfere with the free and unrestricted right of the public....," several other ill-fated projects have included construction of geotubes, jetties, and cement riprap (Figs. 2-2A–2D). Because the supply of sand to the coast is limited, these projects have done little to slow the rate of shoreline retreat. The state has also invested heavily in sand-resource studies along the upper Texas coast and the south Texas coast. None of these studies has led to the discovery of large sand bodies. Currently, the state is about to embark on its largest sand nourishment project on Galveston Island, using the only known large sand resource and leaving no sand source for post-storm damage repair.

Since sand supply along the upper Texas coast is minimal and rates of sea-level rise for the next century are predicted to exceed 3–5 mm/yr (Thomas et al., 2004; Church and White, 2006; Overpeck et al., 2006; IPCC, 2007; Pfeffer et al., 2008), rates of coastal retreat are expected to increase during this century. An understanding of the variable causes of erosion of the upper Texas coast will be vital to developing successful restoration programs and making decisions about sustainability of the coast.

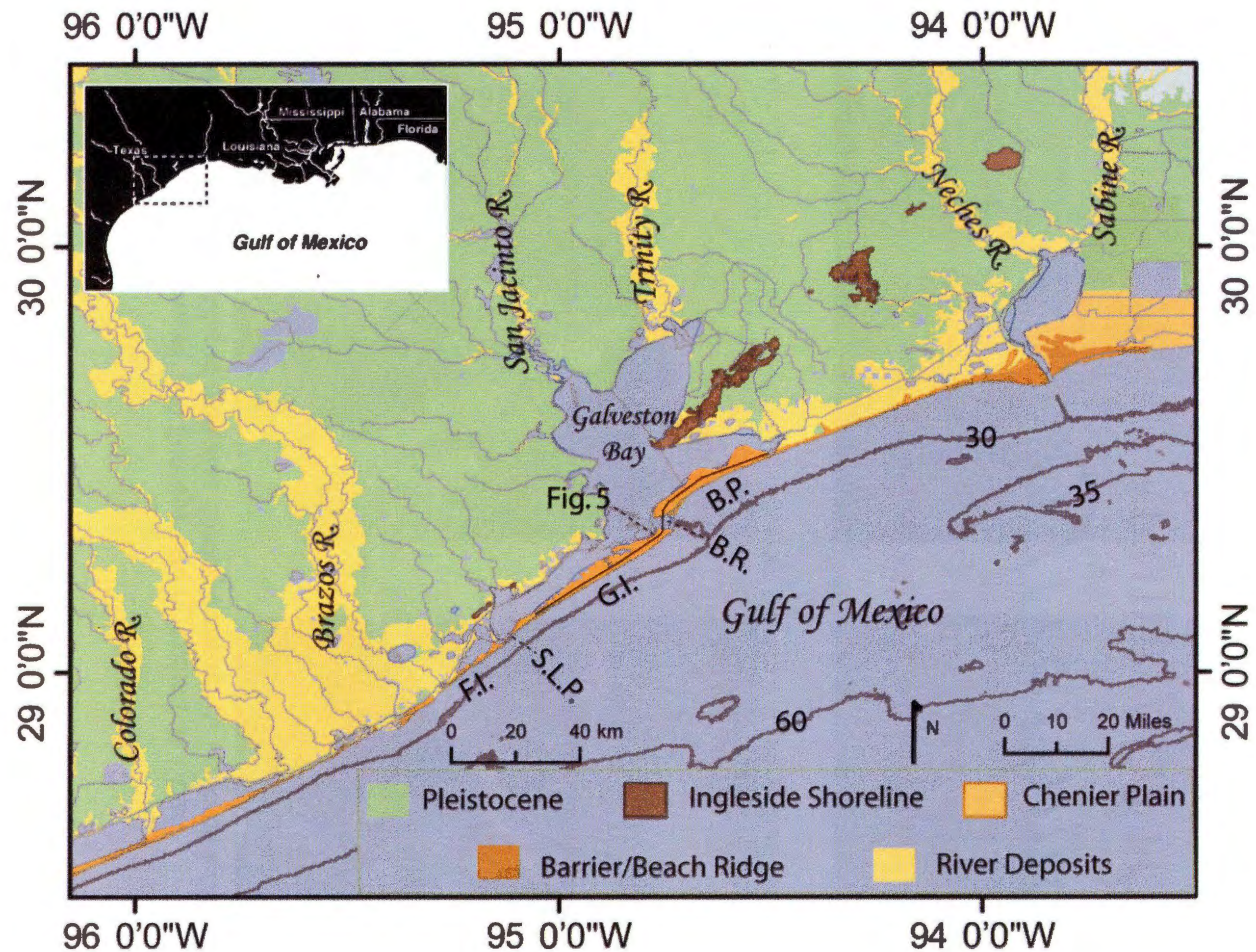


Figure 2-1: Geographic and geologic map of study area (modified from Bernard et al., 1970; Anderson, 2007). Black line indicates transect location of Figure 2-5. Note the 120 ka highstand Ingleside shoreline. B.P.—Bolivar Peninsula; G.I.—Galveston Island; F.I.—Follets Island; B.R.—Bolivar Roads; S.L.P.—San Luis Pass. Contour intervals are in ft (30 ft = 9.1 m, 35 ft = 10.7 m, 60 ft = 18.3 m).



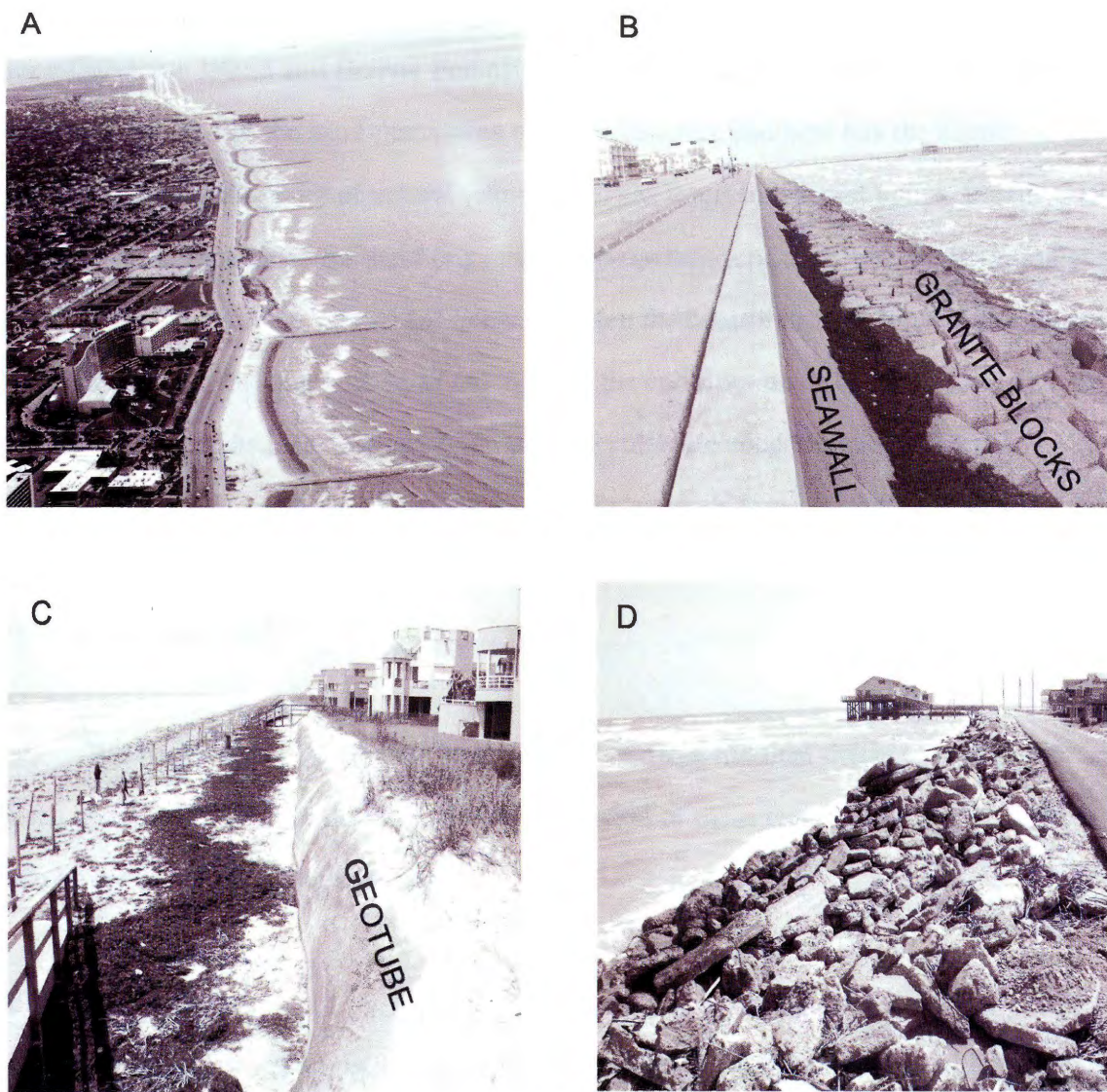


Figure 2-2. Structures used to decrease coastal erosion: (A) Groins along Galveston Island, (B) Galveston Island seawall, (C) geotube, and (D) concrete riprap.

The objective of this paper is to document natural versus anthropogenic causes of erosion along Galveston Island and Bolivar Peninsula. Several questions are addressed, such as: (1) What is the source of the sand that makes up these beaches, and how has the supply of this sand varied, both as a result of natural (climate and sea level) forces and human impacts? (2) What are the natural sinks for sand (e.g., tidal deltas, washovers, and offshore sand bodies), and how has their storage varied? (3) What has been the contribution of tropical storms and hurricane impacts to coastal erosion? (4) What is the contribution of coastal subsidence to erosion? (5) How has local geology (e.g., variable substrate cohesiveness) influenced coastal erosion? (6) What have been the main anthropogenic impacts on the coast, and how fast does the coastal system respond to human impacts? (7) How do current rates of erosion compare to long-term rates?

We begin with a description of the coastal barriers and tidal deltas of the upper Texas coast, followed by a discussion of the evolution of these features. Lastly, we address each of the questions using existing data.

## **Setting**

Prevailing winds along the upper Texas coast are from the southeast, which results in longshore currents that flow dominantly to the west. During winter months, cold fronts approach the region from the north and west, causing winds to blow offshore and from the west and creating associated eastward-flowing longshore currents. Estimates of net transport of sediment along the upper Texas coast range from ~11,800–300,000 m<sup>3</sup>/yr (Johnson, 1956; Hansen, 1960; Carothers and Innis, 1962; Weiser and Armstrong, 1963; Mason and Sorenson, 1972; Morton, 1979; Hall, 1976; Watson and Behrens, 1976; Morang, 2006). The lower numbers are associated with the eastern part of Bolivar Peninsula (Fig. 2-3), where little sand is being added to the longshore transport system, and with the western part of Galveston Island (Fig. 2-4A), adjacent to the Galveston seawall (Fig. 2-2B).

The higher numbers are associated with jetties on either side of the ship channel leading into Galveston Bay.

The Gulf of Mexico along the Texas coast is microtidal, with a tidal range of ~30 cm. Average wave heights are <1.0 m, but they can reach >7 m during extreme events like tropical storms and hurricanes. Since 1527, the start of historical storm records, the upper Texas coast has been impacted by ~42 major storms (8.7% annual landfall probability).

## **2.2 Results**

### **Coastal Evolution**

The key to understanding human influence on coastal change is knowledge of how the coast evolved naturally at centennial to millennial time scales. The following brief discussion is intended to provide some background on the evolution of coastal environments of the upper Texas coast.

#### *Bolivar Peninsula*

Previous researchers have reconstructed Bolivar Peninsula's evolution using geomorphic features and a relatively large number of short (<6-m-long) sediment cores, drill cores (>8 m long), and sandpit observations (Morton, 1994; Rodriguez et al., 2004). These results indicate that the peninsula formed by spit accretion as sand was added to the western end of the peninsula by westward-flowing longshore currents. It is a relatively young barrier, having formed after 1.7 ka (Rodriguez et al., 2004). Westward growth of Bolivar Peninsula has resulted in the barrier having migrated over the Trinity River incised valley, which is ~40 m deep at the coast (Fig. 2-5). Thus, the barrier and associated tidal-inlet and tidal-delta deposits increase in thickness from east to west as a result of having filled the fluvial valley.



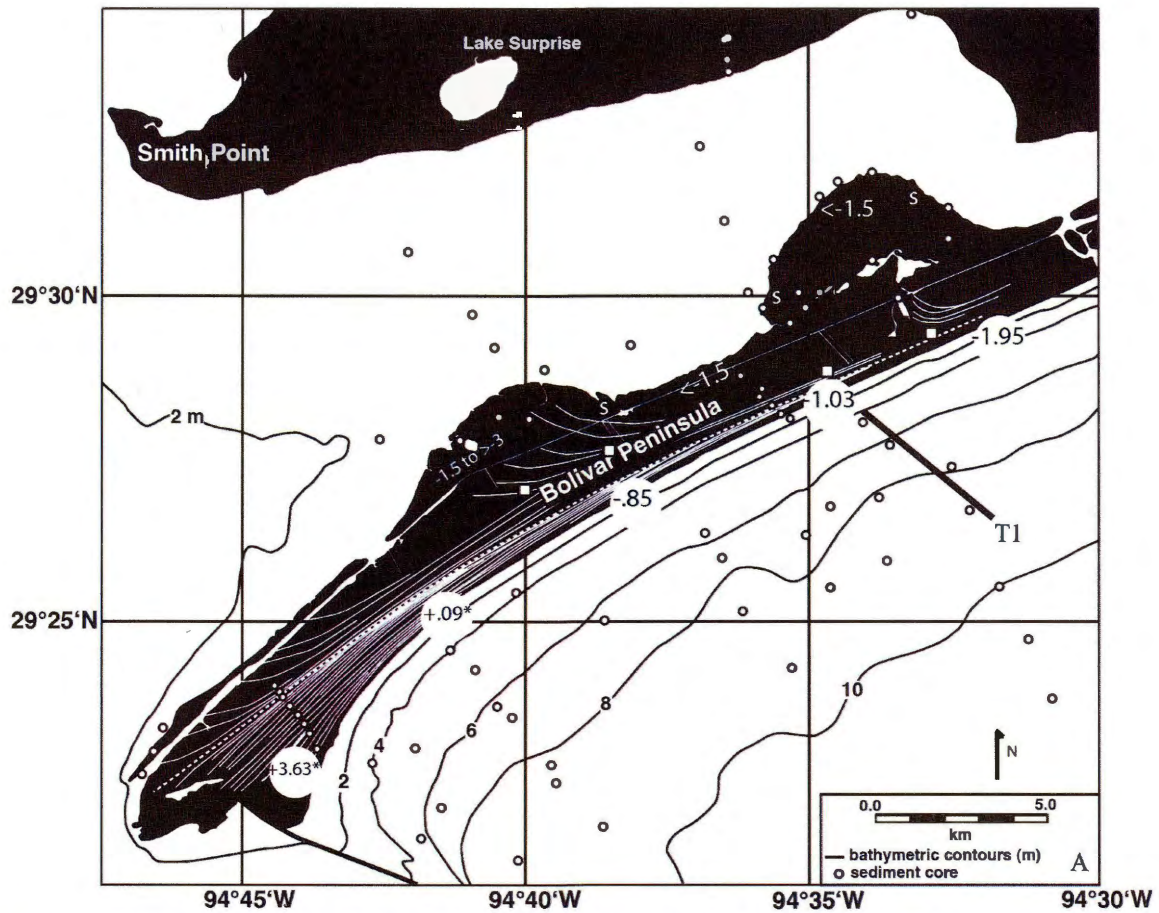


Figure 2-3: Bolivar Peninsula, core locations, approximate location of offshore profile T1 shown in Figure 2-8A, and selected shoreline/bay change rates (from Texas Bureau of Economic Geology) (modified from Rodriguez et al., 2004). Erosion rates are in m/yr; s—stable; \*—rate is heavily influenced by anthropogenic structures. Shoreline change rates are from 1930 to 2000; bay shoreline change rates are from the 1930s to 1982.

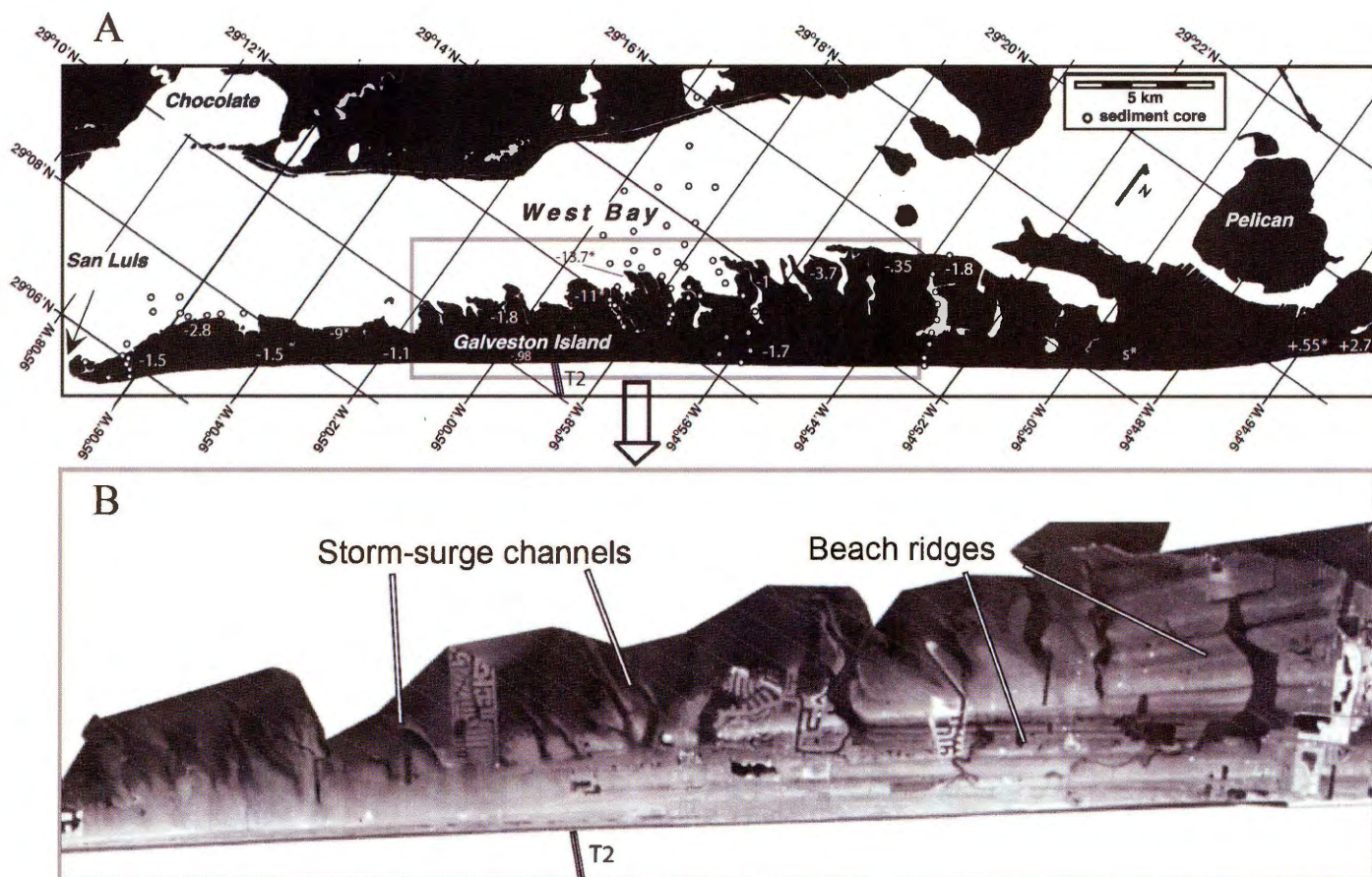


Figure 2-4: (A) Map of Galveston Island showing locations of cores, the offshore transect T2 shown in Figure 2-8B, and selected shoreline/bay change rates (from Texas Bureau of Economic Geology) (modified from Rodriguez et al., 2004). Erosion rates are in m/yr; s—stable; \*—rate is heavily influenced by anthropogenic structures. Shoreline change rates are from 1930 to 2000; bay shoreline change rates are from the 1930s to 1995. Offshore transect T2 is also shown. (B) Light detection and ranging (LIDAR) image showing beach ridges extending approximately two-thirds the length of the island. Location indicated by gray box in Figure 2-4A.

The barrier ranges between 3 and 5 m in thickness up to the edge of the valley, where it rapidly expands to 20 m. Two prominent washover fans occur on the north side of the barrier (Fig. 2-3). Radiocarbon dates from these fans indicate that they both formed between  $1,755 \pm 85$  cal yr B.P. and  $1,530 \pm 85$  cal yr B.P. during the early stages of barrier development (Rodriguez et al., 2004).

The growth of Bolivar Peninsula was relatively continuous until ~700 yr ago, when a hurricane destroyed much of the western end of the barrier now located seaward of the current highway. This is evidenced by a prominent hiatus that separates an older beach ridge set that curves to the north from a series of relatively straight and low beach ridges that parallel the current shoreline (Fig. 2-3). The older ridge set yielded radiocarbon ages that range between ca. 1,500 ka and ca. 1,200 ka, while the younger beach ridge set yielded ages younger than ca. 700 ka (Rodriguez et al., 2004).

### *Galveston Island*

Galveston Island is a typical drumstick-shaped barrier island with prominent beach ridges recording an initial history of barrier growth (Morton, 1994) (Fig. 2-4B). Radiocarbon dates from drill cores (Bernard et al., 1959) and vibracores (Rodriguez et al., 2004) collected in transects oriented perpendicular to the long axis of the barrier indicate that the progradational phase of barrier evolution began ~5,500 yr ago and lasted until at least 1,800 yr ago. Growth of the island was followed by landward retreat.

Like Bolivar Peninsula, Galveston Island has continued to accrete to the west, so the barrier is younger, and therefore narrower and thinner, in that direction. Beach ridges are easily traced in aerial photographs and LIDAR images as far west as ~95°00'W (Fig. 2-4B). West of that location, storm washover features dominate the barrier landscape.



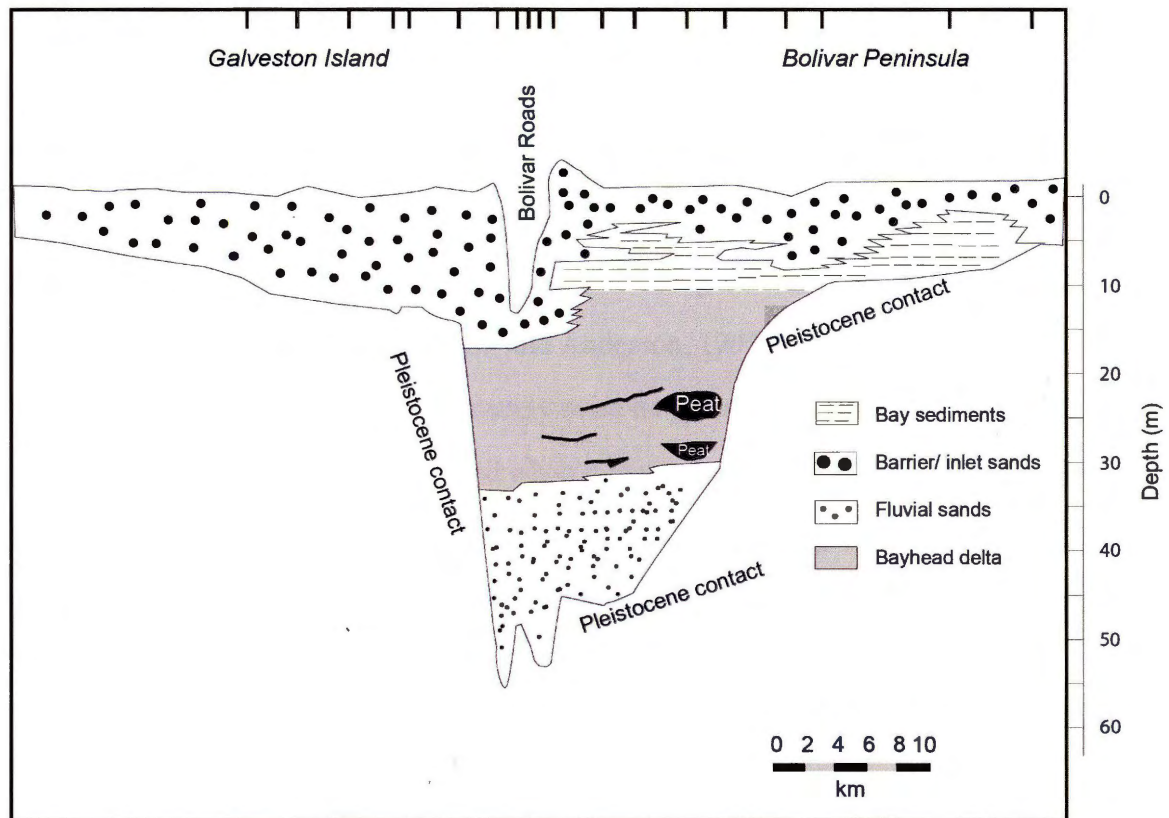


Figure 2-5: Subsurface geology of the study area from the east end of Bolivar Peninsula to the west end of Galveston Island (modified from Siringan and Anderson, 1993; Rodriguez et al., 1999; Anderson et al., 2008). See Figure 2-1 for cross-section location. Core locations are denoted by black hash marks.

### *Bolivar Tidal-Delta Complex*

A prominent tidal-inlet and tidal-delta complex (ebb- and flood-tidal deltas) separates Bolivar Peninsula from Galveston Island (Fig. 2-6). Westward migration of the Bolivar tidal inlet associated with growth of the peninsula is marked by curved beach ridges and prograding clinoforms that thicken toward the west (Siringan and Anderson, 1993). As the barrier grew toward the west, the Bolivar tidal inlet grew narrower and the flood-tidal delta also migrated westward (Siringan and Anderson, 1993). At ca. 1,500 cal yr B.P., the Bolivar flood-tidal delta was approximately twice its present size (Rodriguez et al., 1998). Westward migration of the inlet ceased when it reached the Trinity River incised valley, and the inlet itself correspondingly became deeply incised. Following this, the flood-tidal delta shrank in size, and bay mud buried sandy tidal-delta deposits (Siringan and Anderson, 1994; Rodriguez et al., 1998).

### *San Luis Pass Tidal-Delta Complex*

The San Luis Pass tidal inlet separates Galveston from Follets Island to the west (Fig. 2-1). A large flood-tidal delta that extends into West Bay and Christmas Bay and a much smaller ebb-tidal delta (Fig. 2-7) are associated with the inlet. The age of the delta is constrained by a single radiocarbon date of  $4,150 \pm 190$  cal yr B.P. from bay mud resting below the tidal delta; however, this is a maximum age because the tidal delta is separated from these bay deposits by an erosional surface.

The San Luis Pass flood-tidal delta has a visible influence on the west end of Galveston and eastern Follets Islands. Little is known, however, about the way in which this inlet affects sand transport and storage over geologic time. No migration or sediment accumulation rate data currently exist for this tidal delta.

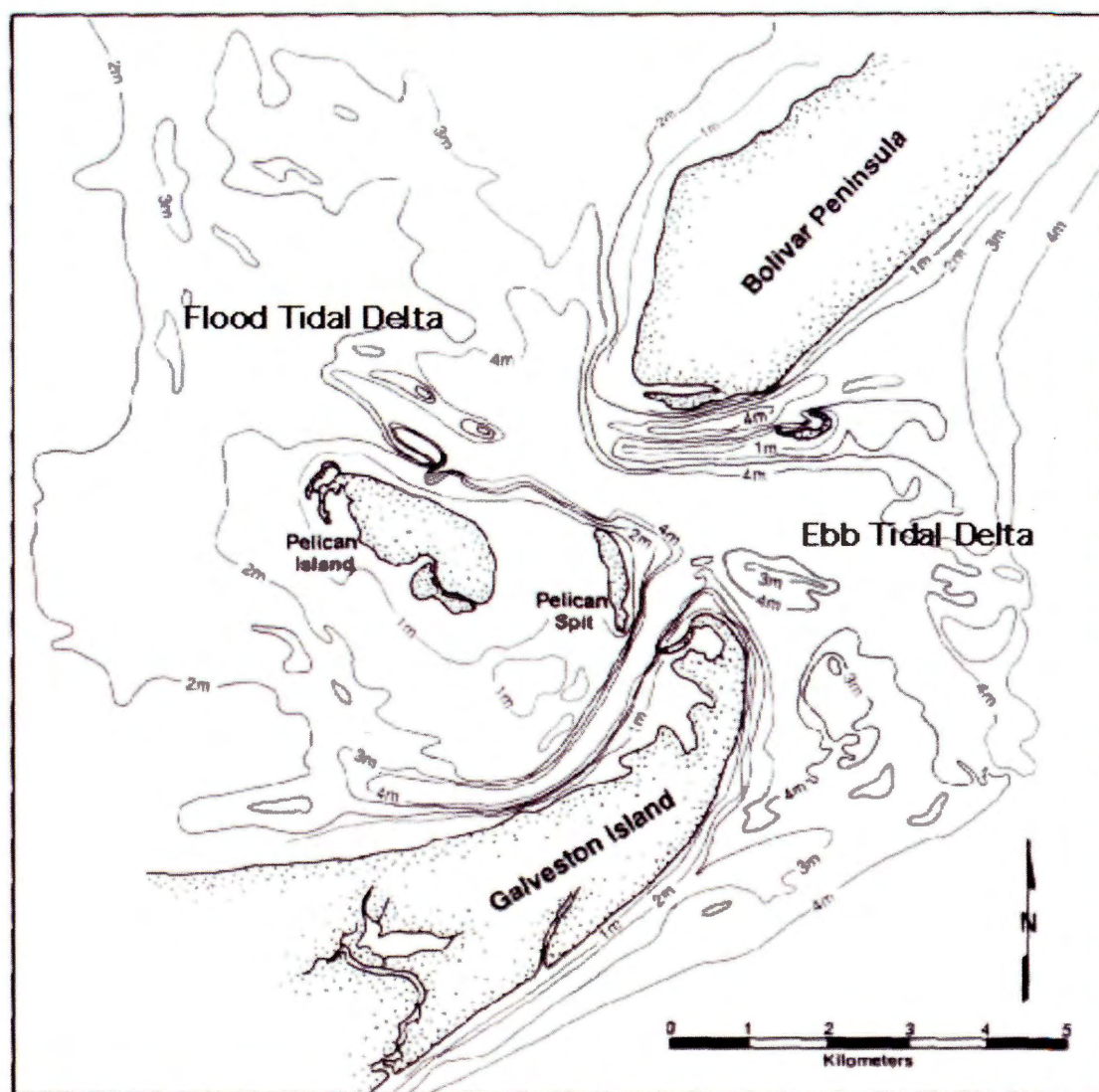


Figure 2-6. The morphology of the Bolivar Roads tidal delta in 1867 prior to jetty construction and dredging of the ship channel (modified from Eyer, 1984).

Previous hypotheses have suggested that the inlet migrated to the southwest, but we recently acquired cores that shed doubt on this interpretation due to the lack of old flood-tidal delta deposits on the back-barrier side of the west end of Galveston Island. Hence, the tidal inlet is now believed to be a more recent feature, and possibly formed by breaching of an earlier continuous barrier and separation of Galveston Island from Follets Island to the west.

Previous work (Morang, 2006) has suggested that a large volume (over 3.1 million  $\text{m}^3$ ) of sand is potentially sequestered in both the San Luis Pass flood- and ebb-tidal delta shoals, making them the main depocenter for sand eroded from Galveston Island (Israel et al., 1987). This number is based on current erosion rates and their contribution of sand to longshore transport. An accurate sediment flux for San Luis Pass is currently being examined.

In summary, Bolivar and Galveston barriers are composed of sand that came mainly from offshore. As the rate of sea-level rise diminished, sand was initially stacked in shingle-like fashion against a wave-cut notch in the Pleistocene surface to create Galveston Island, and later spit accretion resulted in the formation of Bolivar Peninsula. This all occurred after 7,000 yr B.P. when the rate of sea-level rise decreased from an average of 4.1 mm/yr to 0.4 mm/yr (Milliken et al., 2008a). This raises the question: how will these barriers respond to the increase in the rate of sea-level rise that has already begun and is expected to continue this century to the point where it may again exceed 4.0 cm/yr (Church and White, 2006)?



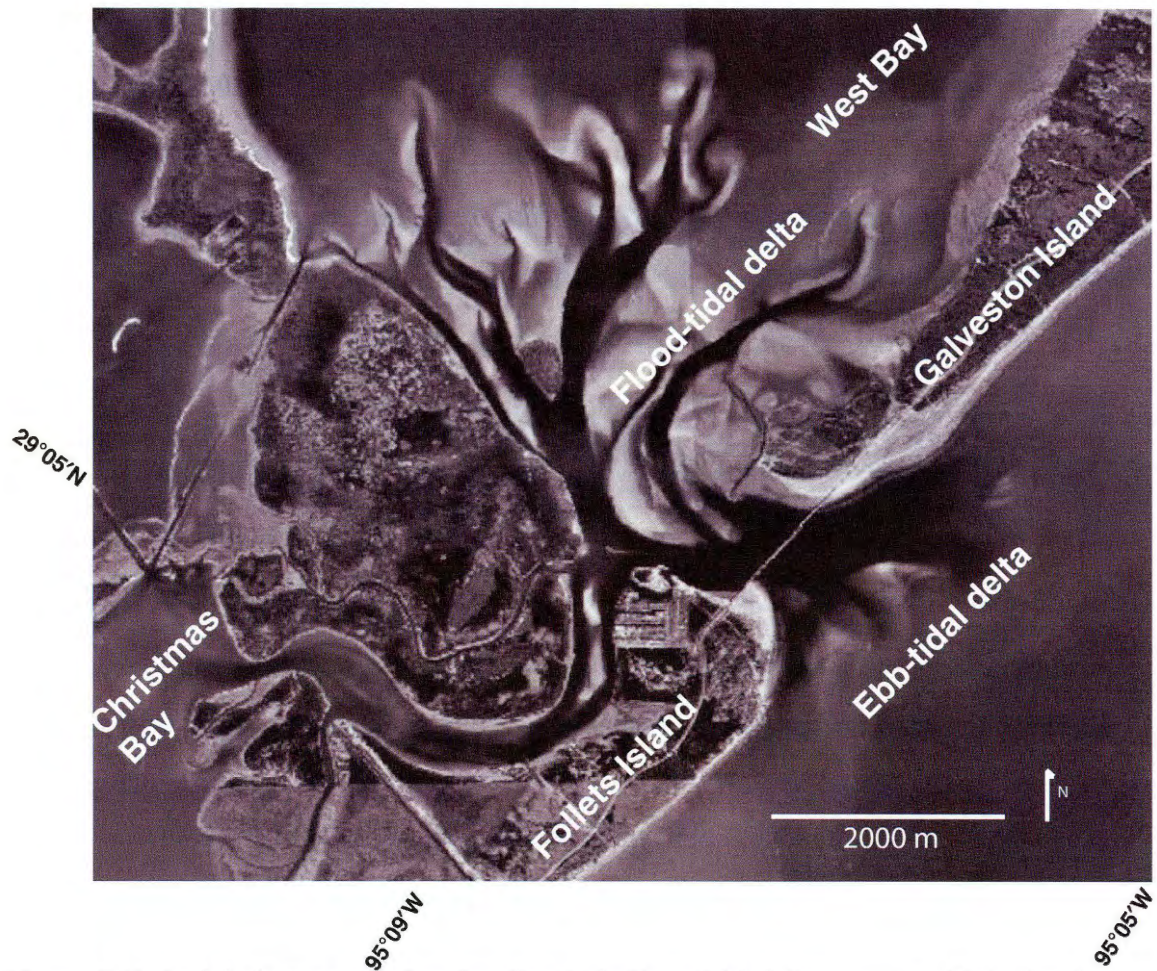


Figure 2-7. Aerial photograph showing San Luis Pass tidal delta complex. Note the size difference between the ebb- and flood-tidal deltas.

## 2.3 Discussion

### Sources of Sand

#### *Sand Supply from Rivers*

The Brazos, San Bernard, and Colorado Rivers flow directly to the upper Texas coast, although the former is the only significant sediment contributor today (Morton and Pieper, 1975b; Mathewson and Minter, 1976). These rivers are located west (down drift) of the study area and are not significant sources of sand for Bolivar and Galveston Island beaches. In addition, there has been limited direct fluvial input to the upper Texas coast since the early Holocene, when the Sabine and Trinity River valleys were flooded to create Sabine Lake and Galveston Bay, respectively (Milliken et al., 2008b; Anderson et al., 2008). These shallow and microtidal estuaries trap sand mostly in their bayhead deltas. Thus, contrary to popular opinion, damming rivers has had minimal impact on the upper Texas coast east of the mouth of the Brazos River.

#### *Offshore Sand Sources*

Sediment cores from offshore Bolivar Peninsula (Fig. 2-8A) and Galveston Island (Fig. 2-8B) have sampled upper shoreface sands that grade offshore into interbedded fine to very fine sand and mud of the lower shoreface. Seaward, at approximately the physiographic toe of the shoreface (~8–10 m), these shoreface deposits are currently being buried beneath marine mud, and there is a virtual absence of sand, including storm sand bodies (Siringan and Anderson, 1994; Rodriguez et al., 2001) (Figs. 2-8A–8B). Hence, premodern shoreface and coastal deposits have been completely eroded below approximately –8 m. This is therefore the depth of the transgressive ravinement surface (Rodriguez et al., 2001).

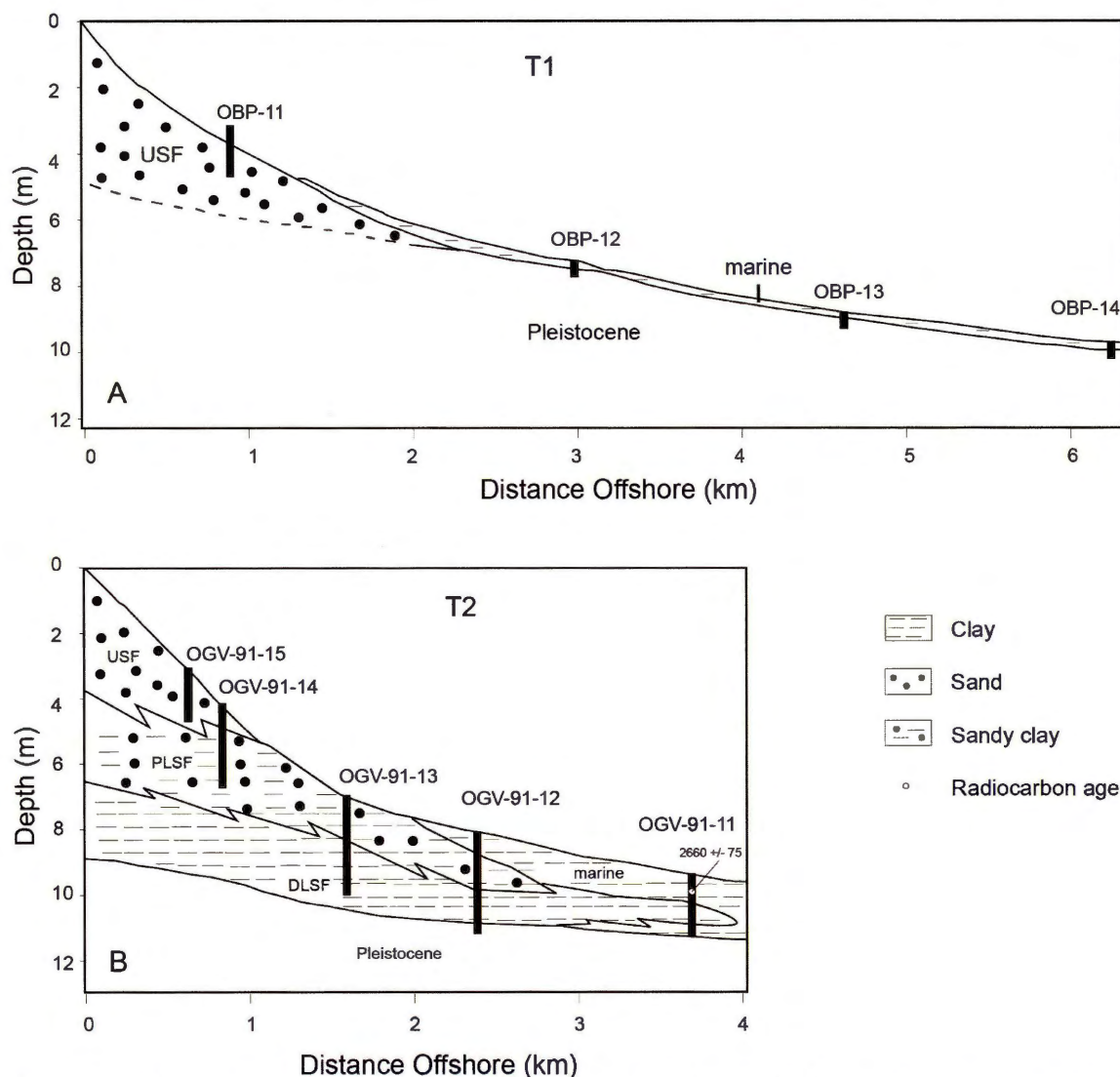


Figure 2-8: Cross section of shoreface offshore Bolivar Peninsula (A) and Galveston Island (B) based on sediment core transects (modified from Rodriguez et al., 2001). See Figures 2-3 and 2-4 for transect locations. USF—upper shoreface, PLSF—proximal lower shoreface, DLSF—distal lower shoreface.

An extensive seismic and core data set from the Texas continental shelf provides evidence that transgressive ravinement during the late Pleistocene–Holocene transgression has incised into the continental shelf (Rodriguez et al., 2004), including cannibalization of sandy delta deposits and fluvial, tidal, and coastal sand bodies within incised valleys (Anderson et al., 2004). While this mechanism was significant in sand delivery to coastal barriers in the past, there are few known localities where relict sand bodies are currently being exhumed. Hence, there is little or no new sand being added to the system. Instead, sand sources for down-drift areas of the coast are currently limited to secondary erosion of beaches, dunes, and bluffs, and that supply is minimal (Morton et al., 1995).

### *Sand Sinks*

There are a number of sand sinks, places where sand is removed from the coastal system for periods of centuries to millennia, within the study area. These include flood-tidal deltas, washover fans, and offshore sand bodies. The latter are restricted to the shoreface at water depths above 8 to 10 m. All of these sinks are temporary at these time scales because sand is ultimately introduced back into the active coastal transport system. Sand that resides in the lower shoreface is continuously being reworked and transported on and along the shore, a process that is most active during tropical storms and hurricanes. The rates at which this happens are measured in decades and are essentially the same as shoreline migration rates, assuming maintenance of a shoreface equilibrium profile (Bruun, 1954, 1962; Swift, 1976; Pilkey et al., 1993). Sand in back-barrier settings is eventually exhumed as the shoreline advances landward and so is brought back into the coastal transport system. At current rates of shoreline migration, this process occurs at millennial time scales.

We estimated the flux of sand within the Bolivar longshore transport system (383,000 m<sup>3</sup>/yr) using the volume of sand that was trapped on the eastern side of the jetties on either side of the Bolivar inlet (Morang, 2006).



However, part of this sand likely came from the Bolivar ebb-tidal delta, which was much larger prior to 1900 (Fig. 2-6). Both the ebb- and flood-tidal deltas diminished in size considerably after the jetties were constructed (Siringan and Anderson, 1993). Thus, construction of the jetties restricted sand supply to the deltas. In particular, the flood-tidal delta was a major sand sink prior to jetty construction. During this time, only a portion of the sand moving within the longshore transport system was making its way onto Galveston Island.

Storm overwash was a significant process only during the early evolution of both barriers. As they grew and gained width and elevation, breaching and washover were restricted to the western end of Galveston Island. Rodriguez et al. (2004) suggested accumulation rates of 0.154 m/100 yr and 0.095 m/100 yr for washover fans on the bayside of Bolivar Peninsula. On the bayside of Galveston Island in West Bay, the rate of washover accumulation is ~0.4 m/100 yr (Rodriguez et al., 2004). Thus, storm washover deposits are not a significant sand sink, at least they have not been during recent time.

### *Hurricane Impacts and Washover Formation*

The most unpredictable influence on coastal evolution is that of tropical storms and hurricanes. Of the hurricanes striking the upper Texas coast during historic time, nine named storms have impacted the study area, including Debra (1959), Carla (1961), Cindy (1963), Edith (1971), Claudette (1979), Alicia (1983), Bonnie (1986), Rita (2005), and Ike (2008). Carla made landfall at Port O'Connor, Texas, and caused a storm surge between 2.7 and 4.6 m, and up to 18.3 m of beach erosion on Bolivar Peninsula (Hayes, 1967; Anderson, 2007). Cindy was significantly smaller, and scoured bar and runnel structures. Alicia, however, passed directly over San Luis Pass, bringing 127–177 mm of rainfall and wave heights of 2.3 m. On West Beach, this storm caused ~45 m of erosion with 1.5 m of vertical scour.

The U.S. Army Corps of Engineers estimated that without the seawall, \$100 million of additional damage would have occurred on Galveston Island during Alicia (Lichter, 2008). Ike made landfall at Galveston Island on 12 September 2008. Damage due to the storm had still not been assessed at the time this paper was written, but it is already clear that the Galveston seawall again protected Galveston during Hurricane Ike. It has also been observed that the greatest impact from Ike occurred on Bolivar Peninsula, where relatively young, low beach ridges provided little protection from storm surge.

### **Relative Sea-Level Rise**

In a recent report on the results of a releveling/benchmark survey in south Louisiana, Shinkle and Dokka (2004) indicated that current rates of subsidence along the south Louisiana coast are as high as 10–15 mm/yr. This is an order of magnitude faster than indicated by sea-level records for the time interval between 4,000 and 1,000 cal yr B.P., suggesting an anthropogenic control, specifically, subsurface fluid extraction (Törnqvist et al., 2004; Morton et al., 2006; Milliken et al., 2008a). This provoked significant concern that the upper Texas coast might be experiencing similar rates. If so, the current rate of relative sea-level rise could exceed the Intergovernmental Panel on Climate Change (IPCC) worse case scenarios for eustatic sea-level rise by the end of this century (Church and White, 2006). Historical subsidence rates along the Texas coast range from 3 to 22 mm/yr, compared to average subsidence rates over geologic time (i.e.,  $10^2$ – $10^3$  yr) of 0.05 mm/yr (Paine, 1993). Areas with the highest subsidence rates are either associated with groundwater or oil and natural gas withdrawal (Paine, 1993).

Although sediment consolidation has been shown to be a dominant Holocene process contributing to subsidence, and therefore coastal erosion, in nearby Louisiana (Penland and Ramsey, 1990; Kulp, 2000; Törnqvist et al., 2004, 2006, 2008), Galveston Island and Bolivar Peninsula do not show the same correlation between erosion rates and subsidence. The reason for this is twofold. First, Holocene mud deposited in incised valleys along the Texas coast accumulated over longer time scales (Milliken et al., 2008a; Anderson et al., 2008; Maddox et al., 2008; Simms et al., 2008), and therefore, subsidence rates due to consolidation have been gradual. Also, the potential effect of higher subsidence within valleys may be compensated by availability of sand bodies within the valleys (e.g., tidal deltas) that contribute to sand supply.

### **Geological Controls on Coastal Erosion**

There are two general categories of substrate along the Texas coast that are being eroded by the advancing shoreline: Pleistocene clay (Beaumont) deposits and Holocene back-barrier and fluvial deposits (mud). Pleistocene substrates are more cohesive than Holocene fluvial and bay sediments. Previous work (Parchure and Mehta, 1985; Amos et al., 1992; Mitchener et al., 1996) has shown that the critical shear stress increases with depth due to changes associated with increasing consolidation. The relief of the Pleistocene surface is quite variable (Simms et al., 2007). When the depth to the Pleistocene surface along the east Texas coast (Fig. 2-5) is compared to current erosion rates (Gibeaut et al., 2006), a correlation exists between erosion rates and substrate type. Isolated areas with shallow depths to the Pleistocene strata (e.g., <8 m) have significantly lower erosion rates (2–3 times). However, there are only a few areas with very shallow underlying Pleistocene depths, so most of the substrate between sea level and –8 m (the depth of the transgressive ravinement) is easily erodible Holocene barrier sand or fluvial and bay mud. Furthermore, areas with the shallowest Pleistocene surface, and therefore thinnest sand, are more vulnerable to storm impact.

## **Comparison of Long-Term and Short-Term Erosion Rates**

Radiocarbon ages have been used to constrain the long-term rates of shoreline retreat along the upper East Texas coast (Rodriguez et al., 2004). These data indicate that the rate of retreat is not only episodic, but it also varies along the coast. As previously stated, Galveston Island was prograding seaward between ca. 5,500 and 1,500 ka, when the barrier shoreline to the east was rapidly retreating landward at an average rate of 7.9 m/yr (Rodriguez et al., 2004). Then, the eastern shoreline stabilized, and Bolivar Peninsula began to form after ca. 1,500 ka. This variability amplifies the importance of factors other than sea-level rise in controlling coastal erosion, in particular, sand supply and antecedent topography.

The Texas Bureau of Economic Geology (BEG) has monitored coastal retreat rates for the past 30 yr. Initial methodology relied upon aerial photographs and field observation, while today, new technology, such as satellite imagery and light detection and ranging (LIDAR), has allowed very precise coastal position measurements to be made. Using these sophisticated technologies, the BEG has reported short-term rates (1930–2000) between +3.63 m/yr to –1.95 m/yr from Bolivar Peninsula (Fig. 2-3) to the west end of Galveston Island (Gibeaut et al., 2006; Fig. 2-4A).

The BEG also monitors bay shore migration rates. Along the East Bay shoreline of Bolivar Peninsula (Fig. 2-3), erosion rates range from <1.5 m to more than 3 m/yr (Gibeaut et al., 2006). Currently, 79% of the West Bay shoreline is retreating, with rates as high as 13.7 m/yr (Fig. 2-4A). Hence, the barriers are shrinking in size, not stepping landward. At the eastern end of Galveston Island, wetlands are being submerged due to inundation by rising sea level and a lack of sediment supply needed to sustain wetlands growth.

The rates of bay shoreline migration are, in fact, similar to those occurring in other back-barrier settings (e.g., Corpus Christi Bay, San Antonio Bay, and Red Fish Bay) where human influence has been negligible. In contrast, bay shoreline erosion near the western end of Galveston Island is in part due to the interruption of storm washover by highways and other human influences.

### **Anthropogenic Influence**

At the turn of the century, Galveston Island was considered the “Wall Street of the South.” Its strong economy was largely driven by the shipping industry, which was made possible by the deep Bolivar tidal inlet that allowed ships to sail through the inlet and dock in the protected waters on the north side of the island. The “Great Storm” of 1900 virtually destroyed the island, killing most of its inhabitants. However, the city rebuilt, including the construction of the Galveston seawall in 1902, which stretches some 15.7 km along the east end of the island. The city again prospered, until the construction of the Houston Ship Channel, which robbed the island of much of its maritime commerce. This period also involved the construction of two large jetties on either side of the entrance to the channel. Since the South Jetty on Galveston Island was built in 1880, the west end of Bolivar Peninsula has accreted  $+3.63$  m/yr due to a predominant southwesterly longshore transport (Gibeaut et al., 2006) and sequesters  $\sim 383,000$  m<sup>3</sup>/yr of sediment. The area west of this jetty (the east end of Galveston Island) has also accreted  $2.71$  m/yr, and roughly  $428,000$  m<sup>3</sup>/yr of sediment accumulates against the jetty, as longshore transport periodically comes from the southeast (Morang, 2006).

Prior to the construction of the jetties at the mouth of the ship channel, there was a large ebb-tidal delta located offshore of Bolivar Inlet (Fig. 2-6). Within a few decades of jetty construction, the ebb-tidal delta shrank to its current size. Part of the sand in the delta was transported landward and accreted to beaches on either side of the jetties.

The more distal part of the ebb-tidal delta was buried beneath marine mud and dredge spoils. Groins were constructed along the Galveston seawall (Fig. 2-2A) and effectively trapped sand moving along the coast; however, relatively little sand is currently moving within the longshore transport system offshore of the seawall.

Construction of the Galveston seawall began in 1902 and was one of the great engineering accomplishments of the time. The seawall still stands as a protective barrier that has withstood a number of tropical storms and hurricanes, most recently, Hurricane Ike. Mostly weekenders and tourists occupy Bolivar Peninsula and the west end of Galveston Island. These areas have largely remained “unprotected” from coastal erosion, but that is rapidly changing.

Between 2000 and 2007, the state of Texas supplied over 44 million dollars for the Coastal Erosion Planning and Response Act (CEPRA; Texas General Land Office, 2007). Thirty-four of these projects were aimed at restoration efforts in Chambers and Galveston Counties, which include Bolivar Peninsula and Galveston Island, respectively (McKenna, 2004). Within the last two decades, the most popular approach to combating coastal erosion has been the placement of “geotubes” along the coast (Fig. 2-2C). Geotubes are soft, textile structures filled with sand designed to act as artificial dunes and protect the beach from storm impacts. Finding sand to fill the geotubes has been a problem. These structures exist both on Bolivar Peninsula (Gilchrist East and Rollover Pass) and on Galveston Island (Dellanera, Beach Pocket Park 2, Riviera, and Pirates Beach) (Gibeaut et al., 2003). There was one large beach nourishment project in 1995, which was considered to have been briefly successful, but that beach fill has now largely eroded away. Otherwise, there have been several small nourishment projects involving truckloads of sand being placed on the beach. Much of this sand has come from pits dug on the barriers.

In general, these small segments of nourished beach have lasted less than a year or two, and none are known to have survived Hurricane Ike. Plans by the BEG are under way for a new beach-nourishment project at the west end of the Galveston seawall that would use the only known large sand deposit on the island. This project has been delayed because this sand may be needed for restoration in the aftermath of Hurricane Ike.

## 2.4 Conclusions

The current rates of retreat along the Gulf of Mexico shoreline are equal to or less than the premodern rates, except in a few isolated areas, such as Rollover Pass on Bolivar Peninsula, where humans have impacted the normal longshore transport of sand. The cause of coastal erosion is known—minimal sand supply and rising sea level. The popular conception that damming rivers has increased rates of erosion is unsupported, since fluvial sand delivery has in fact been relatively minimal over geologic time. However, the impact of the Galveston seawall and its groins has only exacerbated erosion along a shoreline that is currently sand starved. The main impact of the jetties on either side of Bolivar Roads tidal inlet is the trapping of eroded sand from the ebb-tidal delta and longshore-transported sand in locations where it would not have accreted naturally. This starves the down-drift areas of Galveston Island of sand, intensifying erosion rates further west.

To date, efforts to curtail coastal erosion have been largely unsuccessful, with the exception of one large beach-nourishment project. Armoring the beach has protected infrastructure, but it has not slowed the rate of shoreline retreat. The biggest obstacle to large-scale beach-nourishment projects is a virtual absence of offshore sand resources in nearshore areas, although large sand bodies do exist tens of kilometers offshore (Anderson, 2007). Thus, the cost of nourishment would be high.

The short-term and long-term success of these projects remains uncertain until there are better estimates of longshore transport rates and better refinement of the coastal sand budget. Even then, major hurricanes could destroy in a matter of hours what man is able to accomplish.



## CHAPTER 3

### **Transgressive ravinement versus depth of closure: A geological perspective from the upper Texas coast<sup>2</sup>**

#### **3.0 Abstract**

The upper Texas coast is one of the most populated areas along the Gulf of Mexico. Three dynamic barriers along this section of coastline (Bolivar Peninsula, Galveston Island, and Follets Island) have a well-documented history of shoreline change. Numerous engineering studies incorporating both sedimentological data and numerical models have been established for this system to understand sediment fluxes. However, no previous study has examined sediment fluxes for the upper Texas coast in light of certain fundamental concepts of coastal geology. Here, we discuss the current theory and understanding of barrier island dynamics from a geologic standpoint as they relate to sediment budgets for the upper Texas coast. Additionally, we demonstrate that both hurricane overwash and shoreface sands, which previously were not incorporated as sand sinks into sediment budgets for this system, represent a sizable portion of the total budget.

Until now, a depth of closure (beyond which sediment transport is negligible) of 4 m has been used, however, our data suggest a depth of at least 8 m would be more appropriate. We show that the combined upper and lower shoreface has the potential to sequester  $\sim 156,000 \pm 38,000 \text{ m}^3/\text{yr}$  of sand, equaling  $\sim 17\%$  of the entire calculated sediment flux and  $\sim 40\%$  of the total longshore transport flux for the upper Texas coast, based on previous studies. Therefore, we recommend revised approaches to future sediment budget studies in order to establish more robust analyses.

---

<sup>2</sup> This chapter is a reformatted and reprinted (with permission) version of: Wallace, D.J., Anderson, J.B., and Fernández, R. A., 2010, Transgressive ravinement versus depth of closure: A geological perspective from the upper Texas coast, *Journal of Coastal Research*, (in review).

Ultimately, it will be crucial to use both engineering principles and geologic concepts to construct an accurate and realistic scenario for coastal restoration projects.

## **3.1 Introduction**

### **Rationale for Study**

Several studies establish sand budgets for a wide range of coastal systems (Bowen and Inman, 1966; Komar, 1983; Carter, 1988; Best and Griggs, 1991; Schwab et al., 2000; Kelley et al., 2005). The upper Texas coast is one of the most developed sections of the Gulf Coast. Every year, millions of dollars are spent towards coastal nourishment projects aimed at combating coastal erosion. The study area spans some 150 kilometers of coastline, and includes both progradational and regressive barrier systems (Fig. 3-1).

Gibeaut et al., (2006) present shoreline and bayline erosion rates for the upper Texas coast ranging from stable to  $-4$  m/yr. To better understand this variability and ultimately quantify the long-term contributions of different coastal change mechanisms, an accurate sediment budget for the upper Texas Coast is needed. Previous research has focused on engineering practices as they relate to sediment budgets, but few have considered this work in light of geological principles. Specifically, there is a need to better constrain the sand flux at a range of time scales using information gained from sediment cores (Fig. 3-2). Since rates of sea level rise are expected to increase this century, quantifying coastal change mechanisms over decadal and centennial timescales allows us to better predict coastal change and to establish coastal preservation and planning scenarios.

### **Geologic Setting**

Prevailing winds from the southeast create a dominant westward flow along the upper Texas coast, although eastward flow does occur during cold fronts and winter months.

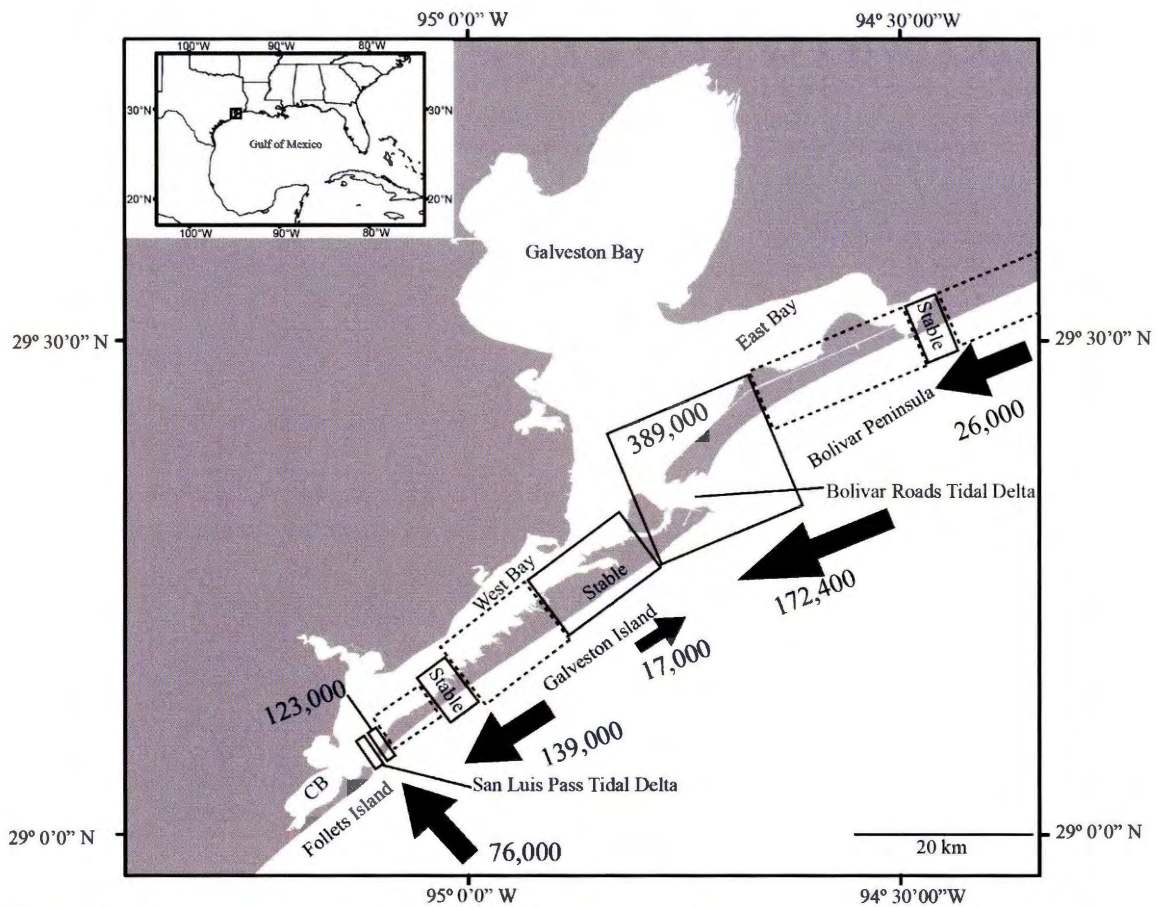


Figure 3-1: Study area map of the upper Texas coast. Also shown are approximate summarized results from an Army Corps of Engineers sand budget analysis (Morang, 2006). Numbers are the flux in  $\text{m}^3/\text{yr}$ . Solid black boxes are progradational shoreline sections, solid boxes marked stable are stable shoreline sections, and dashed boxes represent erosional shoreline sections. Numbers adjacent to arrows represent longshore transport fluxes. CB = Christmas Bay.

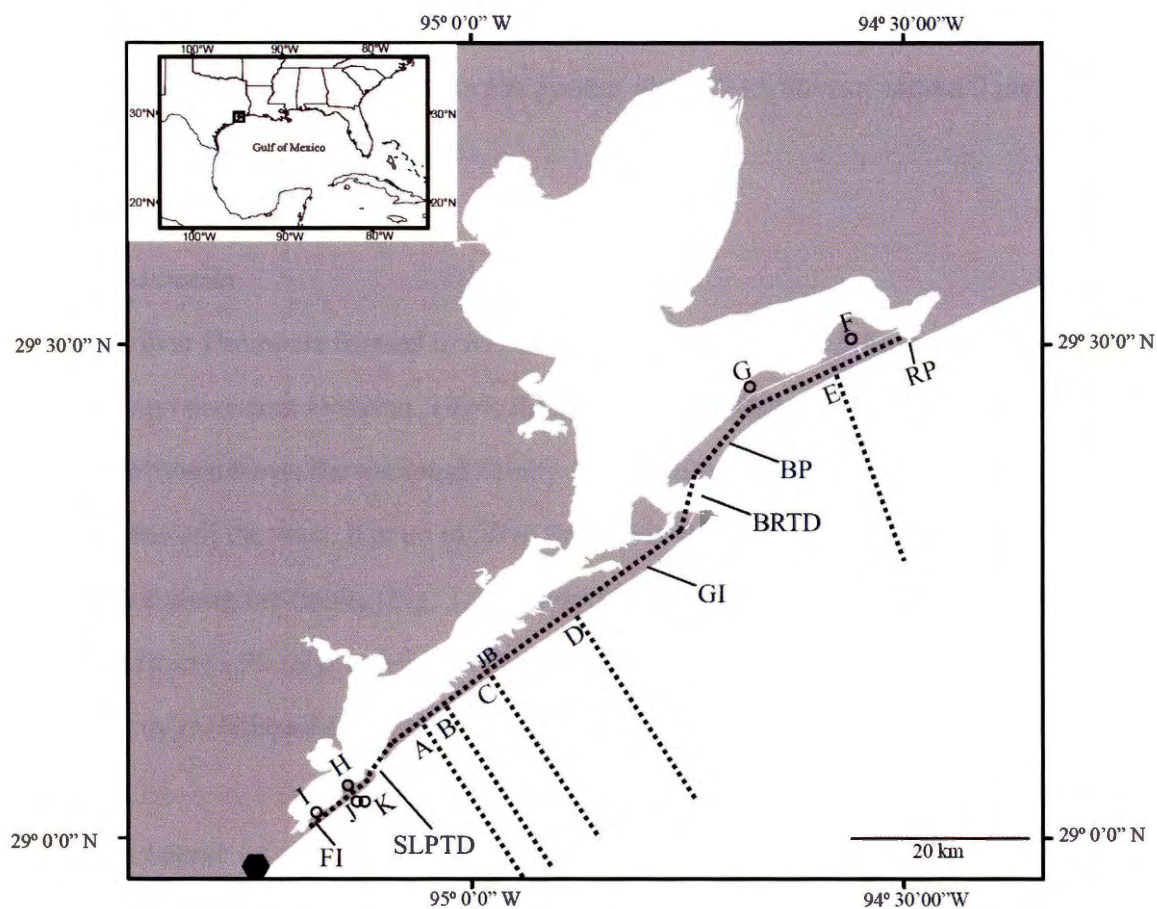


Figure 3-2: Map showing locations of core transects used for this study. Onshore and offshore core transects (dashed lines, letters A-E) and FI, back-barrier core transects (open circles, letters F-I) and nearshore cores (open circles, letters J and K) are shown. Black polygon represents the approximate location of Figure 3-7. RP= Rollover Pass, BP= Bolivar Peninsula, BRTD= Bolivar Roads Tidal Delta, GI= Galveston Island, JB=Jamaica Beach, SLPTD= San Luis Pass Tidal Delta, FI=Follets Island.

Along this section of coastline, a microtidal regime exists, as the tidal range is  $\sim 30$  cm. Average fair-weather wave heights for the system are  $\sim 1.0$  m, but can exceed 7 meters during tropical storms and hurricanes.

### *Bolivar Peninsula*

Bolivar Peninsula formed in its current location between 1,500 and 1,700 yr B.P. by westward spit accretion (Morton, 1994; Rodriguez et al., 2004). As Bolivar Peninsula migrated westward over the ancestral Trinity River incised valley, the barrier's thickness increased toward the west. It is up to 20 m thick over this valley, and ranges between 3 and 5 meters thick along the flanks (Fig. 3-3). Currently, Bolivar Peninsula's shoreline change rates vary from  $-1.95$  m/yr to  $+3.63$  m/yr, while the bayline is eroding at rates from  $-1.5$  m/yr to  $-3$  m/yr (Gibeaut et al., 2006).

### *Galveston Island*

Galveston Island is an elongate barrier, which began to form  $\sim 6,000$  yr B.P (Bernard et al., 1959; Morton, 1994; Rodriguez et al., 2004). Seaward progradation of the barrier island ended  $\sim 2,000$  years ago. Since that time it has been eroding. The island is younger towards the west, as the prevailing longshore currents deposit sand in this direction. It ranges in thickness from 12 m to 2 m from east to west (Fig. 3-3). Currently, Galveston Island's shoreline change rates vary from  $-1.70$  m/yr to  $+2.70$  m/yr, and between  $-0.35$  m/yr to  $-13.7$  m/yr for the bayline (Gibeaut et al., 2006). The island is currently drowning in place.

### *Follets Island*

Follets Island rests on  $\sim 3,000$  yr B.P. paleo Brazos River sediments (Bernard et al., 1970; Morton, 1994). This thin transgressive barrier ranges in sand thickness from  $\sim 1$ -4 m (Fig. 3-3), and the backside of the island is dominated by washover deposits.

Currently, Follets Island's shoreline change rates vary from stable to -3 m/yr, while the bayline varies from stable to +1 m/yr (Gibeaut et al., 2006). We consider this island to be in its "rollover phase", as the rate of shoreline retreat is roughly equal to the rate of landward bayline movement.

### *Tidal Deltas*

Two prominent tidal deltas exist along the upper Texas coast: Bolivar Roads Tidal Delta (BRTD) and San Luis Pass Tidal Delta (SLPTD) (Fig. 3-1; Fig. 3-3). The Bolivar Roads Tidal Delta system formed ~3,300 yr B.P. between the western end of Bolivar Peninsula and the eastern end of Galveston Island, and had both a prominent ebb and flood tidal delta before jetties were constructed in 1846 (Siringan and Anderson, 1993, 1994; Rodriguez et al., 1998). San Luis Pass Tidal Delta is a smaller delta between the west end of Galveston Island and the east end of Follets Island. SLPTD has both a prominent flood and ebb tidal delta (Israel et al., 1987). Today, BRTD is highly anthropogenically influenced by jetties and dredging, while SLPTD is almost entirely natural.

### *Transgressive Ravinement*

Along Galveston Island, shoreface sands extend on average 5 km offshore and rarely into more than 12 m water depth, where there is clear onlap of distal lower shoreface deposits by marine mud (Fig. 3-4). These shoreface sands date back to ~2,660 yr B.P., and rest atop Pleistocene aged sediments, indicating that the entire shoreface profile is migrating landward with the shoreline (Rodriguez et al., 2001). Thus, reworking of sand during transgression (transgressive ravinement) occurs to water depths up to ~12 m, within a distance of ~5 km from the Galveston Island shoreline (Siringan and Anderson, 1994; Rodriguez et al., 2001). On Bolivar Peninsula, shoreface sands are restricted to water depths up to 8 meters, or within 2.5 kilometers of the shoreline (Fig. 3-4).

Hence, the system is more sand deficient and transgressive ravinement occurs at shallower depths, mainly because of this sand deficiency (Rodriguez et al., 2001). On Follets Island, nearshore core data suggests the system is sand starved (Fig. 3-5), as the upper and lower shoreface contain only ~2 m and ~1 m of sand, respectively. Ravinement occurs to the Pleistocene surface (Fig. 3-3), which is more resistant to erosion than the softer Holocene sediment.

Transgressive ravinement has removed old fluvial channels, deltas and coastal deposits on the inner shelf. At the same time, cannibalization of these fluvial, tidal, and coastal deposits has yielded most of the sand that makes up the modern barriers of the upper Texas coast (Anderson et al., 2004).

### **3.2 Equilibrium Profile and Depth of Closure**

The equilibrium profile model describes a beach profile that is bounded seaward by the depth of closure, beyond which there is negligible sediment transport, although the existence of such a profile has been debated (Bruun, 1962; Swift, 1976; Pilkey et al., 1993; Thieler et al., 2000). As the shoreface and shoreline migrate, sand that is removed from the barrier can be deposited into the backbarrier environment by storm washover and/or offshore by storm return flow.

Previous studies in the Gulf of Mexico have determined that storms can transport sediment at velocities up to 200 cm/s out to the edge of the continental shelf (Hayes, 1967; Morton, 1981; Snedden et al., 1988; Pilkey et al., 1993). For the upper Texas coast, however, core data show no modern sand beds beyond ~12 m water depth (Siringan and Anderson, 1994; Rodriguez et al., 2001). The existence of upper and lower shoreface sands directly overlaying Pleistocene sediments also suggests that the toe of the shoreface migrates in accordance with the shoreline position (Fig. 3-4; Fig. 3-6).



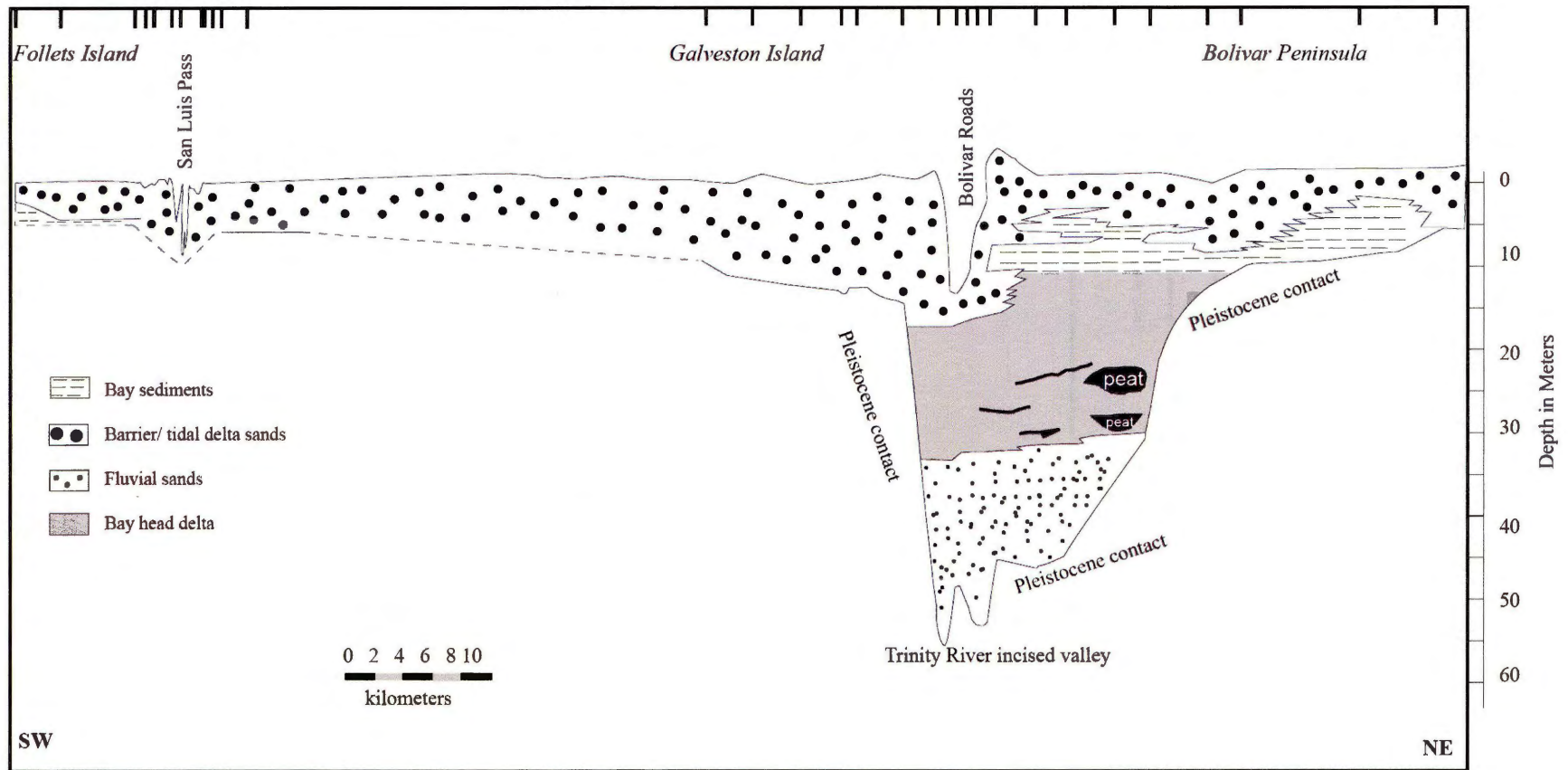


Figure 3-3: Coast-parallel cross section from Bolivar Peninsula to Follets Island (modified from Siringan and Anderson, 1993; Rodriguez et al., 1999; Anderson et al., 2008; Wallace et al., 2009). Note the thinning of sand from Galveston Island westward and on Bolivar Peninsula eastward, which is controlled by the antecedent topography of the Pleistocene surface, the most prominent feature being the ancestral Trinity River incised valley.



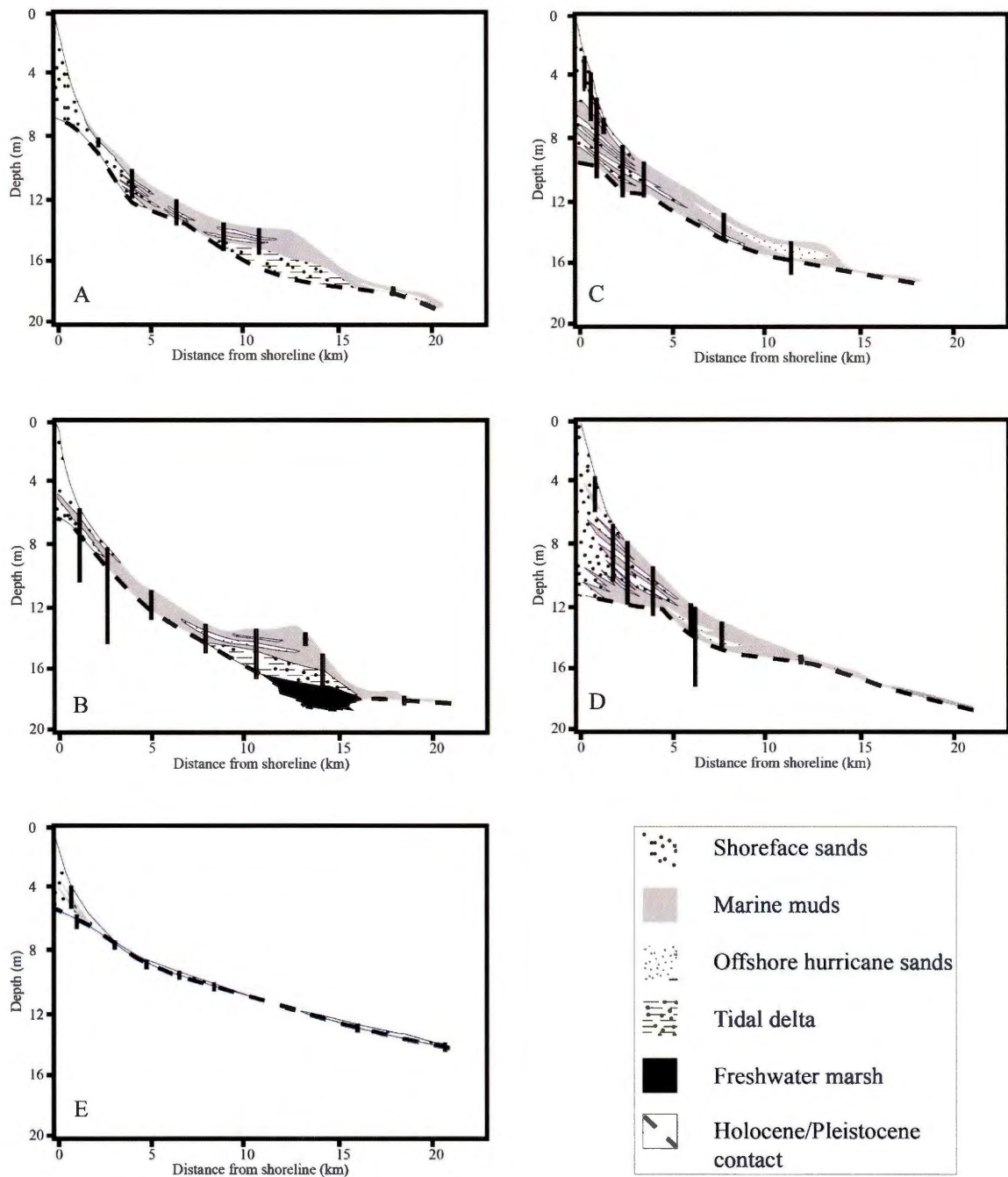


Figure 3-4: Core transects used to approximate sand volumes for the upper Texas coast (modified from Siringan and Anderson, 1993; Siringan and Anderson, 1994; Rodriguez et al., 2001) (see figure 3-2 for transect locations). A shoreface age of 2,660 yr B.P. is used, based on the maximum age of onlapping marine mud along the upper Texas coast (Rodriguez et al., 2001; Rodriguez et al., 2004). Vertical black lines represent core locations. Sand area between 4 and 8 meters is determined for each profile. These profiles are then extrapolated between core transects for each barrier, and a shoreface sand volume is estimated for each barrier island system.

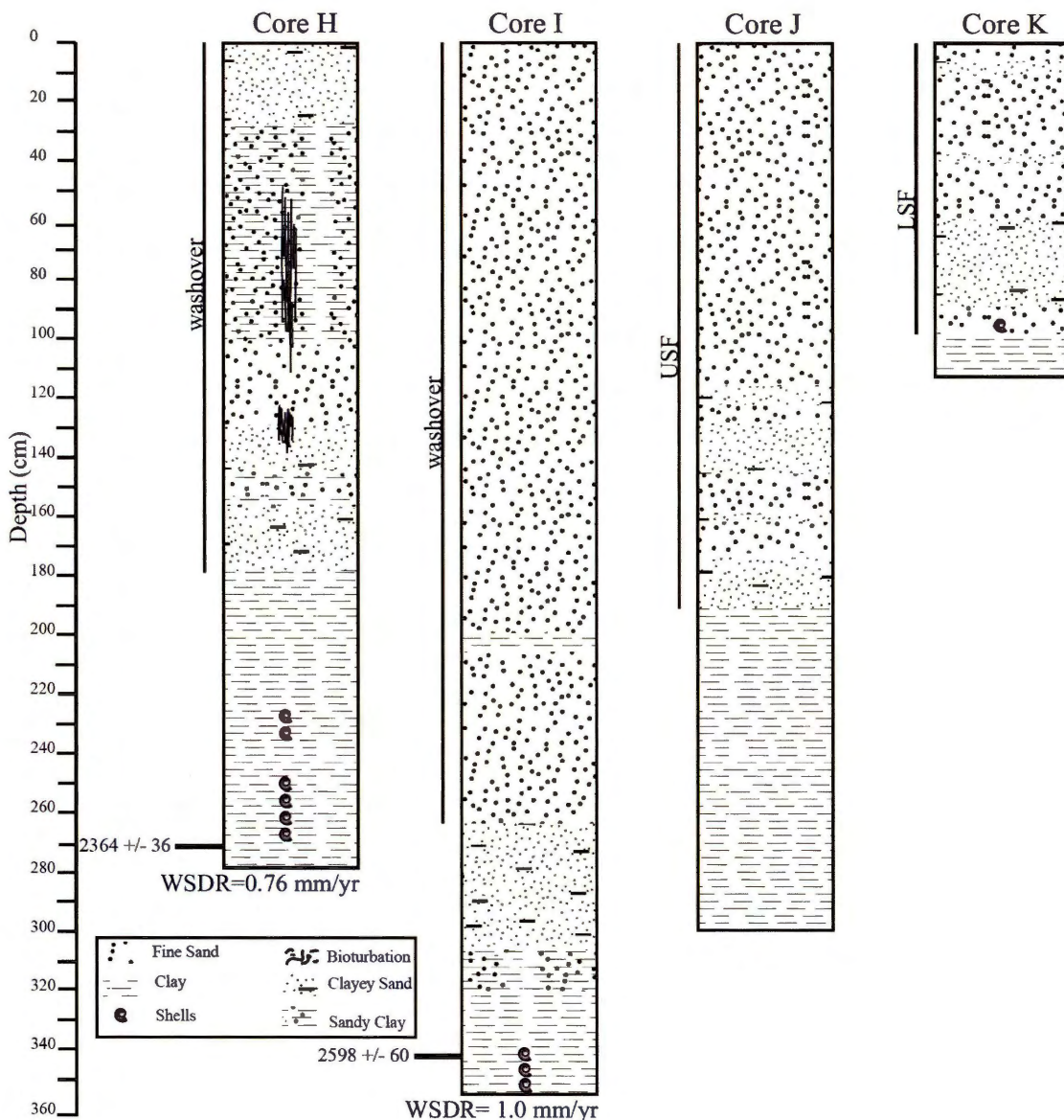


Figure 3-5: Lithologic descriptions and radiocarbon ages from core transects across Follets Island. Locations of cores shown in Figure 3-2. Radiocarbon ages are calibrated from radiocarbon to calendar years using the average one sigma ranges from Marine04 (Hughen et al., 2004). Cores H and I represent hurricane washover sands, and cores J and K represent upper shoreface (USF) and lower shoreface (LSF), respectively. Note the minimal washover sand deposition rates (WSDR) for approximately the past 3,000 years ( $\sim$ 0.76-1.0 mm/yr) in cores H and I. There is also minimal sand present in the upper and lower shoreface, suggesting it is likely being eroded and transported further west. The clay at the bottom of each core is fluvial sediment from the Bastrop channel, described by Bernard et al. (1970).

The process of storm overwash transports sand from offshore, shoreface, and barrier environments into the backbarrier environment. Evidence of past storm deposition is seen on the backsides of Bolivar Peninsula, Galveston Island, and Follets Island as washover fans (Fig. 3-2- Cores F, G, H, and I). Washover fans generally form when barrier islands are narrow, thin, and can easily be overtopped. A recent study showed that the intense hurricane landfall probability for the Gulf coast over the late Holocene is  $\sim 0.46\%$  for south Texas, and the current rate does not seem unprecedented (Wallace and Anderson, 2010). However, little is known about the long-term storm sand fluxes associated with each barrier island along the upper Texas coast.

Measuring the change in sand volumes for any length of beach is the product of shoreline change ( $\Delta s$ ), and the depth of the active beach sediment transport from an equilibrium profile (i.e. the sum of the berm height,  $D_b$ , and the depth of closure,  $D_c$ ) (Dean and Dalrymple, 2002; Ravens and Sitanggang, 2007). Both shoreline change and the berm height are well established from beach profile data, aerial photography, and satellite images (Gibeaut et al., 2006; Ravens and Sitanggang, 2007). The depth of closure, however, is highly controversial. Morang, (2006) and Ravens and Sitanggang, (2007) both use a  $D_c$  value of 4 m, based on negligible changes in before and after bathymetric profiles (i.e.  $< 1$  m). Beumel and Beachler, (1994) calculated a depth of closure for Galveston Island of  $\sim 5$  m. Numerous studies based on seismic, core, and bathymetric data indicate that a  $D_c$  value of at least  $\sim 8$  m would be more appropriate along the upper Texas coast (Siringan and Anderson, 1994; Rodriguez et al., 2001; Anderson et al., 2004). There are several lines of evidence that point to this deeper value. First, the physiographic toe of the shoreface, the defining geological factor in determining the  $D_c$ , is at least 8 m deep (Fig. 3-4; Fig. 3-6). Second, historical bathymetric profiles show that the relief of the shoreface undergoes continuous change to water depths of between 8 and 12 meters (Rodriguez et al., 2001), so sediment transport is active to at least these water depths.

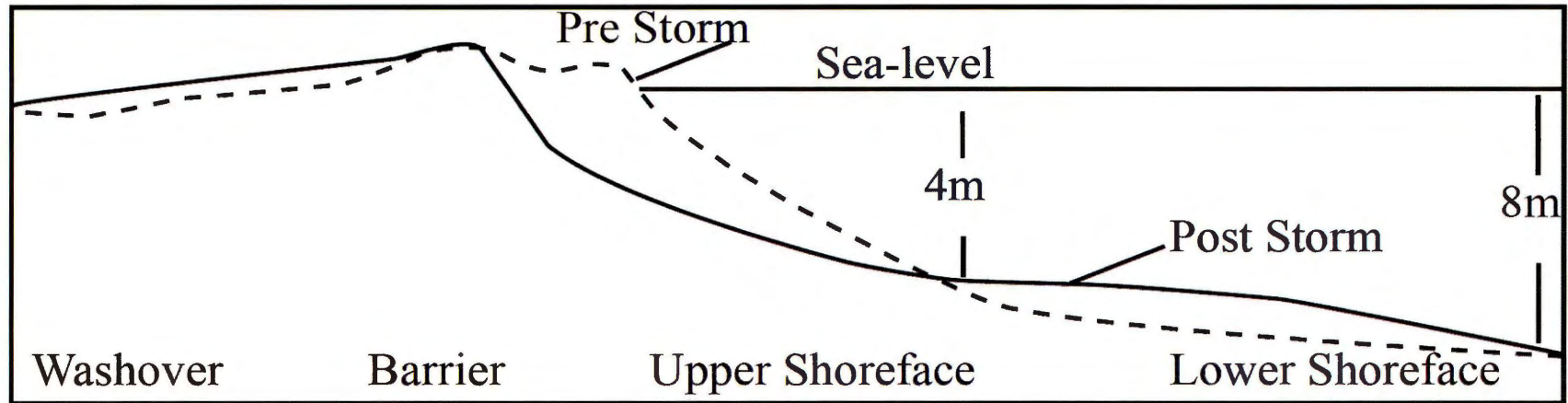


Figure 3-6: Equilibrium profile model for the upper Texas coast (modified from Bruun, 1962; Swift, 1976; Pilkey et al., 1993). The dashed line represents the pre-storm cross-sectional profile, while the solid line represents the post storm cross-sectional profile. Recent sand budgets for the upper Texas coast only consider sediment within 4 meters water depth to be part of the active coastal system (i.e. depth of closure). However, geological studies suggest that a depth of at least 8 meters would be more appropriate (Siringan and Anderson, 1994; Rodriguez et al., 2001; Anderson et al., 2004).



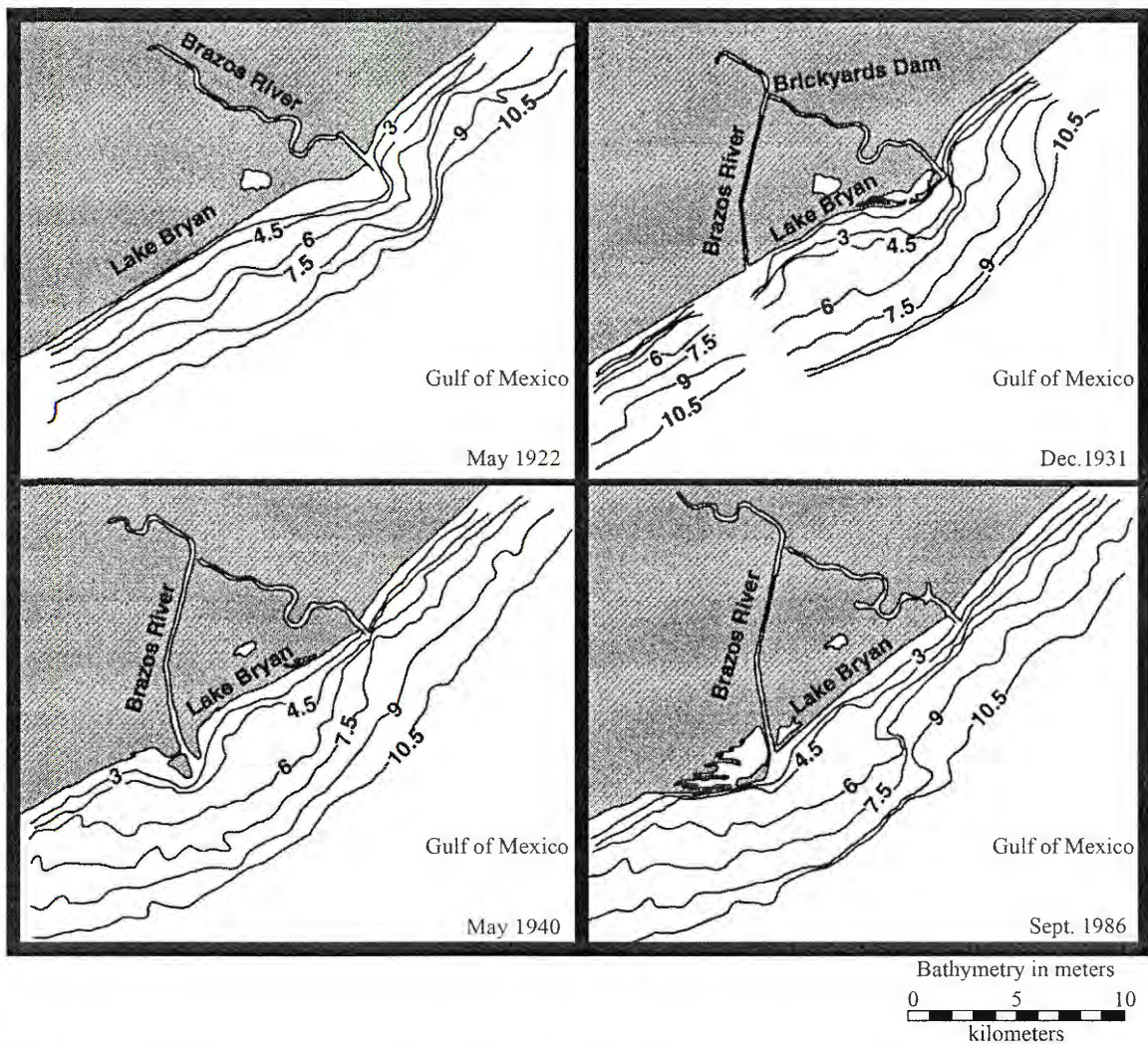


Figure 3-7: Bathymetric maps of the Brazos delta showing changes in the location of the delta from 1922 to 1986 (National Oceanic and Atmospheric Administration (NOAA) nautical chart number 1283) (modified from Rodriguez et al., 2000). Approximate location shown in Figure 3-2. The Brazos River was diverted in 1929 and the old delta was quickly eroded. Note that erosion of the old delta occurred at depths of at least 10.5 meters.

Lastly, the fact that transgressive ravinement occurs at these deeper water depths indicates sand transport during storms and hurricanes is a common process.

The best example of transgressive ravinement at depths well below 4 m is the erosion of the pre-1929 Brazos Delta. Prior to 1929, there was a prominent delta located at Surfside, Texas that extended ~5 km offshore into at least 10.5 m of water (Fig. 3-7). After the Brazos River diversion in 1929, the delta eroded within a matter of a few decades. Most of the sand that was eroded from the old delta was transported westward and accreted to a new delta that formed at the new river mouth within a few decades (Rodriguez et al., 2000) (Fig. 3-7). This example illustrates that wave erosion and redistribution of sand occurs to water depths well below 4 m, and over timescales relevant to coastal nourishment projects. Therefore, we suggest using a  $D_c$  value of at least 8 m to accurately portray the depths of sediment transport. The Brazos Delta example provides a stark reminder that ravinement associated with the  $D_c$  is a very efficient process, and should be taken into account for any sediment budget analyses.

### **3.3 Assessing the Sand Budget Approach**

Several previous studies attempt to develop a sediment and/or sand budget for the upper Texas coast. Ravens and Sitanggang (2007) use a numerical modeling approach to understand and develop a strategy to combat coastal erosion along Galveston Island. This study incorporates shoreline change data with the GENESIS model to determine that approximately 100,000 m<sup>3</sup>/yr of sand might be needed to maintain the 2001 shoreline on Galveston Island, and ~300,000 m<sup>3</sup>/yr would be needed to nourish the more depleted West Beach. A recent US Army Corps of Engineers study (Morang, 2006) develops a sediment budget for the upper Texas coast from the Texas/Louisiana border to SLPTD. This study relies on bathymetric profiles, sediment grab samples, dredging records, aerial photographs, and elevation data.

These studies provide two independent approaches for establishing a sediment budget for the upper Texas coast. However, neither study incorporates data beyond 4 m water depth. Furthermore, neither study incorporates known sand contributions from storm impacts nor potential sources from reworking of sediment. Quantifying these previously overlooked components would provide the necessary information to accurately quantify a sediment budget for the entire system and determine the volume needed for nourishment purposes.

## **Methodology**

Since sand-sized material is the most relevant to coastal nourishment scenarios, we focus the discussion on this size fraction. Currently, new sand delivery from fluvial systems to the upper Texas coast is minimal (Morton et al., 1995; Anderson, 2007). Therefore, it is critical to examine all available potential sources and sinks. The volume of sand within part of the coastal system (i.e. barrier proper, littoral drift, and fluvial sediment supply) for Bolivar Peninsula, Galveston Island, and Follets Island is established by previous studies (Morang, 2006; Ravens and Sitanggang, 2007). From core data, we determine the previously unaccounted volume of sand within the active coastal system (i.e. between 4 and 8 meters water depth) (Rodriguez et al., 2001). The volumes are accurately estimated based on previously collected offshore profiles coupled with calibrated radiocarbon dates (Siringan and Anderson, 1994; Rodriguez et al., 2004) (Fig. 3-4). Radiocarbon ages are calibrated from radiocarbon to calendar years using the average one sigma ranges from Marine04 (Hughen et al., 2004). The upper Texas coast has a ~400 yr radiocarbon reservoir (Milliken et al., 2008a), which is the built-in reservoir used in Marine04. Additionally, the storm sand flux is examined from sediment core data (Fig. 3-2; Fig. 3-4; Fig. 3-5) both over historic and geologic time.

### 3.4 Results

The volume of sand sequestered within the shoreface environment is accurately estimated from core transects (Fig. 3-2; Fig. 3-4; Fig. 3-5). First, the sand area between 4 and 8 meters is determined for each profile. Next, these profiles are extrapolated between core transects for each barrier, and a shoreface sand volume is estimated for each system. Based on the spatial distribution of core transects (Fig. 3-2), this method yields a robust estimation of shoreface sand sequestration. From Rollover Pass to Follets Island (Fig. 3-2), the upper and lower shoreface contains an estimated 426 million m<sup>3</sup> of sand between 4 and 8 meters. For Bolivar Peninsula and Galveston Island, the volume is then time averaged by 2,660 yr B.P., the age of the shoreface deposits, based on the age of onlapping marine mud and the average age of barrier island deposits for the upper Texas coast (Rodriguez et al., 2001; Rodriguez et al., 2004), while the Follets Island shoreface sand volume is averaged by ~3,000 yr B.P. (Bernard et al., 1970; Morton, 1994) to arrive at a total flux of ~160,000 m<sup>3</sup>/yr. Additionally, the error is calculated to be  $\pm$  one standard deviation from the average area of Galveston Island profiles. Additionally, the percentage of the total of this standard deviation (24%) is used to estimate error for all other shoreface profiles (i.e. Bolivar Peninsula and Follets Island).

#### Bolivar Peninsula

The sand volume is determined within the shoreface from Rollover Pass to the west end of Bolivar Peninsula (Fig. 3-2) to be approximately 109,000,000 m<sup>3</sup>. The shoreface sand is only ~6 m thick here, as the underlying Pleistocene topography is shallow in this location (Fig. 3-4). The time averaged sand flux to the Bolivar Peninsula shoreface is thus determined to be  $\sim 41,000 \pm 10,000$  m<sup>3</sup>/yr (Fig. 3-8).



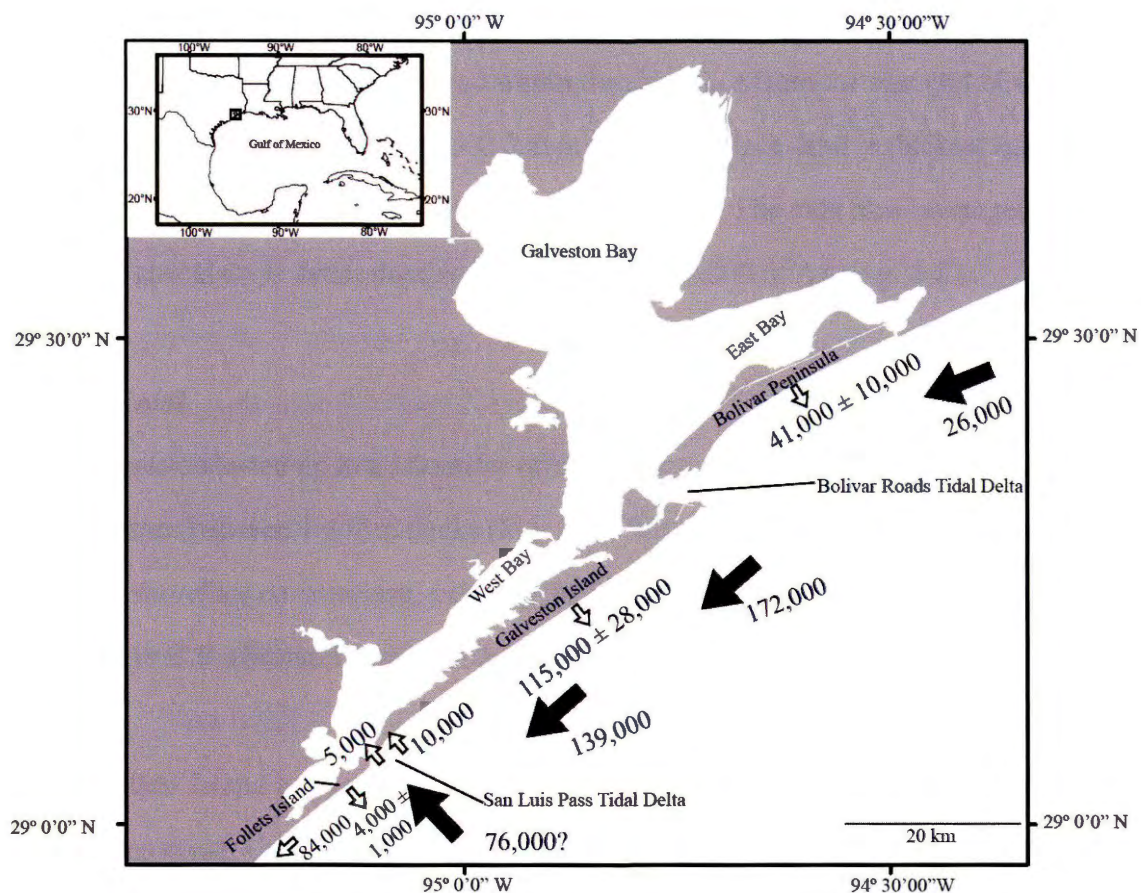


Figure 3-8 Previous longshore transport data (solid arrows- from Morang, 2006) with new data (hollow arrows) for the annual flux of sand to between 4 and 8 m water depth (arrows pointing offshore), into San Luis Pass tidal delta, and further west ( $84,000 \text{ m}^3/\text{yr}$ ). Note that the estimated shoreface flux is equal to  $\sim 17\%$  of the entire calculated sediment flux and  $\sim 40\%$  of the total longshore flux for the upper Texas coast from previous studies (Morang, 2006).

## **Galveston Island**

The sand volume is determined within the shoreface from the east end of Galveston Island to San Luis Pass to be  $\sim 306,000,000 \text{ m}^3$ . The shoreface sand is thickest near the east end ( $\sim 12 \text{ m}$ ), and thins toward the west ( $\sim 8 \text{ m}$ ) (Fig. 3-4). The total time- averaged sand flux to the shoreface is determined to be  $\sim 115,000 \pm 28,000 \text{ m}^3/\text{yr}$  (Fig. 3-8).

## **Follets Island**

Cores collected up to a kilometer offshore show minimal sand in the shoreface of Follets Island (between 1-1.7 m thick) (Fig. 3-5). We estimate  $\sim 11,000,000 \text{ m}^3$  stored within the shoreface environment, meaning the flux is  $\sim 4,000 \pm 1000 \text{ m}^3/\text{yr}$  based on an age of  $\sim 3,000 \text{ yr B.P.}$  (Bernard et al., 1970; Morton, 1994) (Fig. 3-8).

Follets Island has yet to be incorporated into any previous sediment budgets for the upper Texas coast. Using an erosion rate of  $\sim 3 \text{ m/yr}$  for roughly 10 km of shoreline (Gibeaut et al., 2006) averaging 3 m thick (Morton, 1994), we determine an annual sand flux of  $\sim 90,000 \text{ m}^3/\text{yr}$ .

## **San Luis Pass**

Previous studies suggest that the sand flux into the flood tidal delta of the SLPTD is at least  $76,000 \text{ m}^3/\text{yr}$  (Morang, 2006). This number is determined based on the residual flux needed to close the budget from further east. A prior study by Israel et al. (1987) uses an extensive collection of sediment cores to map proximal and distal facies and stratigraphic relationships of the SLPTD. Based on this work, we derive an approximate volume of  $9,000,000 \text{ m}^3$  of sand within the flood tidal delta of San Luis Pass.

This volume is time averaged by the age of when most of the sediments were deposited into San Luis Pass (between  $\sim 2,100$  yr B.P.- 200 yr ago), which yields an annual sand flux of  $\sim 5,000 \text{ m}^3/\text{yr}$ . (Fig. 3-8), which is more than an order of magnitude lower than previous estimates (Morang, 2006). From core data, along with historical charts, we estimate that  $\sim 2,000,000 \text{ m}^3$  of sand has been stored along the far west end of Galveston Island due to the infilling of the San Luis Pass over the past 200 years (Bernard et al., 1970), equaling an average sand flux rate of  $\sim 10,000 \text{ m}^3/\text{yr}$  to the far west end of Galveston Island (Fig. 3-8).

### **Bolivar Roads Flood Tidal Delta**

The sand flux for BRTD is measured from annual dredging records. Both the north and south jetties on the west end of Bolivar Peninsula and the east end of Galveston Island, respectively, have accumulated a significant volume of sand since they were constructed. Morang, (2006) suggest that the sand flux for this system equals  $\sim 389,000 \text{ m}^3/\text{yr}$ , of which  $\sim 189,400 \text{ m}^3/\text{yr}$  ( $172,400 \text{ m}^3/\text{yr} + 17,000 \text{ m}^3/\text{yr}$ ) can be attributed to longshore transport from further to the east and west (Fig. 3-1). Morang, (2006) suggest that since the dominant longshore transport direction is from northeast to southwest, sand is transported and deposited directly adjacent to the north jetty (far west end of Bolivar Peninsula). During winter months and approaching fronts, the dominant longshore transport direction switches to northeast, and thus some sand also accumulates directly against the south jetty (far east end of Galveston Island) (Morang, 2006). Since they are porous, the author suggests that sand moves through the jetties into the channel. However, this estimate does not take into account the large volume of sand sequestered in both the ebb and flood tidal deltas prior to jetty construction (Morton, 1977; Siringan and Anderson, 1993). Morton, (1977) suggests a flux of  $\sim 470,000 \text{ m}^3/\text{yr}$  on both Bolivar Peninsula and Galveston Island from 1867-1974 that could be attributed directly to destruction and reworking of the Bolivar Roads ebb tidal delta.

Therefore, it is likely that the sediment source reported by Morang, (2006) to the western end of Bolivar Peninsula and the eastern end of Galveston Island could likely be the cannibalization of the natural BRTD after jetty construction, with only minimal input from longshore transport.

### **Washover Sands**

Over historical time, Light Detection and Ranging (LIDAR) is used to measure the elevation of subaerial land to within decimeters. Coupled with core data, comparing pre and post hurricane LIDAR data is the most accurate way of understanding the sand fluxes associated with storms. When both pre and post storm LIDAR data for Bolivar Peninsula and Galveston is compared, it is clear that sand is transported only a few hundred meters landward of the shoreline, so washover into East Bay is minimal (United States Geological Survey, 2009).

Wallace et al., (2009) suggest that hurricane washover accumulation rates are  $\sim 0.4$  m/100 yr for Galveston Island, and vary from 0.154 m/100 yr to 0.095 m/100 yr for Bolivar Peninsula (using radiocarbon data from Rodriguez et al., 2004). Recently collected core data on the backside of Follets Island suggest washover rates of  $\sim 0.1$  m/100 yr (Fig. 3-2; Fig. 3-5). Therefore, from both core and LIDAR data, we conclude that the majority of washover sands in East, West, and Christmas Bays (Fig. 3-1) accumulated earlier in the histories of the three barriers, when they were significantly lower and narrower, and that current rates of washover are minimal. These low accumulation rates are consistent with results from south Texas (Wallace and Anderson, 2010).

Rodriguez et al., (2004) determine that beach ridges extending from the east end of Galveston Island to approximately the location of Jamaica beach (Fig. 3-2) formed  $\sim 1,800$  yrs B.P. based on radiocarbon ages.

The continuity of these ridges along much of the coast suggest that hurricane sand transport from the island into West Bay has been minimal throughout modern times.

The washover sand fluxes are quantified first by estimating the area from satellite imagery, then calculating a volume based on known sand thicknesses from cores (Fig. 3-2), and finally using the age of the deposits to derive a time averaged flux (Rodriguez et al., 2004). On Bolivar Peninsula, washover deposit F (Fig. 3-2) formed  $\sim 1,800$  yr B.P., and washover deposit G (Fig. 3-2) formed  $\sim 2,800$  yr B.P. Rodriguez et al., (2004) suggest that these features likely have not been active since  $\sim 700$  yr B.P, based on the continuity of beach ridges of this age and younger on the peninsula. Therefore, the sand flux for washover F was  $\sim 23,000 \text{ m}^3/\text{yr}$  ( $2,300,000 \text{ m}^3/100 \text{ yr}$ ), and  $\sim 3,000 \text{ m}^3/\text{yr}$  ( $300,000 \text{ m}^3/100 \text{ yr}$ ) for washover G from the time they both respectively formed until  $\sim 700$  yr B.P.

On Follets Island, there are no preserved beach ridges, suggesting that during storms, the island is frequently overtopped and the washover fans on the backside of the island have recently been active. Washover H formed  $\sim 2,400$  yrs B.P., meaning the washover sand flux is  $\sim 300 \text{ m}^3/\text{yr}$  ( $30,000 \text{ m}^3/100 \text{ yr}$ ). Washover I formed  $\sim 2,600$  yrs B.P., and the sand flux in this location is  $\sim 2,000 \text{ m}^3/\text{yr}$  ( $200,000 \text{ m}^3/100 \text{ yr}$ ). It appears as though bayline stability on Follets Island is the result of organic marsh accretion and not washover sand deposition. Thus, while washover was an important means of removing sand from these barriers during their early evolution, this process can be considered negligible for sand budget purposes.

### 3.5 Discussion

By incorporating both hurricane overwash and shoreface sand sinks into previous sand budget studies for the upper Texas coast, a more accurate sand and sediment budget is established. We show that the shoreface environment from the east end of Bolivar Peninsula to the west end of Galveston Island sequesters  $\sim 156,000 \pm 38,000 \text{ m}^3/\text{yr}$  of sand. This represents  $\sim 17\%$  of the entire calculated sediment flux onshore, longshore, and offshore from previous studies. Additionally, this flux equals  $\sim 40\%$  of the previously calculated longshore transport flux for the entire region. Most of the error in prior budget analyses stems from using a 4-meter depth of closure, which geological evidence indicates is half the depth of active sediment transport in the region.

Previous sediment budgets have yet to concretely establish the sand flux into SLPTD, and to incorporate Follets Island. The flux of SLPTD was previously thought to be at least  $76,000 \text{ m}^3/\text{yr}$  (Morang, 2006). However, our data suggest a flux of  $\sim 5,000 \text{ m}^3/\text{yr}$  is more reasonable. For Follets Island, it appears as though a unique scenario is taking place. A sand flux of  $\sim 90,000 \text{ m}^3/\text{yr}$  is determined based on current erosion rates. However, only  $\sim 6,000 \text{ m}^3/\text{yr}$  is being sequestered in both the shoreface and washover environments (Fig. 3-8), and there have been no notable elevation changes on the barrier itself. Therefore, since Follets Island is currently sand starved, longshore transport is likely removing and transporting  $\sim 84,000 \text{ m}^3/\text{yr}$  of sand further west (Fig. 3-8).

The magnitude of this volume shows that the current estimates of longshore sand transport west of SLPTD (Morang, 2006) are significantly underestimated, and highlights the importance of taking all possible sand sequestration environments into account for sediment budgets.

### 3.6 Conclusions

Several studies rely on engineering principles to establish sand budget estimations for the upper Texas coast (Morang, 2006; Ravens and Sitanggang, 2007). They determine that the majority of sand is either deposited along jetties and beaches, or erodes and is transported west with the prevailing longshore currents. These studies estimate the total sand flux along the upper Texas coast to be  $\sim 820,000,000 \text{ m}^3/\text{yr}$  (Morang, 2006), and that nourishing the seawall and West Beach along Galveston Island would likely require  $\sim 400,000 \text{ m}^3/\text{yr}$  to maintain the 2001 shoreline (Ravens and Sitanggang, 2007). However, these studies use a closure depth of 4 m, when a depth of at least 8 m is more appropriate based on many lines of geological evidence. Incorporating this new shoreface sand volume equals  $\sim 17\%$  of the entire previously estimated sediment flux, and  $\sim 40\%$  of the previously calculated total longshore flux (using previous estimates from Morang, 2006). Additionally, extending the closure depth to a more geologically reasonable depth increases the volume needed to successfully nourish beaches on Galveston Island by at least  $\sim 115,000 \pm 28,000 \text{ m}^3/\text{yr}$ .

We also show that the modern washover sand flux into the bays behind Bolivar Peninsula, Galveston Island, and Follets Island is quite minimal, and thus not a significant annual contributor to sand sequestration. We determine a sand flux for San Luis Pass that is an order of magnitude lower than previous estimates (Morang, 2006). Consequently, longshore sand transport from the west end of Galveston Island past SLPTD is significantly underestimated. This translates into significant errors in the estimates of sand needed for coastal nourishment projects.

## CHAPTER 4

### **Evidence of similar probability of intense hurricane strikes for the Gulf of Mexico over the late Holocene<sup>3</sup>**

#### **4.0 Abstract**

Hurricane magnitude and landfall probability has been linked to numerous mechanisms, including the steady rise in annual sea surface temperatures, ENSO variations, and atmospheric changes. In order to better understand those factors that control hurricane magnitude and landfall probability, a long-term record spanning the entire Gulf coast is needed. Here, we present a detailed record from ~5,300–900 yr B.P. of past intense hurricane impacts for cores collected from Laguna Madre, TX. Relative storm intensities were calculated for each event, and the average intense storm impact probability for south Texas was determined to be ~.46% (annual landfall probability). Previous field studies in Western Lake, FL, and Lake Shelby, AL, reveal similar probability intense hurricane strikes of ~.39%. Although high frequency oscillations between warm, dry and cool, wet climate conditions have occurred in Texas through the late Holocene, there has been no notable variation in intense storm impacts across the northwestern Gulf Coast during this time interval implying no direct linkage between these changing climate conditions and annual hurricane impact probability. In addition, there have been no significant differences in the landfall probabilities of storms between the eastern and western Gulf during the late Holocene, suggesting storm steering mechanisms have not varied during this time.

---

<sup>3</sup> This chapter has been edited, reformatted, and reprinted with permission: Wallace, D.J., and Anderson, J.B., 2010, Evidence of similar probability of intense hurricane strikes for the Gulf of Mexico over the late Holocene, *Geology*, (in press).



## 4.1 Introduction

Several studies have attempted to study tropical storm frequency and magnitude trends from storm overwash sediment records (Liu and Fearn, 1993; Liu and Fearn, 2000a; Liu and Fearn, 2000b; Donnelly, et al. 2001a; Donnelly, et al. 2001b; Donnelly, et al. 2004; Donnelly and Woodruff, 2007; Woodruff et al., 2008; Mann et al., 2009; Appendix A). Although these studies have provided valuable data for the Atlantic Ocean and eastern Gulf of Mexico (Florida and Alabama), none has targeted the northwestern Gulf of Mexico. In Texas, Laguna Madre (LM) (Fig. 4-1) was assumed to be the most ideal location for paleotempestological studies, as it is an elongate water body sitting behind the narrow, low-elevation barrier (<2 m) of South Padre Island (SPI) (Fig. 4-1). We consider our record to be directly comparable to other paleotempestological studies because all are thought to record intense hurricane activity. This extreme western location was also selected in order to quantify phase relationships between intense hurricanes impacts between the eastern and western Gulf of Mexico. Additionally, extensive Texas climate records (Appendix A) allow relationships between high frequency climate cycles and intense storm impacts to be determined.

Of the hurricanes in which the eye passed directly over SPI during historic time (1854–2009), only Hurricane Allen has been classified as a category three or higher storm (Blake et al., 2007) (~.65% annual landfall probability). Modern intense storm impacts for Lake Shelby, AL, are estimated to be ~.3% (Elsner et al., 2008a), while no category four or higher storms have impacted Western Lake, FL, during historic times (Liu and Fearn, 2000a).

Subsidence of the Rio Grande Delta plain (Fig. 4-1) likely was especially rapid ~5,000 yr B.P., resulting in the formation of LM (Morton, 1994) and locally creating ample accommodation space for preservation of storm washover deposits.

During the late Holocene, the Rio Grande Delta became inundated and reworked: SPI began forming. It is a narrow and thin transgressive barrier, with average widths and height of 3.8 km and 3.75 m, respectively (Morton and McGowen, 1980; Morton and Price, 1987).

Today, because of a restricted tidal exchange, astronomical tides are extremely low in LM (~30 cm) (Rusnak, 1960). Our data suggest that SPI has been relatively stable for at least the last several millennia.

## **4.2 Methods for Identifying Paleohurricanes**

A total of thirty-seven sediment cores were collected along eight transects within LM (Fig. 4-1). Within intervals where radiocarbon dates were taken (Fig. 4-2; Appendix A), grain size analyses were performed every 1 cm. Samples were taken every 5 cm in sections where no radiocarbon dates were taken. These latter intervals also coincided with environments not interpreted to be washover clay couplets. Although a radiocarbon reservoir has been found along some of the bays in Texas (Milliken et al., 2008a), the extremely limited exchange between LM, fluvial systems, and the Gulf of Mexico suggests a negligible effect in LM.

## **4.3 Results**

Not all of the cores yielded a record of storm landfall probability, due mainly to bioturbation. Our initial sampling strategy (core transects) assumed that some cores would be located too close to the barrier, therefore sampling amalgamated storm deposits, others would be too distal to sample storm deposits, and not every transect would occur where there was adequate accommodation for deposition and preservation of washover deposits. However, four cores from two transects yielded a distinct record and enough carbonate material for radiocarbon age dating to constrain the timing of hurricane overwash.

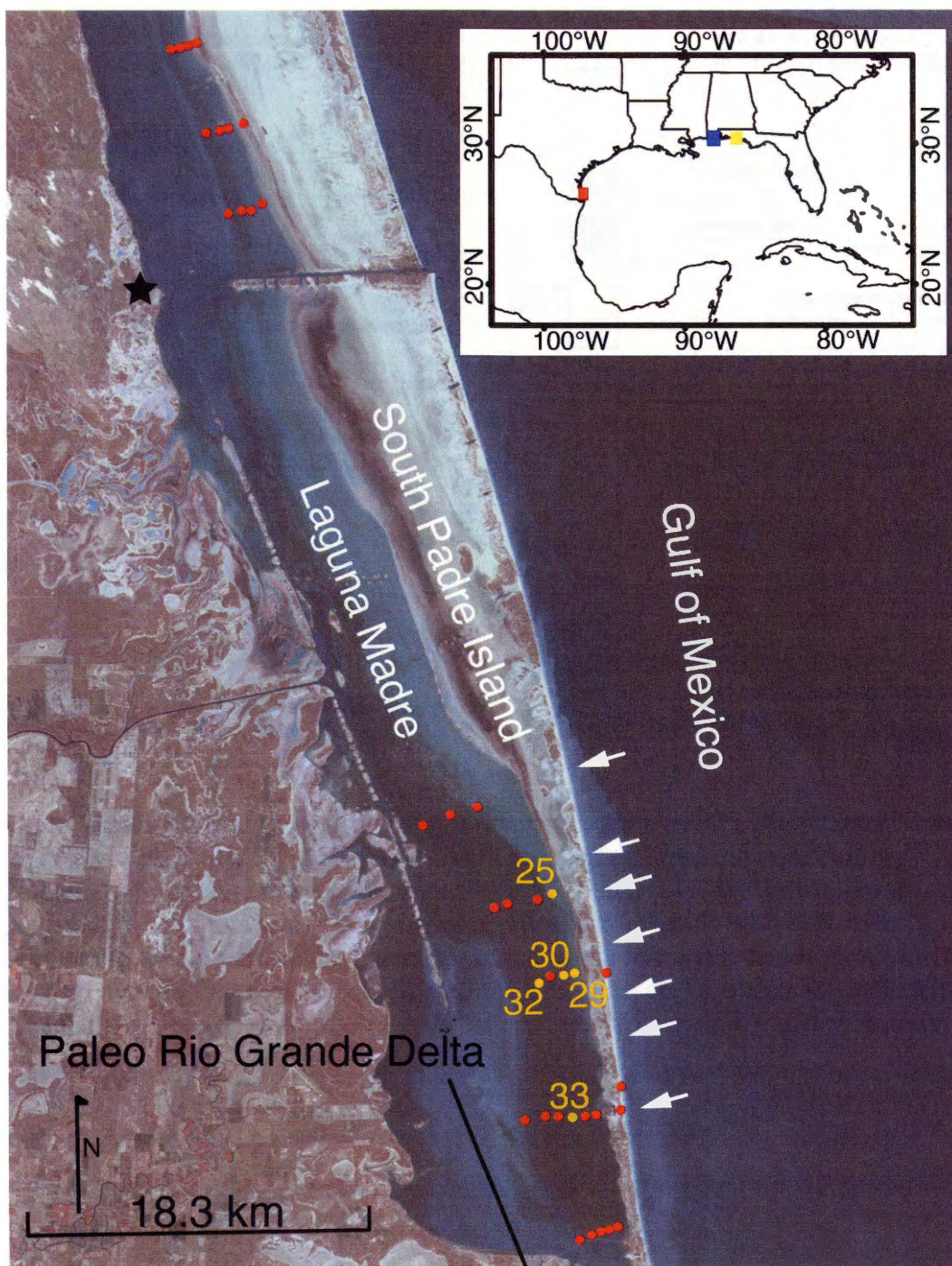


Figure 4-1: Study area and core locations. Map of Laguna Madre (LM), TX (base map from USGS National Map viewer <<http://nmviewogc.cr.usgs.gov/viewer.htm>>). Core locations represented by red dots (all cores collected) and yellow dots (cores used for this study). Inset map indicates this study (LM) (red box), and previous studies in Lake Shelby, Alabama (Liu and Fearn, 1993) (blue box) and Western Lake, FL (Liu and Fearn, 2000a) (yellow box). Note the extensive breaching and overwash features, indicated by white arrows on South Padre Island (SPI). Port Mansfield, where Hurricane Allen's surge was measured in 1980, is identified by black star.



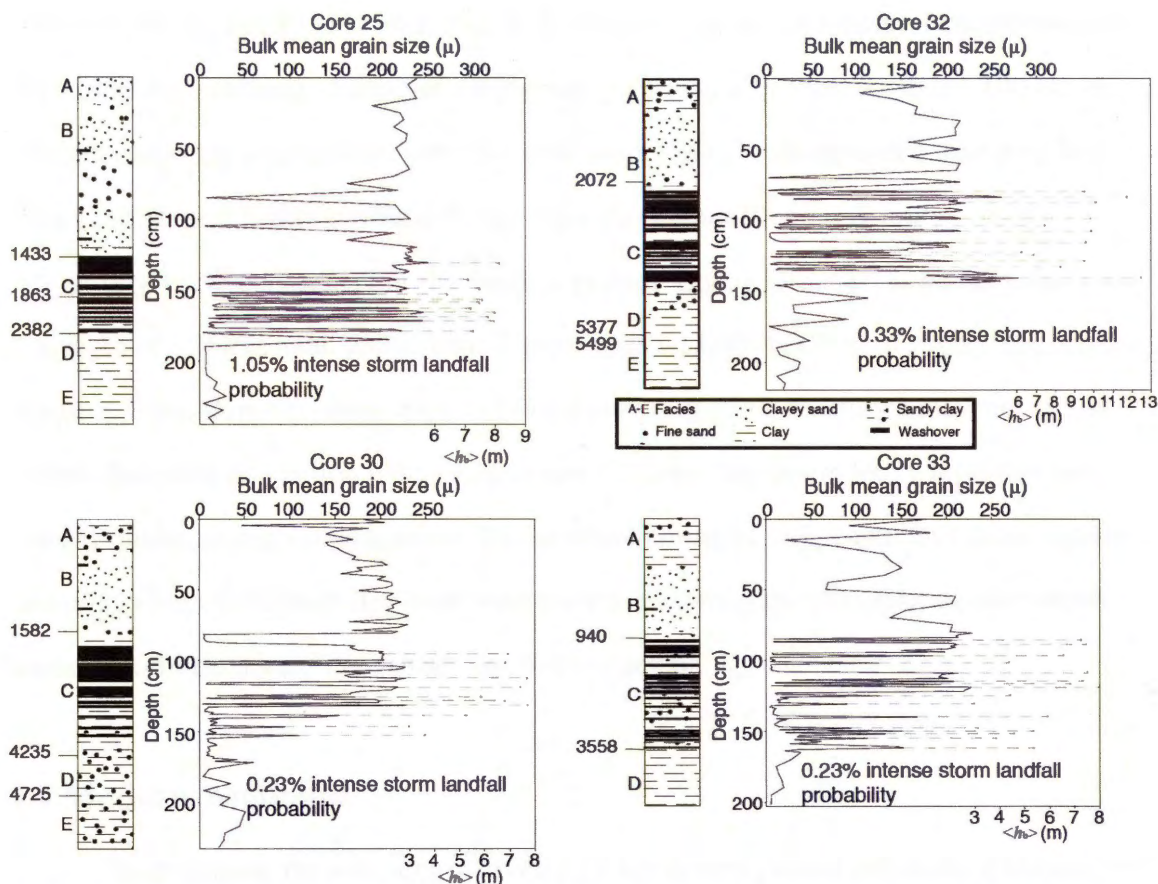


Figure 4-2: Grain size and relative storm intensities for cores 25, 30, 32, and 33 from Laguna Madre (LM), TX. Lithologies, bulk mean grain size, and predicted  $\langle h_b \rangle$  (Appendix A) values (dashed lines) are plotted for each core. Washover deposits are indicated by solid black in lithologic description, and coincide with bulk mean grain size increases. Facies identified by letters to the left of the lithologic description. Age intervals are calibrated radiocarbon dates from mollusc shells within bay sediments (Appendix A). Note the similar probabilities of intense hurricane impacts between cores.

Cores 25, 30, 32, and 33 (Fig. 4-1; Fig. 4-2) sampled ~20 cm of organic-rich, bioturbated clays (unit A), overlying ~60 cm of clayey sand or sandy clay (unit B), then ~100 cm of light gray bay clay interbedded with fine sand units (unit C), all deposited over gray bay clays (unit D) and highly oxidized fluvial plain clays (unit E). Unit A represents the biologically active component of the modern system. Living infauna and plants were found to a depth of ~20 cm in all cores. Unit B represents ~1,000–1,500 yr of highly bioturbated deposits. Other than hurricane impacts (overwash processes), no known mechanism can explain fine sand deposition within LM in unit C. Gray clay layers likely represent fair-weather quiescent lagoon deposition. Radiocarbon dating of indigenous bay fauna (*mulinia lateralis*) within individual clay beds were used to constrain the time interval over which discrete storm beds were deposited (Fig. 4-2; Appendix A).

#### 4.4 Modern Analogue

From historic records, approximately 13 hurricanes passed within 65 kilometers of the SPI area from AD 1854-present (Blake et al., 2007). However, we find evidence of only one modern discrete washover event recorded in our core data. Core 29 contained ~30 cm of a fine sand washover unit sharply overlying a clayey sand unit.  $^{137}\text{Cs}$  measurements yielded a concentration spike (indicating AD  $1963 \pm 2$ ) ~5 cm below the base of the washover unit (Appendix A). This deposit was thus associated with Hurricane Allen (1980), which was a category 3 storm, due to the proximity of this core to the known hurricane track, the age of the deposit, and the fact that no hurricanes passed within 65 kilometers of SPI between 1981 and 2007 (Blake et al., 2007).

#### 4.5 Relative Storm Intensities

A method for predicting flow depth of water over a barrier ( $\langle h_b \rangle$ ) from extreme hurricane flooding events has recently been established (Woodruff et al., 2008) (Appendix A).

This method allows relative comparisons of storm intensities between discrete storm deposits. Since Hurricane Allen was the only modern storm known to have left a deposit in LM and it was the only intense storm to impact SPI during historic times, this event was used to establish a modern analogue for predicted  $\langle h_b \rangle$  values (Appendix A). Wave heights over the barrier were calculated to be 6.6 m for Hurricane Allen. The measured surges associated with this storm were up to 3.7 m at Port Mansfield, TX (Fig. 4-1) (Roth, 2000), although the highest surges occurred in uninhabited regions of the coast and thus were not measured. Woodruff et al. (2008) cautioned that predicted  $\langle h_b \rangle$  values could overestimate exact storm surges from modern deposits. Still, we consider this method to be the best quantitative means of deriving relative differences in storm intensity within a given location. Thus, to constrain high intensity storms, we use the predicted  $\langle h_b \rangle$  values from Hurricane Allen as a baseline. For SPI,  $\langle h_b \rangle$  values were calculated for each hurricane event from the four cores (Fig. 4-2). Our data yield  $\langle h_b \rangle$  values between 3 and 13 m, but only inundation heights  $\geq 6.6$  m were classified as intense storms. Intense storm predicted values of  $\langle h_b \rangle$  ranged from 7.1 to 8.1 m in core 25, from 6.8 to 7.7 m in core 30, from 6.9 to 12.4 m in core 32, and from 6.8 to 7.9 m in core 33 (Fig. 4-2; Appendix A). SPI has extremely uniform sand grain-size, so overwash events recorded in our cores reflect the maximum grain sizes available for transport from the barrier into the lagoon. This explains the observed lack of lateral sorting in washover events (Fig. 4-2). By spacing cores apart large distances, using an advective model (Woodruff et al., 2008) to calculate relative storm intensity seems appropriate due to a wide range of sample distances from the barrier (Fig. 4-1).

## 4.6 Holocene Gulf of Mexico Intense Hurricane Activity

The storm overwash record from the four cores spans 20 km of backbarrier shoreline (Fig. 4-1) and shows little variability in intense hurricane landfall probabilities for the time interval 5,377–940 yr B.P.



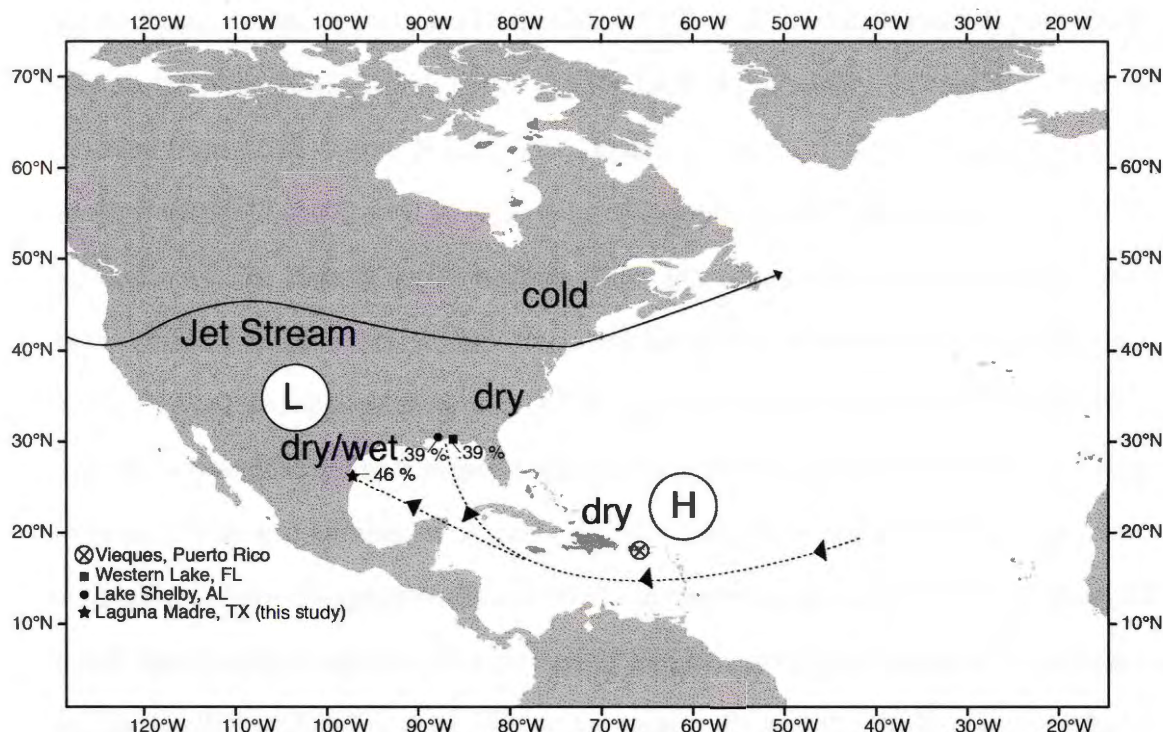


Figure 4-3: Gulf of Mexico intense hurricane landfall probability comparison for the late Holocene. Intense hurricane landfall probabilities for Lake Shelby, AL (Liu and Fearn, 2000b), Western Lake, FL (Liu and Fearn, 2000a), and Laguna Madre (LM), TX (this study). Average landfall probabilities between four cores from LM calculated to be ~.46%. Note the similar probabilities for all three sites, indicating a regional signature. Location of Vieques, Puerto Rico indicates recent study (Donnelly and Woodruff, 2007) where intense hurricane activity occurred from i.e., ~4,400–3,600 yr B.P., 2,500–1,000 yr B.P., and 250 yr B.P.–present. These time intervals overlap with all three studies. Note the location of the jet stream and Bermuda High (Forman et al., 1995). Dry conditions near southeastern North America (Forman et al., 1995; Liu and Fearn, 2000a), and shifting dry/wet conditions over Texas are also represented. Black dashed line represents hypothetical intense hurricane tracks under these conditions.

Six hurricane events are recorded from 4,235–1,582 yr B.P. (0.23% landfall probability) in core 30, ten from 2,382–1,433 yr B.P. (1.05% landfall probability) in core 25, six are recorded from 3,558–940 yr B.P. (0.23% landfall probability) in core 33, and a total of eleven from 5,377–2,072 yr B.P. (0.33% landfall probability) in core 32 (Fig. 4-2; Appendix A). The slightly higher landfall probability observed in core 25 could be due to its more northerly location that, perhaps, recorded storms not affecting the more southern cores. Due to low sedimentation rates in LM, it is possible that one storm bed could potentially represent multiple events, although the similar hurricane counts between cores separated by tens of kilometers suggests this effect might be negligible. Due to lagoon morphology, there is a range in the observed age intervals. However, these time intervals significantly overlap and all yield consistently similar landfall probabilities. Therefore, an average landfall probability within the 20 km wide study area of  $\sim 0.46\%$  was calculated from these four cores between  $\sim 5,300$ –900 yr B.P. (Appendix A).

A recent study concluded that 12 hurricanes likely of category 4 or higher intensity impacted Western Lake, Florida from 3,543–492 yr B.P. ( $\sim 0.39\%$  landfall probability) (Liu and Fearn, 2000a; Appendix A) (Fig. 4-3). In coastal Alabama, Lake Shelby has yielded evidence of 11 hurricane impacts of category 4 or higher from 3,500–700 yr B.P. ( $\sim 0.39\%$  landfall probability) (Liu and Fearn, 2000b) (Fig. 4-3). A recent modeling study (Elsner et al., 2008a) estimated a modern landfall probability of intense storms for this area to be  $\sim 0.3\%$ . In the western Gulf of Mexico, we show average landfall probabilities from  $\sim 5,300$ –900 yr B.P. of  $\sim 0.46\%$  (Fig. 4-2; Fig. 4-3). Our average landfall probabilities are possibly slightly higher due to sampling a longer time interval and wider geographic area. However, these remarkably similar landfall probabilities shed light on a regional hurricane record along the Gulf of Mexico coast.

Additionally, our findings seem to correlate well with two recent paleotempestological studies in the Caribbean and North America. A 5,000 yr hurricane record from Laguna Playa Grande in Vieques, Puerto Rico (LPG) (Fig. 4-3) showed that intense hurricanes impacted from ~4,400–3,600 yr B.P., 2,500–1,000 yr B.P., and from 250 yr B.P.-present (Donnelly and Woodruff, 2007). During historic times, hurricanes impacting LPG generally have been steered towards the Atlantic, although some have entered the Gulf of Mexico. The hurricane record presented in this study from LM, Texas included three overlapping intervals similar to LPG: ~4,235–1,582 yr B.P., 2,382–1,433 yr B.P., and 3,558–940 yr B.P. Recent work from North America compiles several sedimentary records and creates statistical models yielding evidence for a peak in Atlantic hurricane activity around AD 1,000, followed by a period of inactivity (Mann et al., 2009). Aside from the modern deposit from Hurricane Allen, we see little evidence of discrete storm bed preservation from ~1,000 yr B.P.- present.

The geological record becomes better constrained with the addition of properly located study areas within the Gulf of Mexico and Caribbean and the analysis of robust data sets. We consider our dataset to be accurate and robust because of the regularly spaced distribution of cores in the area. In addition, our study area encompasses ~20 km of coastline and shows little variability in paleohurricane landfall probabilities. Lastly, our data set suggests remarkably similar intervals of intense hurricane impacts as other paleotempestological sites around the Gulf Coast and Caribbean separated by hundreds of kilometers (Fig. 4-3; Appendix A).

## 4.7 Intense Hurricane Impact Climate Forcings

A recent study suggests that warmer sea surface temperatures (SST) in the Atlantic were not the main mechanism for increased intense hurricane activity for the past several millennia at LPG (Donnelly and Woodruff, 2007), although SST change cannot be completely ruled out. Rather, intervals of frequent intense hurricane impacts (i.e., ~4,400–3,600 yr B.P., 2,500–1,000 yr B.P., 250 yr B.P.-present) can be correlated with periods of fewer El Niño events and increased precipitation in tropical Africa. It has also been suggested that the jet stream and the Bermuda High have shifted south and southwest, respectively, since the mid-Holocene Thermal Maximum (Fig. 4-3) (Forman et al., 1995). This claim is bolstered by the fact that oxygen isotopic records from Lake Miragone, Haiti suggest an abrupt shift toward dry conditions in the late Holocene (Hodell et al., 1991). A shift in circulation patterns likely explains the observed change in the probabilities of impacts in northwestern Florida (Western Lake) and coastal Alabama (Lake Shelby) (Liu and Fearn, 2000a) (Fig. 4-3).

Paleoclimate data spanning much of Texas shows oscillations between warm, dry and cool, wet conditions in the late Holocene (Fratlicelli, 2003; Appendix A). It has been hypothesized that high pressure (associated with westward flowing cool, wet air masses) would effectively steer storms away from an area (Liu and Fearn, 2000a). Although this likely explains intense hurricanes being steered toward the Atlantic Ocean (Liu and Fearn, 2000a), our data indicate that despite high frequency (lasting ~500–1,000 yrs) climate oscillations, there has been no significant change in storm landfall probability over this time interval for the Gulf of Mexico. Furthermore, there is no evidence of any clear out-of-phase relationship that would indicate a direct correlation between climate and storm steering mechanisms for this area.

## 4.8 Conclusions

A detailed record from ~5,300–900 yr B.P. of past intense hurricane impacts from Laguna Madre, TX is presented. For each event, relative storm intensities were estimated. Average intense storm impact probability for south Texas was determined to be ~.46%. By combining our results with previous field studies from Western Lake, FL, and Lake Shelby, AL, which provide a record of intense storm impacts from the eastern Gulf, the intense hurricane impact history of the Gulf of Mexico for the Holocene can be constrained. These studies reveal similar probability intense hurricane strikes of ~.39%. Current rates of intense hurricane impacts for Western Lake, FL, Lake Shelby, AL, and Laguna Madre, TX, do not seem unprecedented when compared to intense strikes over the past 5,000 yr. In Texas, the probability of intense storm impacts does not appear to have varied during the late Holocene, although this was a period of high frequency oscillations between cool, wet and warm, dry climate conditions. Lastly, similar probabilities in high intensity hurricane strikes for the eastern and western Gulf of Mexico do not show any clear cut out-of-phase relationship, which would enlighten us as to those climate controls on storm pathways. Thus, in the northern Gulf of Mexico, there have been no significant variations in storm impact probabilities and/or storm steering mechanisms from ca. 5300-900 yr B.P.

## CHAPTER 5

### **Response of a low-gradient coast to global change: A case study of the Galveston Island and San Luis Pass inlet complex, Texas**

#### **5.0 ABSTRACT**

Along the Gulf of Mexico coast, there are many tidal inlets and deltas, most of which are anthropogenically altered and engineered. San Luis Pass is one of the only natural tidal inlet and delta complexes that remains, allowing the unique opportunity to study a natural system's response to accelerating sea-level rise and other forcing mechanisms over both geologic and historic time. Here, we describe the coupled evolution of Galveston Island and the San Luis pass tidal delta through time. We attempt to constrain sediment supply, relative sea-level rise (subsidence and eustasy) and hurricane landfall probability in order to assess the relative influence of these forcing mechanisms in regulating coastal change over geological and historical time. We show that the tidal inlet initially formed ~7 km east of the modern location ~3,500 yr B.P., when the rate of sea-level rise slowed from 2 mm/yr to 0.6 mm/yr. After an avulsion event in which the inlet moved ~4 km to the west, the system migrated ~3 km west between ~2,800 yr B.P. and ~2,100 yr B.P. to reach its current location. This chronology is consistent with the evolution of the adjacent Galveston Island, as the island began retreating sometime after ~1,800 yr B.P. Sediment cores reveal that the flux of sand from Galveston Island into San Luis Pass over the past 200 years has more than doubled relative to the past several millennia. Since sand is delivered by the longshore transport system, this suggests that erosion along Galveston Island has significantly increased in recent time. Additionally, inlet migration rates appeared to have nearly tripled (from ~2.9 m/yr to ~7.5 m/yr) over historic relative to geologic time, suggesting the system is becoming increasingly unstable. These changes can be most directly linked with the acceleration in relative sea-level rise over historic time, but hurricane impacts may also be a contributor.



## 5.1 INTRODUCTION

There is little question that the rate of sea-level rise has increased this century, and there is growing consensus that the frequency and magnitude of tropical storm impacts along the Atlantic, Pacific, and Indian Oceans has and could continue to increase in the near future due to global change (Emanuel, 2005; Webster et al., 2005; Mann and Emanuel, 2006; Elsner et al., 2008b). For the Gulf of Mexico, however, the current rate of intense hurricane impacts does not appear to be unprecedented when compared to the late Holocene (Wallace and Anderson, 2010). The impact of global change, as opposed to anthropogenic influence, on coasts is poorly documented. Our research is aimed at measuring long-term (millennial) versus historical changes that have occurred along the upper Texas coast, which because of its low gradient, limited sediment supply and variable climate, is among the world's most vulnerable coasts to global change (Anderson, 2007).

There are a number of reasons to expect significant change along the upper Texas coast this century. The first is the recent acceleration in the rate of sea-level rise, which for the Atlantic coast was initiated between 1879 and 1915 (Kemp et al., 2009). Eustatic sea-level is currently rising about 2 mm/yr, about 1 mm/yr less than the global average, and both the magnitude and rate is expected to increase by at least two to three times in the coming century (Thomas et al., 2004; Church and White, 2006; Overpeck et al., 2006; IPCC, 2007; Pfeffer et al., 2008). Current subsidence along the upper Texas coast varies along the coast, but averages 3 mm/yr (NOAA, 2010), bringing the rate of relative sea-level rise to ~5 mm/yr. Hurricanes, the most unpredictable control on coastal evolution, have and likely will continue to increase both in magnitude and frequency due to current climate change (Emanuel, 2005; Webster et al., 2005; Mann and Emanuel, 2006; Elsner et al., 2008b). Additionally, sediment supply to the coast is minimal (Anderson, 2007).

Tidal inlets and deltas are particularly sensitive to change, especially changes in longshore sediment supply. In addition, studying tidal inlet and delta evolution provide insight into the evolution of adjacent barrier island systems.

Galveston Island formed ~ 5,500 yrs B.P. (Bernard et al., 1959; Rodriguez et al., 2004) when the rate of sea-level rise was similar to today (Milliken et al., 2008a). The evolution of the island is linked to two tidal inlet and delta systems: Bolivar Roads tidal delta (BRTD), located east of the island, and San Luis Pass tidal delta (SLPTD), located west of the island. Detailed studies of Galveston Island show that sand supply to the barrier is minimal and that very little of the sand that is eroded from the island is transported either offshore or into backshore environments (Siringan and Anderson, 1994; Rodriguez et al., 2001, 2004; Wallace and Anderson, 2009). Rather, most of the sand is transported in the east-to-west flowing longshore currents and ultimately ends up in the SLPTD. For this reason, examining the historical sand flux for the SLPTD provides a record of the island's erosion history. There is also a long historical record of the migration of SLPTD (~200 years) from relatively detailed navigational charts, allowing placement of historical changes into geological context. Finally, SLPTD is the only natural tidal delta on the upper Texas coast, allowing the unique opportunity to examine how a barrier and tidal inlet/delta complex responds to changes in different forcing mechanisms, such as sea-level rise, sediment supply and the potential increase in hurricane frequency. This information, in turn, provides a framework for predicting coastal response to global change.

## **5.2 GEOLOGICAL SETTING**

SLPTD is a natural, microtidal (<30 cm; Morton and McGowen, 1980) tidal delta situated along the Texas Gulf coast between the west end of Galveston Island (N29.084°, W95.116°) and the east end of Follets Island (N29.077°, W95.123°) (Fig 5-1; Fig 5-2).

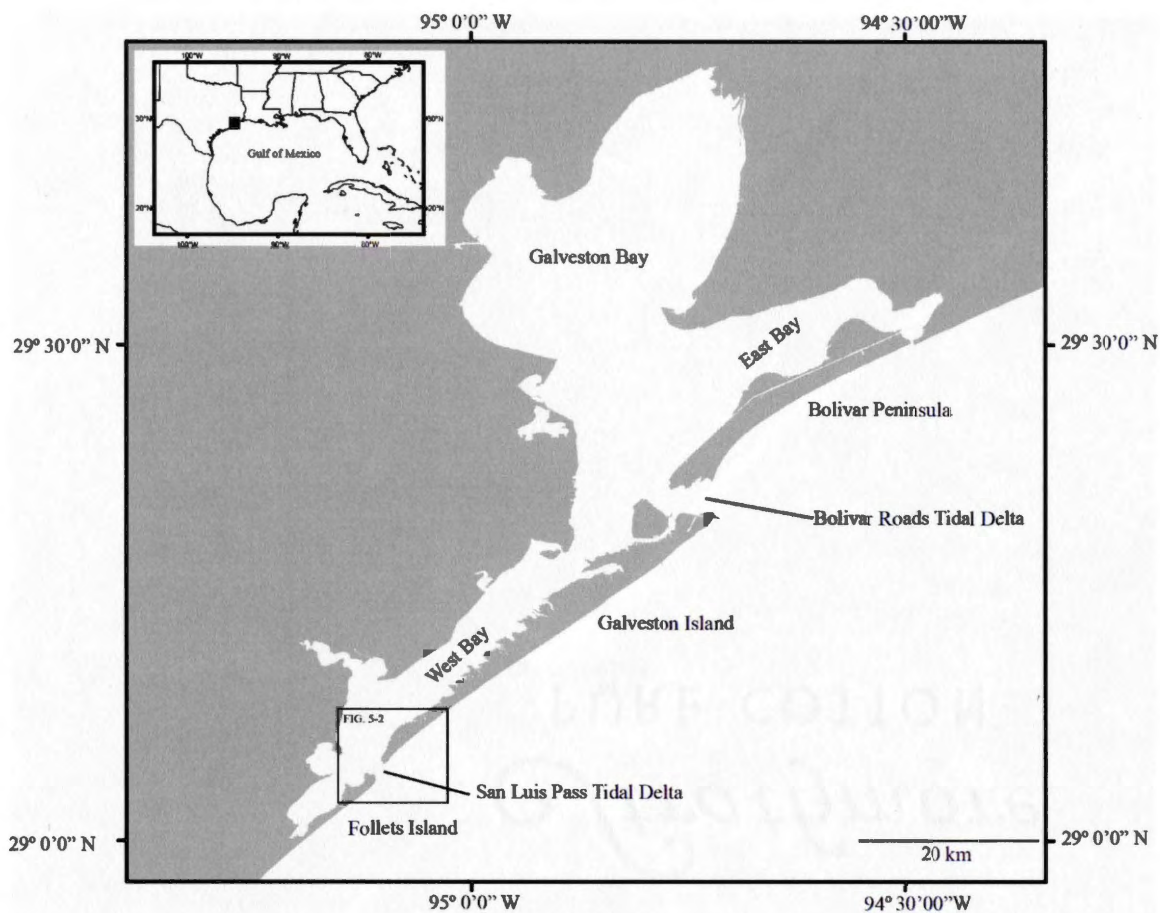


Figure 5-1: Study area map of the upper Texas coast. Box indicates the approximate location of Figure 5-2.

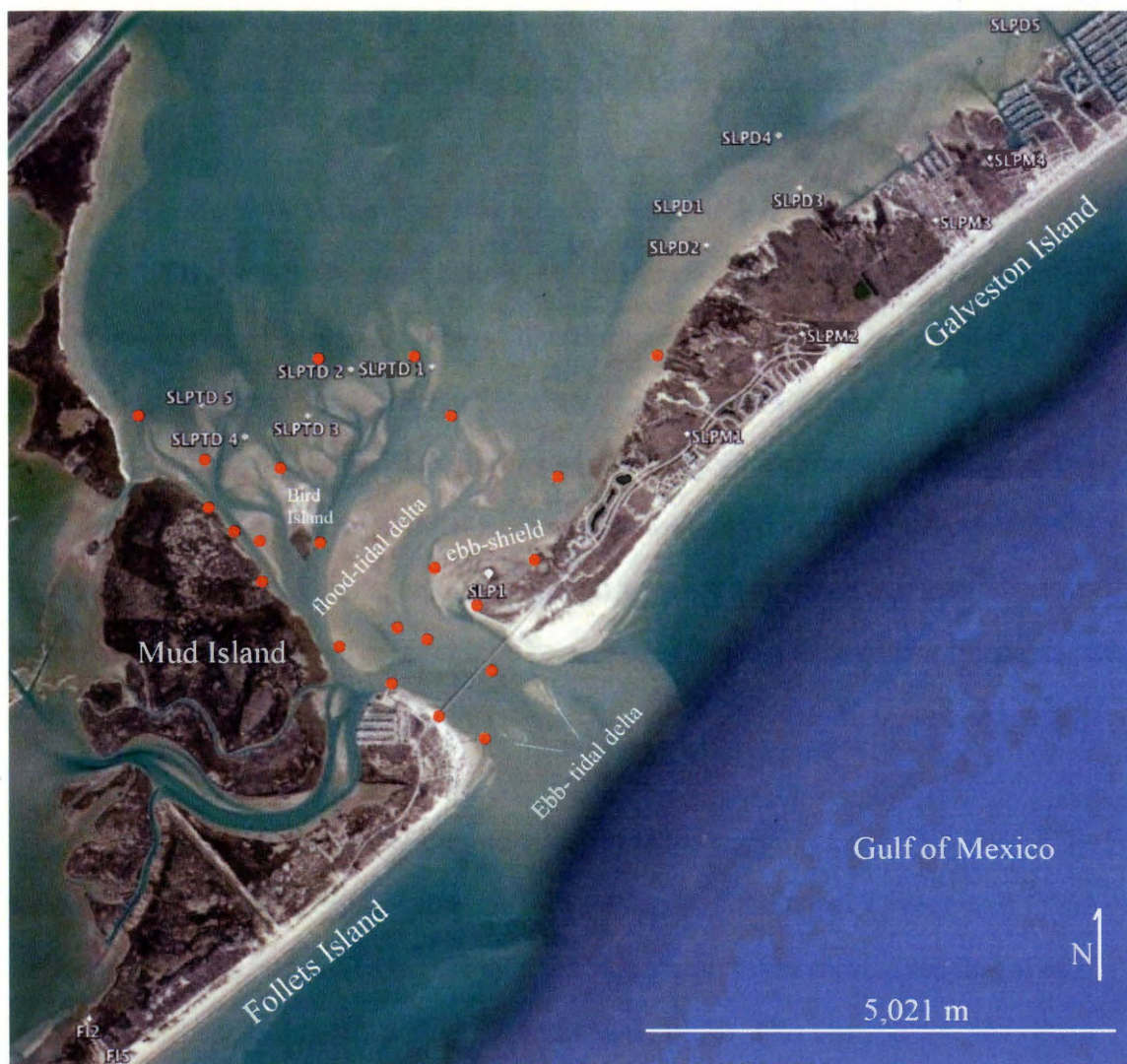


Figure 5-2: Satellite image of San Luis Pass tidal delta (base map modified from Texas General Land Office-Google Earth). Location shown in Figure 5-1. Cores from this study denoted by white circles with labels. Red circles are approximate locations of cores from Israel et al, (1987). Note the prominent flood- and ebb- tidal delta components, as well as the ebb-shield environment.

The ebb tidal section of the delta extends into the Gulf of Mexico, and the flood tidal delta extends into West Bay (Fig. 5-1). The flood tidal delta includes several subaerially exposed islands, an extensive channel system, sand bars, and shoals (Israel, 1987) (Fig. 5-2).

SLPTD is a late Holocene feature, as it bisects Galveston (formed ~5,500 yrs BP) and Follets Islands (formed ~3,000 yrs BP) (Bernard et al., 1959; Morton, 1994; Rodriguez et al., 2004). As these islands migrated landward due to sea-level rise, SLPTD has presumably followed. The SLPTD overlies ~4,000 year old Brazos River sediments that were deposited when the river flowed within a channel located very near the current inlet (Bernard et al., 1970). No tidal delta deposits exist seaward of the modern shoreline, as sediments below ~10 m water depth have been ravined during sea-level rise (Siringan and Anderson, 1994; Rodriguez et al., 2001).

The prevailing longshore current direction in the region is southwest (Fig. 5-1). For the most part, little sand exists within the barrier islands of the upper Texas coast; thicknesses range from ~2-10 m. Much of the upper east Texas coast is eroding at an average rate of approximately 3 m/yr (Gibeaut et al., 2006). This erosion coupled with a steady longshore current annually transports significant sand volumes.

## **5.3 CONTROLS ON COASTAL CHANGE**

### **Relative sea-level rise**

Sea-level rise over the late Holocene in the Gulf of Mexico is shown to be ~.6 mm/yr over the last 3,000 years B.P. (Milliken et al., 2008a). The average long-term subsidence rate for the Texas coast over geologic time (i.e.  $10^2$  -  $10^3$  yrs) is ~.05 mm/yr (Paine, 1993). Thus, relative sea-level rise for the past 3,000 years averages ~.65 mm/yr.

Over decades to centuries, local subsidence rates due to consolidation could be as high as 10 mm/yr (Törnqvist et al., 2008). These high rates are associated with areas consisting of thick, highly compressible Holocene sediments. Based on Holocene sediment thicknesses ranging from 9-21 m along the upper Texas coast, consolidation rates were likely high when Galveston Island initially formed ~ 5,500 yr B.P. However, since the island formed much of the sediment has mostly dewatered, so subsidence due to consolidation is believed to be negligible at present.

Estimates of current relative sea-level rise from the Pier-21 tide gauge record, located in the southern part of Galveston Bay, exceed 6 mm/yr (NOAA, 2010). Of this, ~2.1 mm/yr can be attributed to regional sea-level rise in the Gulf of Mexico, as these are the observed trends from the stable Pensacola, FL tide gauge (NOAA, 2010). Therefore, ~3.9 mm/yr can be attributed to local subsidence in recent time. This subsidence is mostly due to anthropogenic activities, such as groundwater, oil, and natural gas extraction, because the natural subsidence rates due to consolidation and/or tectonics are lower. In addition, the current rate of subsidence is believed to vary locally due to variable anthropogenic influence and growth fault activity.

### **Hurricane impacts and erosion**

Over both historical and geological timescales, hurricanes have the potential to drastically alter the evolution of coastal systems. Hurricanes deliver sand to back-barrier environments (washover) and contribute significantly to shoreline erosion. After a hurricane impact, shoreface profile adjustments occur, as sediment is eroded and transported offshore. However, an absence of storm beds seaward of the modern shoreface indicates that sand delivered offshore during severe storms is ultimately transported landward and back into the longshore transport system. Thus, the main impact of hurricanes is to increase sand transport by longshore currents over centennial to millennial timescales.



Wallace and Anderson, (2010) suggest that the rate of intense hurricanes impacting the Gulf coast over the late Holocene has been relatively constant at  $\sim 0.46\%$  annual landfall probability. Since 1900, Chambers, Galveston and Brazoria Counties have had 7 direct impacts from category 4 and 5 storms ( $6.4\%$  annual landfall probability) (Blake et al., 2007). There have been two hurricane landfalls on Galveston Island and Bolivar Peninsula this century and each resulted in an average of 10 meters of permanent shoreline retreat in areas unprotected by man-made structures.

## 5.4 METHODS

We rely on three types of data: aerial and satellite imagery, bathymetric data, and vibracore data. Israel et al. (1987) present an extensive coring program in the SLPTD, from which a detailed facies analysis is developed. Their work provides an important framework for our work and is used to conduct volumetric analyses of the tidal delta. In addition, we use their results to select core transects designed to sample both proximal and distal flood tidal delta deposits (Fig. 5-2). In addition to Israel et al., (1987), we use the results of Bernard et al., (1970) to constrain the evolution of SLPTD over the past 200 years.

Five 7.6 cm diameter vibracores are taken across the delta and are sampled for radiocarbon-datable material to establish a chronostratigraphic framework. Four cores are collected on the far west end of Galveston Island for datable material in order to establish a migration chronology of the inlet. Five cores are taken on the backside of Galveston Island to establish the extent of paleo-inlet deposits. A GARMIN® handheld GPS unit is used for obtaining horizontal core location coordinates to within about 10 m. Aerial photographs are analyzed when available to detect changes in flow patterns or deposition locales within the flood and ebb tidal shoals.



Sample name	Depth (cm)	Material	<sup>14</sup> C Age	Cal. <sup>14</sup> C Age
SLPTD1-1_70.5-72.5cm <sup>1</sup>	70.5-72.5	Gemma cf. <i>G. purpurea</i> Lea & <i>Psuedomiltha floridana</i>	1410 ± 20	947 ± 28
SLPTD1-2_30-32cm	165-167	<i>Mulinia lateralis</i>	710 ± 20	349 ± 40
SLPTD1-2_85cm	220	<i>Mulinia lateralis</i>	755 ± 20	406 ± 41
SLPTD2-1_47-49cm	47-49	<i>Chione grus</i> & fragments	1735 ± 20	1284 ± 22
SLPTD3-1_76cm <sup>1</sup>	76	<i>Mulinia lateralis</i>	(-)760 ± 20	Modern
SLPTD3-2_25-27cm	162-164	<i>Chione grus</i>	1545 ± 20	1100 ± 38
SLPTD5-2_6cm <sup>1</sup>	138	Oyster fragment	2770 ± 20	2497 ± 71
SLPTD5-2_50.5-53cm	182.5-185	Gemma cf. <i>G. purpurea</i> Lea & <i>Pyrgiscus</i> cf. <i>portoricana</i>	2435 ± 20	2076 ± 41
SLPM1_176cm	1.76	<i>Mulinia lateralis</i> & <i>Ervilia</i> cf. <i>E. concentrica</i>	2895 ± 15	2696 ± 22
SLPM1_178cm	1.78	<i>Anadara transversa</i>	3100 ± 15	2874 ± 38
SLPM2_197cm	1.97	<i>Noetia ponderosa</i>	5545 ± 15	5922 ± 26
SLPM2_230-235cm	2.3-2.35	shell fragments	2255 ± 15	1857 ± 32
SLPM3_181cm	1.81	juvenile <i>Tagelus divisus</i>	295 ± 15	Modern
SLPM3_306cm	3.06	<i>Tagelus divisus</i>	1415 ± 15	950 ± 27
SLPM3_318cm	3.18	<i>Tagelus divisus</i>	1550 ± 15	1105 ± 36
SLPM4_254cm	2.54	<i>Cyclinella tenuis</i>	3050 ± 20	2808 ± 35
SLPM4_270cm	2.7	<i>Cyclinella tenuis</i>	3210 ± 15	3015 ± 44
SLPM4_365cm	3.65	<i>Chione cancellata</i>	3340 ± 15	3205 ± 41
SLPM4_392-393cm	3.92-3.93	<i>Mulinia lateralis</i>	3575 ± 15	3463 ± 39
SLP1_365-370cm <sup>2</sup>	3.65-3.7	<i>Cyrtopleura costata</i>	4100 ± 140	4152 ± 190
SLP1_560-581cm <sup>2</sup>	5.6-5.81	organic-rich clay	6560 ± 110	7494 ± 75

<sup>1</sup> sample reworked

<sup>2</sup> sample from Rodriguez et al., (2004)

Table 5-1: San Luis Pass tidal delta radiocarbon results.

Grain size data are obtained using a MALVERN Mastersizer 2000. AMS radiocarbon dating is performed at Keck Carbon Cycle AMS Facility at UC-Irvine. Radiocarbon ages are calibrated from radiocarbon to calendar years using Marine04 (Hughen, et al., 2004) (Table 5-1).

## **5.5 FACIES, ENVIRONMENTS AND MIGRATION DYNAMICS**

Understanding the history of formation and migration of the tidal inlet and delta complex relies on proper identification of depositional environments and their stratigraphic associations. Cores recovered from the SLPTD sample sediments representing a number of depositional environments including fluvial, bay, marsh, washover deposits, proximal tidal delta, or distal tidal delta (Israel et al., 1987). Brazos fluvial deposits are oxidized, stiff, red clays, which occasionally are gradational with overlying bay clays (Fig. 5-3). Bay sediments include structureless or mottled, homogenous mud with shell material (Fig. 5-3). Marsh environments contain clayey sand and/or sandy clay with abundant plant material, roots and shells. Washover deposits consist of fine sand with clay mottles, and typically are highly bioturbated near the surface. Proximal tidal delta deposits consist of mottled sand with abundant shell material, and occasionally contain clay laminae. Distal tidal delta deposits include highly bioturbated sandy clay to clayey sand, with interbeds of tidal couplets (Fig. 5-3) (Israel et al., 1987).

Bernard et al., (1970) show that tidal delta deposits are found at least ~6 km northeast of the SLPTD current location. They describe interbedded, burrowed and laminated tidal delta deposits, as well as a channel sequence composed of sand and shell hash that filled the migrating inlet and channels. Cores collected from the modern SLPTD sample a stratigraphic succession that indicates progressive growth of the delta as it migrated into its current location.

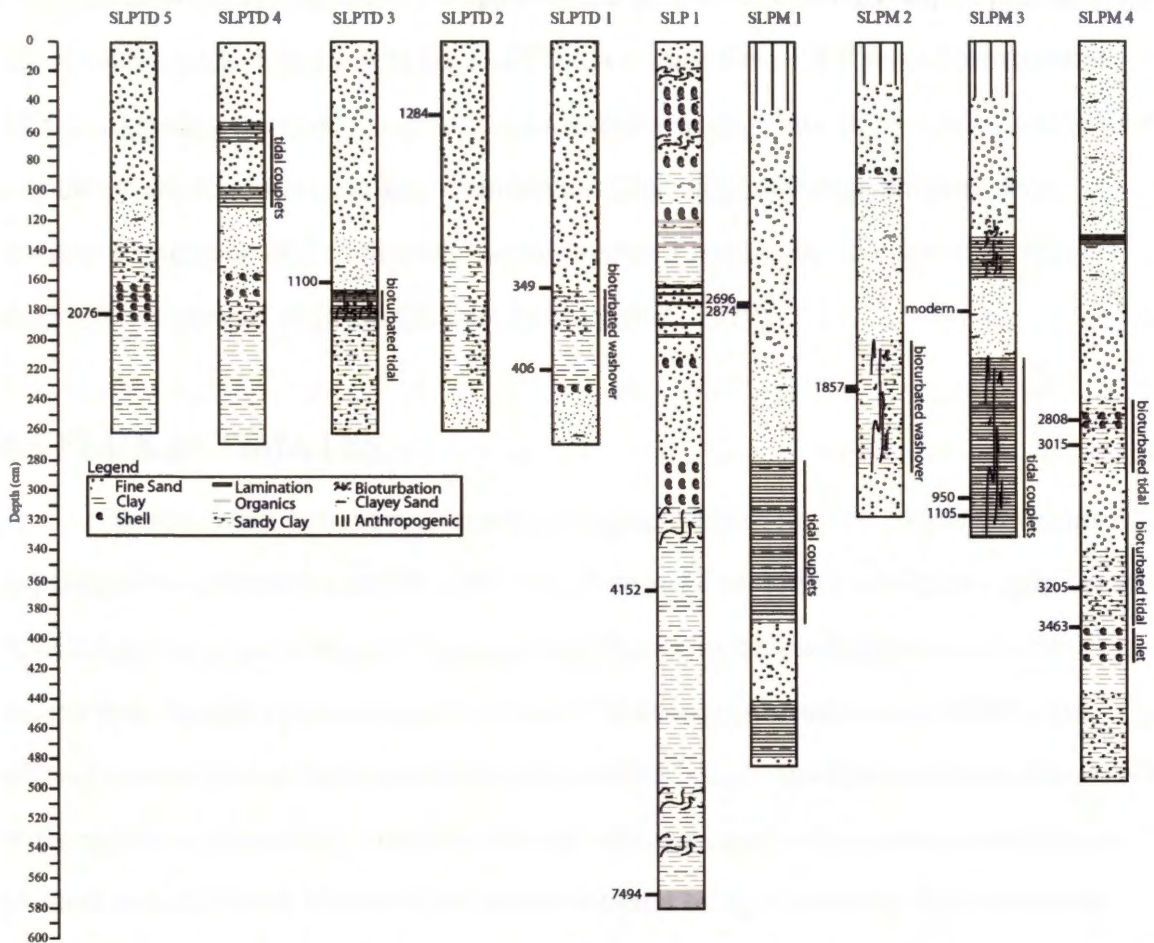


Figure 5-3: Lithologic descriptions of cores. See Figure 5-2 for locations. Numbers indicate calibrated radiocarbon ages from mollusc shells (Table 5-1). Note the minimum age of San Luis Pass tidal delta of ~2,100 yr B.P. (core SLPTD5). Also, note the tidal deposits in most cores. Tidal couplet deposits are also present in most cores, and the paleo-inlet deposit in core SLP M 4 dates to ~3,500 yr B.P. The radiocarbon data suggest that the inlet described in core SLP M 3 and SLP M 4 occupied this location between ~1,000 and ~3,500 yr B.P. Additionally, the tidal deposits in core SLP M 1 appear to be associated with the modern inlet based on two ages ~2,800 yr B.P., suggesting it migrated from this location to its near modern location. Therefore, due to a lack of tidal deposits in core SLP M 2, we suggest that the migration of San Luis pass tidal delta was not continuous; it appears to have rapidly avulsed between the locations of SLP M 3 and SLP M 4, to the location of SLP M 1 (see Figure 5-2 for core locations).

From old aerial photographs and navigational charts, it is estimated that approximately 1-1.5 km of southwestern migration of the SLPTD has occurred over 200 years (Bernard et al., 1970), suggesting the system migrated at a maximum average rate of  $\sim 7.5$  m/yr. As the inlet migrates to the southwest, the deep channels are filled with sand several meters deep. Westward migration of the inlet may have slowed as it reached the location of an ancestral Brazos River channel (Bastrop Channel, Bernard et al., 1970).

## 5.6 FLUX ESTIMATES

Previous work has shown that a significant portion of modern coastal sediments is sequestered in tidal inlets and tidal deltas (Moslow and Tye, 1985). Along the upper Texas Coast, rivers have had minimal direct sand contribution to the coast system since river valleys were flooded to create bays by the early Holocene (Anderson et al., 2008). The primary source of sand that has nourished the barrier islands and tidal inlet/delta complexes of the region has been from cannibalization of offshore sand bodies during transgression (Anderson et al., 2004). However, the amount of sand being supplied by this mechanism today is believed to be negligible (Wallace and Anderson, 2009). Therefore, it appears that the primary sediment source to the longshore transport system, and ultimately the SLPTD, is from erosion of Galveston Island. This being the case, our assumption is that sand supply to the SLPTD varies in response to rates of erosion of Galveston Island, which is controlled by such factors as rates of relative sea level rise and hurricane frequency. Our analysis focuses on establishing the rate of SLPTD migration and sand volumes in order to establish the long-term flux rate. This information in turn is used to estimate the long-term and short-term erosion rates for Galveston Island.

## 5.7 RESULTS

### Modern flood- tidal delta

#### *Formation*

We attempt to sample and date cores from both distal tidal delta locations, however, almost all of the radiocarbon ages from proximal delta locations appear to be reworked (Table 5-1). Samples from cores collected in more distal locations (Fig. 5-3) offer the most precise age constraint, because tidal ravinement and reworking appear to be minimal. Using these data, SLPTD appears to have formed at least by ~2,100 yr B.P., based on the oldest age of proximal tidal sands directly overlaying distal tidal couplets (Fig. 5-3). Thus, the tidal delta is a late Holocene feature.

During its early formation, Galveston Island accreted westward (Bernard et al., 1959; Rodriguez et al., 2004), and the formation of the SLPTD suggests that the island reached its present location ~2,100 yrs B.P. Additionally, this chronology is consistent with when Galveston Island is known to have stopped prograding (~1,800 yr B.P.), and began to retreat (Rodriguez et al., 2004). It is believed that Galveston Island stopped prograding and accreting westward due to a decrease in sediment supply.

#### *Sedimentation rates*

Cores collected across the distal tidal delta (Fig. 5-3), shed light on accumulation rates in this environment. For the modern delta, average sedimentation rates range from ~1 – 5 mm/yr over the past ~2,100 yr B.P.

#### *Sand sequestration*

Coupling our data with previous core data (Israel et al., 1987), we estimate an approximate sand volume of 9,000,000 m<sup>3</sup> for the SLPTD.



Time averaging this volume by when this sediment was mostly deposited into SLPTD (~2,100 yr B.P.- 200 yr ago) yields an annual sand flux of  $\sim 4,700 \text{ m}^3/\text{yr}$ . This value represents the long-term average sand sequestration rate. From core data, along with historical charts, we estimate that  $\sim 2,000,000 \text{ m}^3$  of sand has been stored along the far west end of Galveston Island due to lateral accretion of the barrier and infilling of the San Luis Pass paleo-inlet over the past 200 years (Bernard et al., 1970), equaling an average sand flux rate of  $\sim 10,000 \text{ m}^3/\text{yr}$ .

Cores collected up to  $\sim 7 \text{ km}$  east and  $\sim 5 \text{ km}$  west of the modern tidal delta are used to help constrain the migration history for San Luis Pass (Fig. 5-2). Cores taken east of the delta recovered tidal deposits (Fig. 5-3), while cores taken to the west on Follets Island (Fig. 5-2) showed no evidence of tidal deposits. Paleo tidal inlet deposits were penetrated in core SLPM4 at  $\sim 4 \text{ m}$  depth (Fig. 5-3). This facies consists of mixed clay and shell hash, is a facies consistently observed in modern inlet deposits (Israel et al., 1987). A radiocarbon age from an inlet inhabiting mollusc shell species of  $\sim 3,500 \text{ yr B.P.}$  (Table 5-1) suggests that an inlet formed at this time  $\sim 7 \text{ km}$  east of the modern location (Fig. 5-2; Fig. 5-3- core SLPM4; Fig. 5-4).

Tidal couplets in core SLPM3 (Fig. 5-2; Fig. 5-3) are determined to be  $\sim 1,000 \text{ yr B.P.}$ , suggesting an inlet was located between cores SLPM3 and SLPM4 from  $\sim 3,500 \text{ yr B.P.}$  to  $\sim 1,000 \text{ yr B.P.}$  No tidal deposits are found in core SLPM2 (Fig. 5-2; Fig. 5-3), as this section is dominated by highly bioturbated washover deposits. In core SLPM1 (Fig. 5-2; Fig. 5-3), no datable material is found in the tidal couplet unit. However, two dates from barrier island sands just above tidal couplets (Fig. 5-2; Fig. 5-3- SLPM1) yield ages of  $\sim 2,800 \text{ yr B.P.}$ , suggesting that a tidal delta was in this location just before this time (Fig. 5-4). Therefore, the modern SLPTD appears to have migrated at least  $2 \text{ km}$  (at a rate of  $\sim 2.9 \text{ m/yr}$ ) to reach the approximate location 200 years ago.

Cores SLPM1, SLPM3, and SLPM4 (Fig. 5-2; Fig. 5-3) sample modern barrier island sand sharply overlaying slightly bioturbated tidal couplets, just above proximal tidal delta sands. These results indicate that the SLPTD avulsed from an easterly location (Fig. 5-2; Fig. 5-3-SLPM3 and SLPM4) to a more westerly location (Fig. 5-2; Fig. 5-3-SLPM1), with the older, more shallow ( $\sim 4$  m deep) inlet being rapidly filled with sand by longshore transport. The modern SLPTD then began migrating westward from the location of SLPM1 (Fig. 5-2), and was able to stabilize over an abandoned Brazos River channel (Bastrop Channel)  $\sim 2,100$  yrs B.P. (Fig. 5-4). In the near modern location, the inlet has incised deeply into soft fluvial sediments to its current depth of  $\sim 10$  meters.

### **Modern ebb-tidal delta**

Based on observed geomorphic features associated with San Luis Pass ebb-tidal delta, it is believed to be located on an ebb-tidal shield (Hayes, 1979) composed of interbedded fine sand and oyster shell hash (Israel et al., 1987). Directly underlying these ebb-shield deposits, prominent distal flood tidal couplets exist (Fig. 5-3 – Core SLP 1). A radiocarbon age of  $\sim 4,150$  yr B.P. (Rodriguez et al., 2004) within bay sediments that underlie these tidal couplets confirms that SLPTD was not in its current location between  $\sim 4,150$  yr B.P. and  $\sim 2,100$  yr B.P.

## **5.8 DISCUSSION**

Evolution of SLPTD was punctuated by thresholds in its stability. After the inlet initially formed  $\sim 3,500$  yr B.P., it did not stabilize until the rate of sea-level rise slowed from  $\sim 2$  mm/yr to  $\sim 0.6$  mm/yr (Milliken et al., 2008a). Bolivar Roads tidal delta also stabilized in its current location  $\sim 3,300$  yr B.P. (Siringan and Anderson, 1993). From  $\sim 2,800$  yr B.P. to  $\sim 2,100$  yr B.P., SLPTD migrated west at a rate of  $\sim 2.9$  m/yr. During the past 200 yrs, SLPTD has migrated west at a rate of up to  $\sim 7.5$  m/yr (Bernard et al., 1970). Thus, migration rates have nearly tripled over historic time relative to the late Holocene.



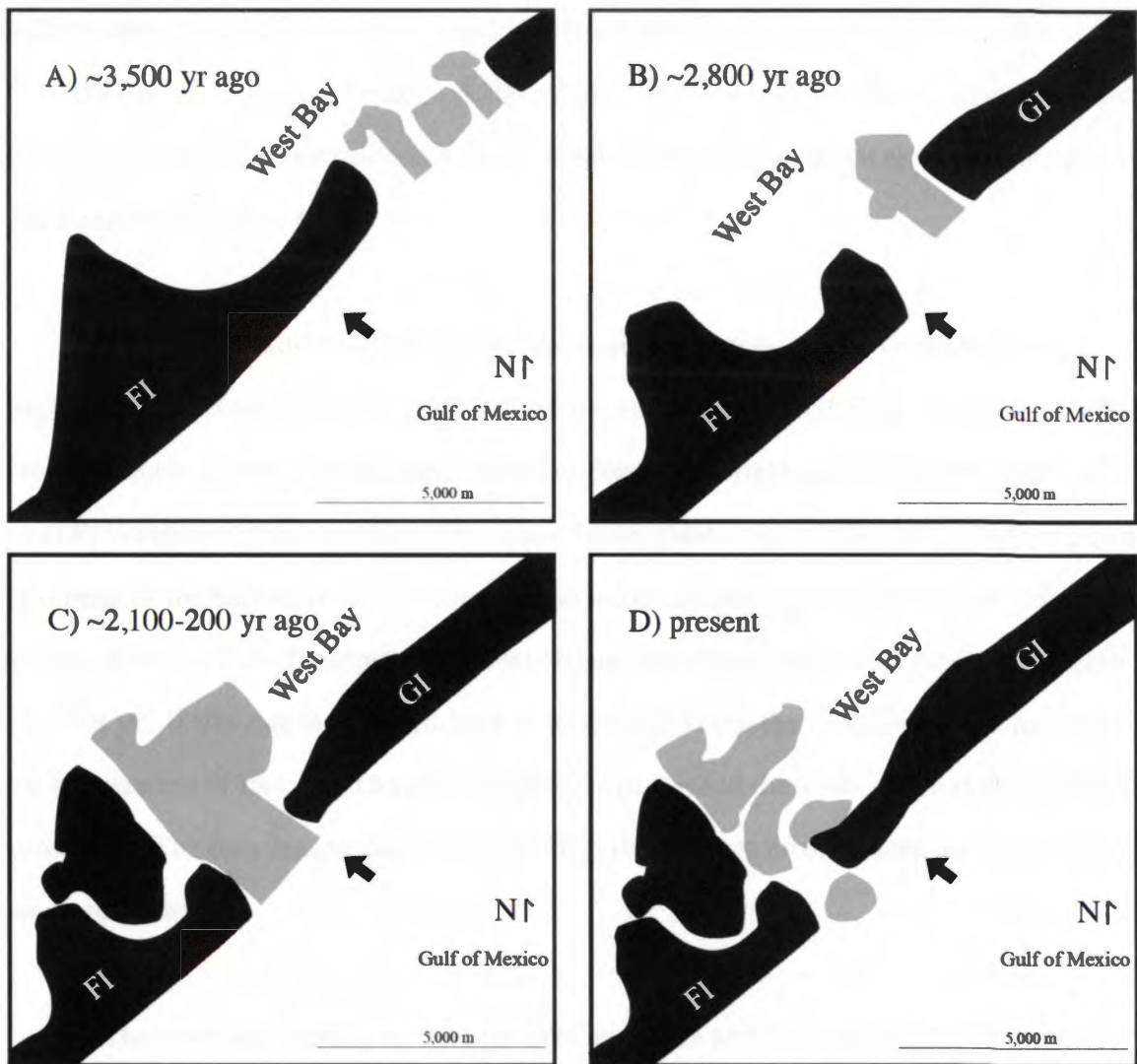


Figure 5-4: Diagram illustrating the evolution of Galveston Island, Follets Island, and San Luis Pass tidal delta through time. A) A radiocarbon age of ~3,500 yr B.P. suggests that an inlet formed at this time ~7 km east of the modern location. B) A radiocarbon age of ~2,800 yr B.P. suggests that a tidal delta was in a location several km east of A. C) San Luis Pass tidal delta is in its current location by ~2,100 yr B.P. The modern inlet and delta appears to have migrated at least 2 km (at a rate of ~2.9 m/yr) to reach its near modern location between ~2,800 yr B.P. and ~2,100 yr B.P. D) The present day system. Note that Galveston Island has migrated ~1.5 km southwest in the past 200 years. GI= Galveston Island, FI=Follets Island. Black shapes represent barrier island deposits, and gray shapes represent tidal and inlet deposits. Reference point indicated by arrow.

Additionally, the flux of sand into San Luis Pass has more than doubled over historic ( $\sim 10,000 \text{ m}^3/\text{yr}$ ) to geologic time ( $\sim 4,700 \text{ m}^3/\text{yr}$ ). Since the only significant source of sand to the tidal delta is from erosion of Galveston Island, this suggests that erosion of the island has doubled in historic time.

Accelerated erosion of Galveston Island during historic time is consistent with preliminary observations from Follets Island, located west of the SLPTD. Sediment cores from washover deposits on the back side of Follets Island yield ages dating back to  $\sim 2,900$  yr B.P. Washover processes along the upper Texas coast are currently restricted to within a kilometer of the back-barrier, so Follets Island must have been close to its present location since  $\sim 2,900$  yr B.P. Presently, the Follets Island shoreline is migrating landward at a rate of  $\sim 3 \text{ m/yr}$ . If this rate is extended back in time 2,900 years, the shoreline would have been  $\sim 9 \text{ km}$  seaward of its current location, which is well beyond the limits of the storm washover processes. The only reasonable interpretation is that modern erosion rates on Follets Island are unprecedented.

The observed changes in both the inlet migration and flux rate of SLPTD occurred at the same time the rate of sea-level rise increased, having gone from an average rate of  $\sim .6 \text{ mm/yr}$  during the late Holocene to a current rate of  $\sim 2.1 \text{ mm/yr}$ . (Milliken et al., 2008a). This recent acceleration in the rate of sea-level rise was initiated between 1879 and 1915 (Kemp et al., 2009). Currently, the rate of intense hurricane impacts does not seem unprecedented for the Gulf of Mexico when compared to the late Holocene (Wallace and Anderson, 2010), though the frequency and magnitude of hurricanes in some oceans has and could potentially continue to increase due to future global change (Emanuel, 2005; Webster et al., 2005; Mann and Emanuel, 2006; Elsner et al., 2008b).

Therefore, the best explanation for the dramatic changes observed within the SLPTD system is that the accelerated rate of sea-level rise over modern times has resulted in a significant increase in erosion of Galveston Island.

## 5.9 CONCLUSIONS

San Luis Pass tidal delta, one of the only natural tidal inlets and deltas along the Texas coast, provides a unique opportunity to examine and compare long-term (millennial) versus historical rates of coastal change of a barrier island (Galveston Island) and tidal inlet/delta complex. The maximum age from several radiocarbon ages of the San Luis Pass tidal inlet is determined to be ~2,100 yr B.P. Since its formation, the migration rate of the inlet has nearly tripled, from ~2.9 m/yr to ~7.5 m/yr (geologic versus historic time, respectively). Additionally, sand sequestration along the far west end of Galveston Island and within the delta has more than doubled over historic time compared to geologic time (rates = 4,700 m<sup>3</sup>/yr for past 2,100 yrs; 10,000 m<sup>3</sup>/yr for past 200 yrs). These rate increases appear to correlate with an acceleration of sea-level rise resulting in enhanced erosion of Galveston Island during historic time relative to the past ~3,000 yr B.P.

## References

- Amos, C.L., Christian, H.A., Grant, J., and Paterson, D.M., 1992, A comparison of in-situ and laboratory methods to measure mudflat erodibility, *in*: Falconer, R.A., Chandler-Wilde, S.N., and Liu, S.Q., eds., *Hydraulic and Environmental Modeling, Proceedings of the Second International Conference on Hydraulic and Environmental Modeling of Coastal, Estuarine and River Waters*, Bradford, UK, University of Bradford, v. 1, pp. 325–336.
- Anderson, J.B., 2007, *Formation and Future of the Upper Texas Coast*, College Station, Texas A&M Press, 163p.
- Anderson, J.B., Rodriguez, A., Abdulah, K., Banfield, L.A., Bart, P., Fillon, R., McKeown, H. and Wellner, J., 2004, Late Quaternary stratigraphic evolution of the northern Gulf of Mexico: a synthesis, *in*: Anderson, J.B., Fillon, R.H. eds., *Late Quaternary Stratigraphic Evolution of the Northern Gulf of Mexico Margin*, Society of Sedimentary Research Special Publication No. 79, pp. 1-24.
- Anderson, J.B., Rodriguez, A.B., Milliken, K., and Taviano, M., 2008, The Holocene evolution of the Galveston estuary complex, Texas: Evidence for rapid change in estuarine environments, *in*: Anderson, J.B., and Rodriguez, A.B., eds., *Response of Upper Gulf Coast Estuaries to Holocene Climate Change and Sea-Level Rise*, Geological Society of America Special Paper 443, pp. 89–104.
- Banfield, L., and Anderson, J.B., 2004, The Late Quaternary Evolution of the Rio Grande Delta, Special Publication, Society of Sedimentary Research, v. 79, pp. 289–306.
- Bernard, H.A., Major, C.F. Jr., Parrot, B.S., 1959, The Galveston barrier island and environments: A model for predicting reservoir occurrence and trend, *Transactions Gulf Coast Association Geological Society* 9, pp. 221-224.
- Bernard, H.A., Major, C.F., Parrot, B.S., and Leblanc, R.J., 1970, Recent sediments of southeast Texas, a field guide to the Brazos alluvial and deltaic plains and the Galveston barrier island complex, Bureau of Economic Geology, The University of Texas at Austin, Guidebook No. 11, 132p.
- Best, T.C., and Griggs, G.B., 1991, A sediment budget for the Santa Cruz littoral cell, California, *in*: Osborne, R.H., ed., *From Shoreline to Abyss: Contributions in Marine Geology in Honor of Francis Parker Shepard*, Special Publication, Society of Economic Paleontology and Mineralogy, v. 46, pp. 35–50.
- Beumel, N.H., and Beachler, P.E., 1994, Beach nourishment design within an existing groin field at Galveston, Texas, *in*: Tait, L.S., eds., *Alternative Technologies in Beach Preservation, Proceedings of the 1994 National Conference on Beach Preservation Technology*, 9–11 February, Tampa, Florida, Florida Shore and Beach Preservation Association, pp. 183–197.
- Blake, E.S., Rappaport, E.N., and Landsea, C.W., 2007, Historical hurricane tracks, <http://csc-s-maps-q.csc.noaa.gov/hurricanes> (last accessed: December 2009).
- Bowen, A.J., Inman, D.L., 1966, Budget of littoral sands in the vicinity of Point Arguello, California Technical Memoir: U. S. Army, Coastal Engineering Resource Center, 56p.

Bruun, P., 1962, Sea-level rise as a cause of storm erosion, *Proceedings of the American Society of Civil Engineers, Journal of the Waterways and Harbors Division*, 88(WWI), pp. 117-130.

Bruun, P., 1954, Coastal Erosion and Development of Beach Profiles, U.S. Army Beach Erosion Board Technical Memorandum 44, Vicksburg, Mississippi, U.S. Army Corps of Engineers, Waterways Experiment Station, 79p.

Carothers, H.P., and Innis, H.C., 1962, Design of inlets for Texas coastal fisheries, *Transactions of the American Society of Civil Engineers*, v. 127, pp. 231-256.

Carter, R.W.G., 1988, *Coastal Environments*, Academic Press, London, 617p.

Church, J.A., and White, N.J., 2006, A 20th century acceleration in global sea-level rise, *Geophysical Research Letters*, v. 33, pp. L01602, doi: 10.1029/2005GL024826.

Dean, R.G., and Dalrymple, R.A., 2002, *Coastal Processes*, New York, Cambridge University Press, 475p.

Donnelly, J.P., Bryant, S.S., and Butler, J., Dowling, Fan, L., Hausmann, N., Newby, P., Shuman, B., Stern, J., Westover, K., and Webb, III, T., 2001b, 700 yr sedimentary record of intense hurricane landfalls in southern New England, *Geological Society of America Bulletin*, v. 113, pp. 714-727.

Donnelly, J.P., Butler, J., Roll, S., Wengreen, M., and Webb, T., 2004, A backbarrier overwash record of intense storms from Brigantine, New Jersey, *Marine Geology*, v. 210, pp. 107-121, doi: 10.1016/j.margeo.2004.05.005.

Donnelly, J.P., Roll, S., Wengren, M., Butler, J., Lederer, R., and Webb, T., 2001a, Sedimentary evidence of intense hurricane strikes from New Jersey, *Geology*, v. 29, pp. 615-618, doi: 10.1130/0091-7613(2001)029<0615:SEOIHS>2.0.CO;2.

Donnelly, J.P., and Woodruff, J.D., 2007, Intense hurricane activity over the past 5,000 years controlled by El Niño and the West African monsoon, *Nature*, v. 447, pp. 465-468, doi: 10.1038/nature05834.

Elsner, J.B., Jagger, T.H., and Liu, K.B., 2008a, Comparison of hurricane return levels using historical and geological records, *Journal of Applied Meteorology and Climatology*, v. 47, pp. 368-374, doi: 10.1175/2007JAMC1692.1.

Elsner, J.B., Kossin, J.P., and Jagger, T.H., 2008b, The increasing intensity of the strongest tropical cyclones, *Nature*, v. 455, pp. 92-95.

Emanuel, K., 2005, Increasing destructiveness of tropical cyclones over the past 30 years, *Nature*, v. 436, pp. 686-688.

Eyer, A.D., 1984, Geomorphology and morphologic development of Bolivar Roads Inlet and Bolivar Peninsula, Texas [unpublished M.S. thesis], University of Houston, Texas, 261p.

Ferguson, R.I., and Church, M., 2004, A simple universal equation for grain settling velocity, *Journal of Sedimentary Research*, v. 74, pp. 933-937.

Forman, S.L., Oglesby, R., Markgraf, V., and Stafford, T., 1995, Paleoclimatic significance of Late Quaternary eolian deposition on the Piedmont and High Plains, Central United States, *Global and Planetary Change*, v. 11, pp. 35–55, doi: 10.1016/0921-8181(94)00015-6.

Fratlicelli, C., 2003, Linking Climate, Sea Level, and Sedimentary Response on the Texas Shelf and Upper Slope: Examples from the Brazos and Colorado Fluvial-Deltaic Systems [Ph.D. Thesis], Rice University, 312p.

Gibeaut, J.C., Gutierrez, R., Waldinger, R., White, W.A., Hepner, T.L., Smyth, R.C., Andrews, J.R., and Crawford, M., 2006, The Texas Shoreline Change Project, <http://www.beg.utexas.edu/coastal/coastal01.htm> (last accessed: February 19).

Gibeaut, J.C., Hepner, T.L., Waldinger, R., Andrews, J.R., Smyth, R.C., and Gutierrez, R., 2003, Geotubes for temporary erosion control and storm surge protection along the Gulf of Mexico shoreline of Texas, Austin, Texas, Bureau of Economic Geology, John A. and Katherine G. Jackson School of Geosciences, The University of Texas at Austin, 6p.

Hall, G.L., 1976, Sediment Transport Processes in the Nearshore Waters Adjacent to Galveston Island and Bolivar Peninsula [Ph.D. thesis], College Station, Texas, Texas A&M University, 325p.

Hansen, E.A., 1960, Studies of a channel through Padre Island Texas, American Society of Civil Engineers, Journal of the Waterways and Harbors Division, v. 86, no. WW3, pp. 63–82.

Hayes, M.O., 1979, General morphology and sediment patterns in tidal inlets, *Sedimentary Geology*, v. 26, pp. 139–156.

Hayes, M.O., 1967, Hurricanes as geological agents, case studies of Hurricanes Carla, 1961 and Cindy, 1963, University of Texas Bureau of Economic Geology Report Investigation, Report 61, 54p.

Hodell, D.A., Curtis, J.H., Jones, G.A., Higuera-Gundy, A., Brenner, M., and Binford, M., W., and Dorsey, K.T., 1991, Reconstruction of Caribbean climate change over the past 10,500 years, *Nature*, v. 361, pp. 430–432.

Hughen, K.A., Baillie, M.G.L., Bard, B.E., Beck, J.W., Bertand, C.J.H., Blackwell, P.G., Buck, C.E., Burr, G.S., Cutler, K.B., Damon, P.E., Edwards, R.L., Fairbanks, R.G., Friedrich, M., Guilderson, T.P., Kromer, B., McCormac, G., Manning, S., Ramsey, C.B., Reimer, P.J., Reimer, R.W., Remmele, S., Southon, J.R., Stuiver, M., Talamo, S., Taylor, F.W., van der Plicht, J. and Weyhenmeyer, C.E., 2004, Marine04 Marine radiocarbon age calibration, 0–26 ka BP, *Radiocarbon*, v. 46, pp. 1059–1086.

Humphrey, J.D., and Ferring, C.R., 1994, Stable isotopic evidence for latest Pleistocene and Holocene climatic change in North-Central Texas, *Quaternary Research*, v. 41, pp. 200–213.

IPCC, 2007, Climate Change 2007: The Physical Science Basis: Contribution of Working Group 1 to the Fourth Assessment Report of the Intergovernmental Panel on Climate Change, <http://www.ipcc.ch/ipccreports/ar4-wg1.htm> (last accessed: March 18).

Israel, A.M., Ethridge, F.G., and Estes, E.L., 1987, A sedimentologic description of a micro-tidal, flood-tidal delta, San Luis Pass, Texas, *Journal of Sedimentary Petrology*, 47(2), pp. 288-300.

Johnson, J.W., 1956, Dynamics of nearshore sediment movement, *The American Association of Petroleum Geologists Bulletin*, v. 40, pp. 2211-2232.

Kelley, J.T., Barber, D.C., Belknap, D.F., FitzGerald, D.M., van Heteren, S., and Dickson, S.M., 2005, Sand budgets at geological, historical and contemporary time scales for a developed beach system, Saco Bay, Maine, USA, *Marine Geology*, v. 214, pp. 117-142.

Kemp, A.C., Horton, B.P., Culver, S.J., Corbett, D.R., van de Plassche, O., Gehrels, W.R. and Douglas, B.C., 2009, The timing and magnitude of recent accelerated sea-level rise (North Carolina, USA), *Geology*, v. 37, pp. 1035-1038.

Komar, P.D., 1983, Beach processes and erosion: an introduction, *in*: Komar, P.D., ed., *CRC Handbook of Coastal Processes and Erosion*, CRC Press, Boca Raton, FL, pp. 1-20.

Kulp, M.A., 2000, Holocene Stratigraphy, History, and Subsidence of the Mississippi River Delta Region, North-Central Gulf of Mexico [Ph.D. thesis], Lexington, University of Kentucky, 336p.

Lichter, J., 2008, Tropical cyclone climatology for the upper Texas coast, National Oceanic and Atmospheric Association, <http://www.srh.weather.gov/hgx/hurricanes/1980s.htm> (last accessed: August 2009).

Liu, K.B., and Fearn, M.L., 2000a, Reconstruction of prehistoric landfall frequencies of catastrophic hurricanes in northwestern Florida from lake sediment records, *Quaternary Research*, v. 54, pp. 238-245, doi: 10.1006/qres.2000.2166.

Liu, K.B., and Fearn, M.L., 2000b, Holocene history of catastrophic hurricane landfalls along the Gulf of Mexico coast reconstructed from coastal lake and marsh sediments, *in*: Ning, Z.H., Abdollahi, K.K., eds., *Current Stresses and Potential Vulnerabilities: Implications of Global Change for the Gulf Coast Region of the United States*, Baton Rouge, Gulf Coast Regional Climate Change Council, pp. 38-47.

Liu, K.B., and Fearn, M.L., 1993, Lake-sediment record of late Holocene hurricane activities from coastal Alabama, *Geology*, v. 21, pp. 793-796, doi: 10.1130/0091-7613(1993)021<0793:LSROLH>2.3.CO;2.

Maddox, J.K., 2005, Holocene Evolution of the Matagorda/Lavaca Bay Complex, Central Texas Coast [M.S. thesis], Houston, Rice University, 124p.

Maddox, J., Anderson, J.B., Milliken, K., Rodriguez, A.B., Dellapenna, T.M., and Giosan, L., 2008, The Holocene evolution of the Matagorda and Lavaca estuary complex, Texas, USA, *in*: Anderson, J.B., and Rodriguez, A.B., eds., *Response of Upper Gulf Coast Estuaries to Holocene Climate Change and Sea-Level Rise*, Geological Society of America Special Paper 443, pp. 105-119, doi: 10.1130/2008.2443(07).

Mann, M.E., and Emanuel, K.A., 2006, Atlantic hurricane trends linked to climate change, *Eos*, v. 87, pp. 233, 238, 241.



- Mann, M.E., Woodruff, J.D., Donnelly, J.P., and Zhang, Z., 2009, Atlantic hurricanes and climate over the past 1,500 years, *Nature*, v. 460, pp. 880–883, doi: 10.1038/nature08219.
- Mason, C., and Sorenson, R.M., 1972, Character and stability of a natural tidal Inlet, *Proceedings of the 13th Coastal Engineering Conference*, New York, American Society of Civil Engineers, pp. 781–800.
- Mathewson, C.C., and Minter, L.L., 1976, Impact of water resource development on coastal erosion, Brazos River, Texas, Texas A&M University, Texas Water Resources Institute, Technical Report 77, 8p.
- McKenna, K.K., 2004, Texas coastal erosion response plan, Austin, Texas, Texas General Land Office, 61p.
- Milliken, K.T., Anderson, J.B., and Rodriguez, A.B., 2008a, A new composite Holocene sea-level curve for the northern Gulf of Mexico, *in*: Anderson, J.B., and Rodriguez, A.B., eds., *Response of Upper Gulf Coast Estuaries to Holocene Climate Change and Sea-Level Rise*, Geological Society of America Special Paper 443, pp. 1–11.
- Milliken, K.T., Anderson, J.B., and Rodriguez, A.B., 2008b, Tracking the Holocene evolution of Sabine Lake through the interplay of eustasy, antecedent topography, and sediment supply variations, Texas and Louisiana, USA, *in*: Anderson, J.B., and Rodriguez, A.B., eds., *Response of Upper Gulf Coast Estuaries to Holocene Climate Change and Sea-Level Rise*, Geological Society of America Special Paper 443, pp. 65–88.
- Mitchener, H.J., Torfs, H., and Whitehouse, R.J.S., 1996, Erosion of mud/ sand mixtures, *Coastal Engineering*, v. 29, pp. 1–25, doi: 10.1016/ S0378-3839(96)00002-6.
- Morang, A., 2006, North Texas sediment budget, Galveston, Texas, U.S. Army Corps of Engineers, Engineer Research and Development Center, 55p.
- Morton, R.A., 1994, Texas barriers, *in*: Davis, R.A., ed., *Geology of Holocene Barrier Island Systems*, New York, Springer-Verlag, pp. 75–114.
- Morton, R.A., 1981, Formation of storm deposits by wind-forced currents in the Gulf of Mexico and the North Sea, *in*: NIO, S.D., ed., *Holocene Marine Sedimentation in the North Sea Basin*, International Association of Sedimentologists, Special Publication No. 5, pp. 385–396.
- Morton, R.A., 1979, Temporal and spatial variations in shoreline changes and their implications, examples from the Texas Gulf Coast, *Journal of Sedimentary Petrology*, v. 49, no. 4, pp. 1101–1112.
- Morton, R.A., 1977, Nearshore changes at jettied inlets, Texas coast, *Coastal Sediments 1977 Symposium*, American Society of Civil Engineers, pp. 267–286.
- Morton, R.A., Bernier, J.C., and Barras, J.A., 2006, Evidence of regional subsidence and associated interior wetland loss induced by hydrocarbon production, Gulf Coast region, USA, *Environmental Geology*, v. 50, pp. 261–274, doi: 10.1007/s00254-006-0207-3.
- Morton, R.A., Gibeaut, J.C., and Paine, J.G., 1995, Meso-scale transfer of sand during and after storms: Implications for prediction of shoreline movement, *Marine Geology*, v. 126, pp. 161–179, doi: 10.1016/0025-3227 (95)00071-6.

Morton, R.A., and McGowen, J.H., 1980, Modern depositional environment of the Texas Coast, University of Texas, Bureau of Economic Geology, Guidebook 20, Austin, 167p.

Morton, R.A., and Pieper, M.J., 1975a, Shoreline changes on Brazos Island and South Padre Island (Mansfield Channel to mouth of the Rio Grande), University of Texas, Bureau of Economic Geology, Geological Circulation, v. 75-2, 39p.

Morton, R.A., and Pieper, M.J., 1975b, Shoreline Changes in the Vicinity of the Brazos River Delta (San Luis Pass to Brown Cedar Cut), Austin, Texas, University of Texas, Bureau of Economic Geology, Geology Circular, v. 75-4, 47p.

Morton, R.A., and Price, W.A., 1987, Late Quaternary sea-level fluctuations and sedimentary phases of the Texas coastal plain and shelf, *in*: Nummedal, D., Pilkey, O.H., Jr., Howard, J.D., eds., Sea-level Fluctuations and Coastal Evolution, Tulsa, Society of Economic Paleontology and Mineralogy Special Publication, v. 41, pp. 181-198.

Moslow, T.F., and Tye, R.S., 1985, Recognition and characterization of Holocene tidal inlet sequences, *Marine Geology*, v. 63, pp. 129-151.

NOAA, 2010, Tides and Currents, <http://tidesandcurrents.noaa.gov> (last accessed: March 4).

NOAA, Nautical chart number 1283.

Nordt, L.C., Boutton, T.W., Jacob, J.S., and Mandel, R.D., 2002, C<sub>4</sub> plant productivity and climate-CO<sub>2</sub> variations in south-central Texas during the Late Quaternary, *Quaternary Research*, v. 58, pp. 182-188.

Nordt, L.C., Boutton, T.W., Hallmark, C.T., and Waters, M.R., 1994, Late Quaternary vegetation and climate changes in Central Texas based on the isotope composition of organic carbon, *Quaternary Research*, v. 41, pp. 109-120.

Overpeck, J.T., Otto-Bliesner, B.L., Miller, G.H., Muhs, R., Alley, R.B., and Kiehl, J.T., 2006, Paleoclimatic evidence for future ice-sheet instability and rapid sea-level rise, *Science*, v. 311, pp. 1747-1750.

Paine, J.G., 1993, Subsidence of the Texas coast: Inferences from historical and late Pleistocene sea levels, *Tectonophysics*, v. 222, pp. 445-458, doi:10.1016/0040-1951(93)90363-O.

Parchure, T., and Mehta, A.J., 1985, Erosion of soft cohesive sediment deposits, *Journal of Hydrologic Engineering*, v. 111, no. 10, pp. 1308-1326.

Penland, S., and Ramsey, K.E., 1990, Relative sea-level rise in Louisiana and the Gulf of Mexico: 1908-1988, *Journal of Coastal Research*, v. 6, pp. 323-342.

Pfeffer, W.T., Harper, J.T., and O'Neel, S., 2008, Kinematic constraints on glacier contributions to 21<sup>st</sup>-century sea-level rise, *Science*, v. 321, pp. 1340-1343.

Pilkey, O.H., Young, R.S., Riggs, S.R., Smith, A.W.S., Wu, H., and Pilkey, W.D., 1993, The concept of shoreface profile of equilibrium, a critical review, *Journal of Coastal Research*, v. 9, no. 1, pp. 255-278.

Ravens, T.M., and Sitanggang, K.I., 2007, Numerical modeling and analysis of shoreline change on Galveston Island, *Journal of Coastal Research*, 23(3), pp. 699-710.

Rodriguez, A.B., Anderson, J.B., and Bradford, J., 1998, Holocene deltas of the Trinity Valley: analogs for exploration and production, Gulf Coast Association of Geological Societies Transactions, XLVIII, pp. 373-380.

Rodriguez, A.B., Anderson, J.B., Siringan, F.P., and Taviani, M., 2004, Holocene evolution of the east Texas coast and inner shelf: along-strike variability in coastal retreat rates, *Journal of Sedimentary Research*, 74 (3), pp. 405-421.

Rodriguez, A.B., Anderson, J.B., Siringan, F.P., and Taviani, M., 1999, Sedimentary facies and genesis of Holocene sand banks on the East Texas inner continental shelf, *in*: Bergman, K.M., and Snedden, J.W., eds., *Isolated Shallow Marine Sand Bodies: Sequence Stratigraphic Analysis and Sedimentologic Interpretation*, Society for Sedimentary Geology Special Publication (SEPM) Special Publication 64, pp. 165-178.

Rodriguez, A.B., Fassell, M.L., and Anderson, J.B., 2001, Variations in shoreface progradation and ravinement along the Texas coast, Gulf of Mexico, *Sedimentology*, v. 48, pp. 837-853.

Rodriguez, A.B., Hamilton, M.D., and Anderson, J.B., 2000, Facies and evolution of the modern Brazos Delta, Texas: Wave versus flood influence, *Journal of Sedimentary Research*, 70 (2), pp. 283-295.

Roth, D., 2000, Texas hurricane history, <http://www.srh.noaa.gov/lch/research/txhur.php> (last accessed: September 2009).

Rusnak, G.A., 1960, Sediments of Laguna Madre Texas, *in*: Shepard, F.P., Phleger, F.B., van Andel, T.J., eds., *Recent Sediments, Northwest Gulf of Mexico*, Tulsa, American Association of Petroleum Geology, pp. 153-196.

Russ, J., Loyd, D.H., and Boutton, T.W., 2000, A paleoclimate reconstruction for southwestern Texas using oxalate residue from lichen as a paleoclimate proxy, *Quaternary International*, v. 67, pp. 29-36.

Schwab, W.C., Thieler, E.R., Allen, J.R., Foster, D.S., Swift, B.A., and Denny, J.F., 2000, Influence of inner continental shelf framework on the evolution and behavior of the barrier island system between Fire Island Inlet and Shinnecock Inlet, Long Island, New York, *Journal of Coastal Research*, v. 16, pp. 396-407.

Shinkle, K.D., and Dokka, R.K., 2004, Rates of vertical displacement at benchmarks in the Lower Mississippi Valley and the Northern Gulf Coast, National Oceanographic and Atmospheric Administration Technical Report NOS/NGS 50, 135p.

Simms, A.R., Anderson, J.B., Milliken, K.T., Taha, Z.P., and Wellner, J.S., 2007, Geomorphology and age of the oxygen isotope stage 2 (last lowstand) sequence boundary on the northwestern Gulf of Mexico continental shelf, *in*: Davies, R.J., Posamentier, H.W., Wood, L.J., and Cartwright, J.A., eds., *Seismic Geomorphology: Applications to Hydrocarbon Exploration and Production*, Geological Society of London Special Publication 277, pp. 29-46.

Simms, A.R., Anderson, J.B., Rodriguez, A.B., and Taviani, M., 2008, Mechanisms controlling environmental change within an estuary: Corpus Christi Bay, Texas, USA, *in*: Anderson, J.B., and Rodriguez, A.B., eds., *Response of Upper Gulf Coast Estuaries to*

Holocene Climate Change and Sea-Level Rise, Geological Society of America Special Paper 443, pp. 121-146, doi 10.1130/2008.2443(08).

Siringan, F.P., and Anderson, J.B., 1994, Modern shoreface and inner-shelf storm deposits off the east Texas coast, Gulf of Mexico, *Journal of Sedimentary Research*, v. 64, pp. 99–110.

Siringan, F.P. and Anderson, J.B., 1993, Seismic facies, architecture, and evolution of the Bolivar Roads tidal inlet/delta complex, east Texas Gulf Coast, *Journal of Sedimentary Petrology*, 63, pp. 794–808.

Snedden, J.W., Nummedal, D., and Amos, A.F., 1988, Storm- and fair-weather combined flow on the central Texas continental shelf, *Journal of Sedimentary Petrology*, 58 (4), pp. 580-595.

Swift, D.J.P., 1976, Continental shelf sedimentation, *in*: Stanley, D.J., and Swift, D.J.P., eds., *Marine Sediment Transport and Environmental Management*, New York, Wiley, pp. 311–350.

Texas General Land Office, 2007, Coastal Erosion Planning & Response Act (CEPRA), Austin, Texas, Report to the 80th Texas Legislature, 83p.

Thieler, E.R., Pilkey, O.H., Jr., Young, R.S., Bush, D.M., and Chai, F., 2000, The use of mathematical models to predict beach behavior for coastal engineering— A critical review, *Journal of Coastal Research*, v. 16, pp. 48–70.

Thomas, R., Rignot, E., Casassa, G., Kanagaratnam, P., Acuña, C., Akins, T., Brecher, H., Frederick, E., Gogineni, P., Krabill, W., Manizade, S., Ramamoorthy, H., Rivera, A., Russell, R., Sonntag, J., Swift, R., Yungel, J., and Zwally, J., 2004, Accelerated Sea-Level Rise from West Antarctica, *Science*, v. 306, pp. 255-258.

Toomey, R.S., III, Blum, M.D., and Valastro, S., Jr., 1993, Late Quaternary climates and environments of the Edwards Plateau, Texas, *Global and Planetary Change*, v. 7, pp. 299-320.

Törnqvist, T.E., Bick, S.J., Van der Borg, K., and De Jong, A.F.M., 2006, How stable is the Mississippi Delta?, *Geology*, v. 34, pp. 697–700, doi: 10.1130/G22624.1.

Törnqvist, T.E., González, J.L., Newsom, L.A., Van der Borg, K., Dejong, A.F.M., and Kurnik, C.W., 2004, Deciphering Holocene sea-level history on the U.S. Gulf Coast: A high-resolution record from the Mississippi Delta, *Geological Society of America Bulletin*, v. 116, pp. 1026–1039, doi:10.1130/B2525478.1.

Törnqvist, T.E., Wallace, D.J., Blaauw, M., Derksen, M.S., Klerks, C.J.W., Meijneken, C., Snijders, E.M.A., Storms, J.E.A., Van Dam, R.L., and Wallinga, J., 2008, Mississippi Delta subsidence primarily caused by compaction of Holocene strata, *Nature Geoscience*, v. 1, pp. 173–176, doi:10.1038/ngo129.

Wallace, D.J., and Anderson, J.B., 2010, Evidence of similar probability intense hurricane strikes for the Gulf of Mexico over the late Holocene, *Geology*, (in press).

Wallace, D.J., Anderson, J.B., and Rodriguez, A.B., 2009, Natural versus anthropogenic mechanisms of erosion along the upper Texas Coast, *in*: Kelley, J.T., Pilkey, O.H., and Cooper, J.A.G., eds., *America's Most Vulnerable Coastal Communities*, The Geological

Society of America Special Paper 460, pp. 137-147.

Watson, R.L., and Behrens, E.W., 1976, Hydraulics and dynamics of new Corpus Christi Pass: A case history, 1973–75, U.S. Army Corps Engineers, General Investigation of Tidal Inlets Report 9, 175p.

Webster, P.J., Holland, G.J., Curry, J.A., and Chang, H.R., 2005, Changes in tropical cyclone number, duration, and intensity in a warming environment, *Science*, v. 309, pp. 1844-1846.

Weiser, E.A., and Armstrong, J., 1963, Design of deep draft navigation channel from Gulf of Mexico into Matagorda Bay, Texas, *in*: Proceedings of the 8th Coastal Engineering Conference, New York, American Society of Civil Engineers, pp. 578–597.

Wilkins, D.E., and Currey, D.R., 1999, Radiocarbon chronology and  $^{13}\text{C}$  analysis of mid- to late-Holocene aeolian environments, Guadalupe Mountains National Park, Texas, USA, *The Holocene*, v. 9, no. 3, pp. 363-371.

Woodruff, J.D., Donnelly, J.P., Mohrig, D., and Geyer, W.R., 2008, Reconstructing relative flooding intensities responsible for hurricane-induced deposits from Laguna Playa Grande, Vieques, Puerto Rico, *Geology*, v. 36, pp. 391–394, doi: 10.1130/G24731A.1.

United States Geological Survey, 2009, Coastal change hazards: Hurricanes and extreme storms, <http://coastal.er.usgs.gov/hurricanes/ike/lidar/bolivar.html> (last accessed: February 2010).

## APPENDIX A

### APPENDIX A: Methods, Calculating $\langle h_b \rangle$ , Error analysis, Total hurricane counts, Radiocarbon reservoir effect, and Geologic history for paleotempestological study<sup>4</sup>

#### A.0 Methods

Thirty-seven 7.6 cm diameter vibracores up to 2m in length were collected for this study. Core locations were determined using a GARMIN® hand-held GPS unit, which provided an approximate horizontal accuracy within 10 m. Mollusc shells were radiocarbon dated at the Keck Carbon Cycle AMS Facility at UC-Irvine. Radiocarbon ages were calibrated from radiocarbon to calendar years using Marine04 (Hughen et al., 2004). All 554 samples were deflocculated in deionized water with a magnetic stirrer, and grain size measurements were performed using a Malvern Mastersizer 2000 particle analyzer. In core 32, the sediments below 146 cm were bioturbated and thus no washover deposits were identified below this depth. Grain size measurements were taken at 1 cm intervals from 80-147 cm in this core. Core Scientific International performed measurements of  $^{137}\text{Cs}$  activity. Cesium samples were taken approximately every 5 cm, so as to capture the age of the washover deposit in core 29.

Liu and Fearn (2000a) presented the lowermost age constraint of  $3310 \pm 80$   $^{14}\text{C}$  yr B.P. from organic lake mud, and an uppermost age of 400  $^{14}\text{C}$  yr B.P. from the subsequent sedimentation age model. In order to directly compare all ages presented in this paper, these ages were calibrated using IntCal04 (Hughen et al., 2004) for terrestrial samples. The results of the calibration yield a lowermost age constraint of  $3543 \pm 90$  yr B.P., and an uppermost age constraint of  $492 \pm 7$  yr B.P.

---

<sup>4</sup> This appendix has been edited, reformatted, and reprinted with permission from the online supplementary information: Wallace, D.J., and Anderson, J.B., 2010, Evidence of similar probability of intense hurricane strikes for the Gulf of Mexico over the late Holocene, *Geology*, (in press).

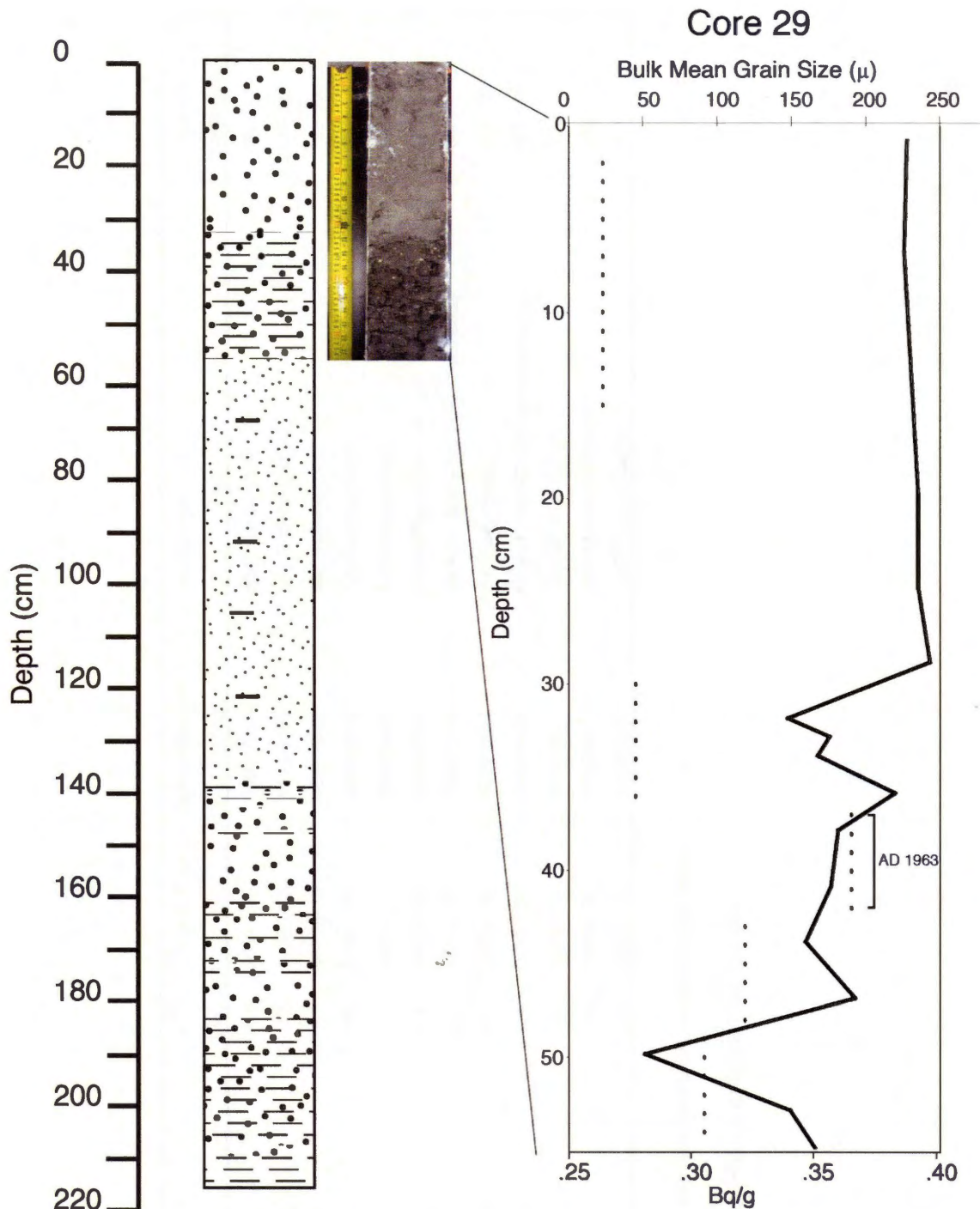


Figure A-1: Lithology and bulk mean grain size of core 29. Note the ~30 cm thick clean sand deposit at the top of the core, attributed to Hurricane Allen (1980). This core was dated using  $^{137}\text{Cs}$  (black circles), and yielded a cesium spike (indicating AD 1963  $\pm$  2) at ~38 cm depth. The predicted  $\langle h_b \rangle$  value for this deposit was 6.6 m, while the measured surges were 3.7 m (Roth, 2000). The highest surges occurred in uninhabited areas and were not measured. The predicted  $\langle h_b \rangle$  value from this event was used as a baseline to constrain intense storms. Lithologic legend in Figure 4-2.



Core	Sample name	$\delta^{13}\text{C}$ (‰)	$^{14}\text{C}$ yr B.P.	Calibrated yr B.P. (1 sigma)	sample type	sample depth (cm)
30	LM30-1_80-81	-1.9	2010 ± 15	1509-1654	bay mollusc shell	80-81
30	LM30-2_171-173	-0.3	4155 ± 15	4141-4329	bay mollusc shell	171-173
30	LM30-2_199-200	-0.7	4520 ± 15	4641-4808	bay mollusc shell	199-200
32	LM32-1_79-80.3	-1.0	2440 ± 15	2000-2143	bay mollusc shell	79-80.3
32	LM32-2_190-191.5	-0.9	4620 ± 15	5308-5445	bay mollusc shell	190-191.5
32	LM32-2_195-197	-0.8	5115 ± 15	5438-5559	bay mollusc shell	195-197
25	LM25_127cm	0.9	1885 ± 20	1362-1503	shell ( <i>m. lateralis</i> and <i>P. multilineata</i> )	127
25	LM25_154-158cm	-0.7	2260 ± 15	1830-1895	shell fragments	154-158
25	LM25_180-182cm	0.4	2685 ± 20	2315-2448	shell ( <i>P. multilineata</i> ) and fragments	180-182
33	LM33_83cm	0.0	1390 ± 15	890-989	shell ( <i>P. multilineata</i> )	83
33	LM33_96cm*	0.6	1130 ± 15	644-721	shell ( <i>E. concentrata</i> )	96
33	LM33_167cm	-2.2	3335 ± 15	3484-3632	shell ( <i>P. multilineata</i> )	167

\*too young based on older date from *Parvilucina multilineata* shell above

Figure A-Table 1: Laguna Madre radiocarbon results.

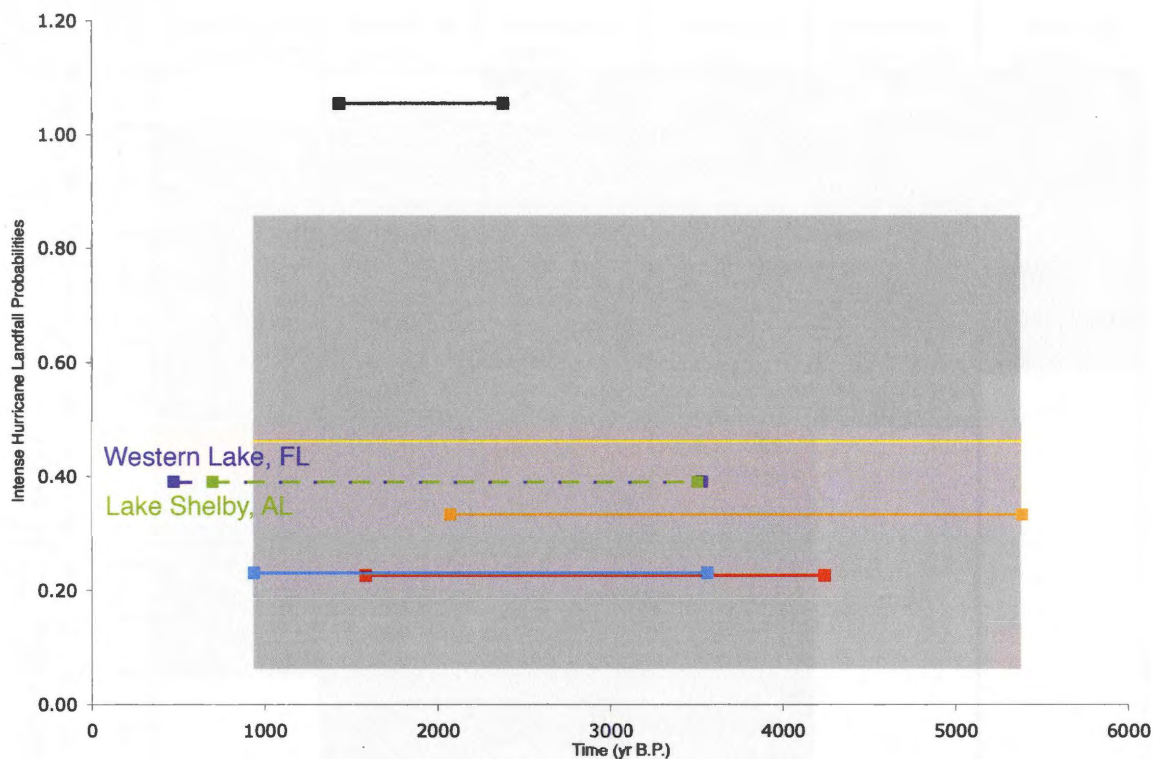


Figure A-2: Plot showing intense hurricane landfall probabilities between paleotempestological studies from Lake Shelby, AL (Liu and Fearn, 2000b – dashed green), Western Lake, FL (Liu and Fearn, 2000a-dashed purple), and Laguna Madre (LM), TX (solid black, orange, blue, red). X-axis is calibrated radiocarbon age intervals. Yellow line represents the average landfall probability (0.46%) between cores from LM, and the gray box represents  $\pm$  one standard deviation from the average landfall probability between cores from LM. Note the similar intense hurricane landfall probabilities and time intervals between sites.

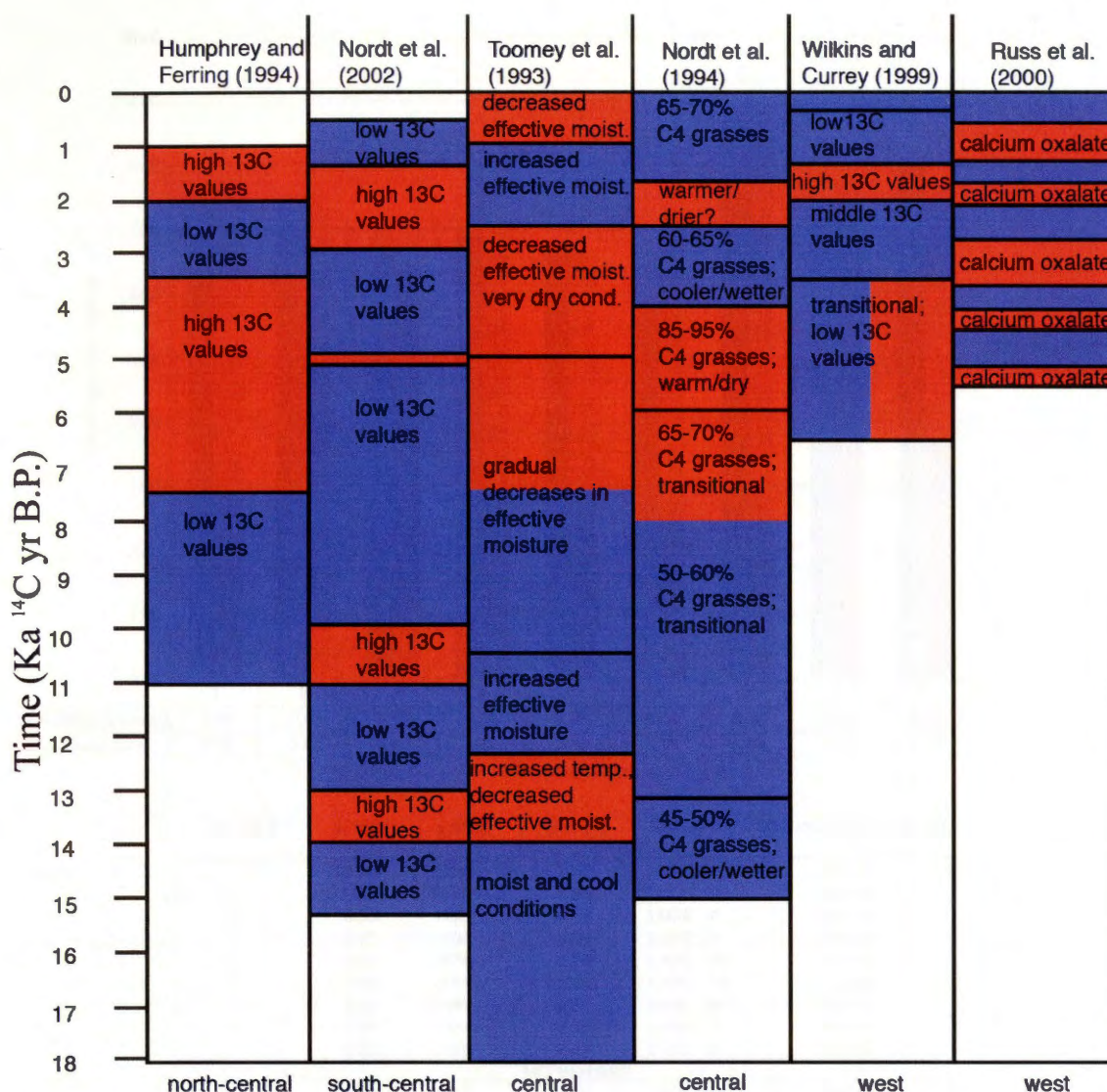
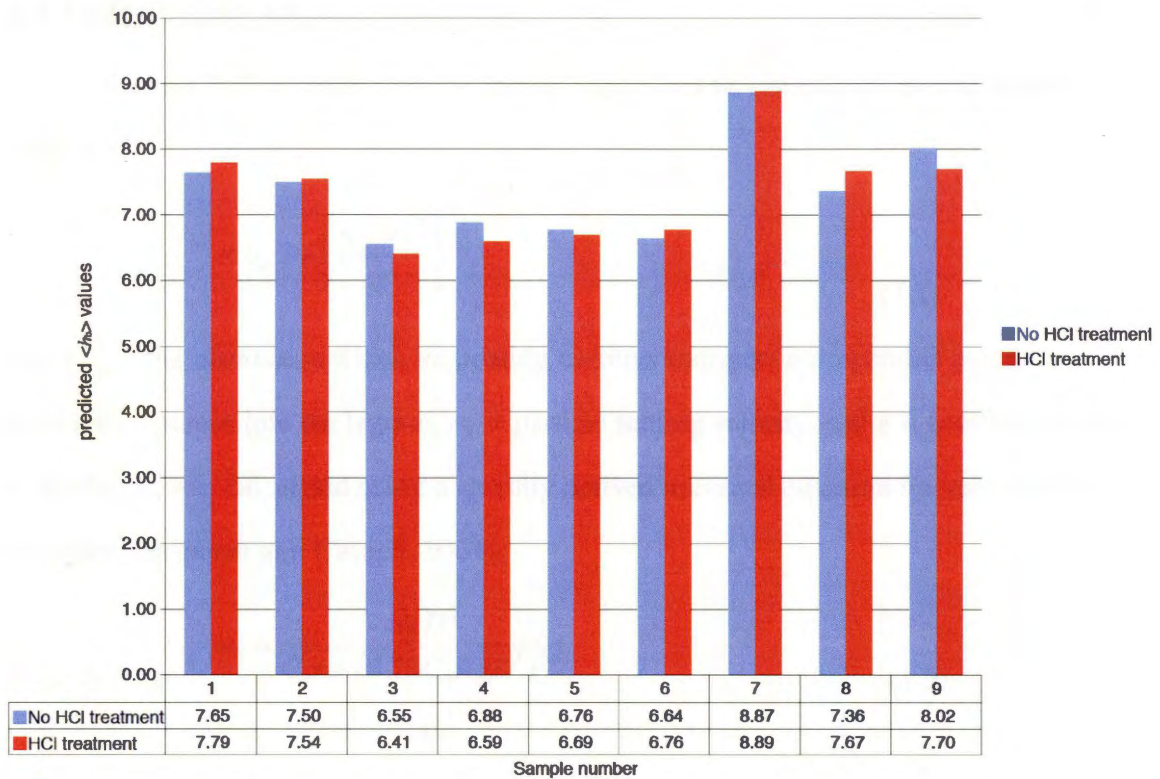


Figure A-3: Compilation of climate studies for the past ~18,000 years (modified from Maddox, 2005). Red represents warm, dry conditions, and blue represents cool, wet conditions. Texas regional location indicated at bottom of each study.





sample #	$w_s$ (m/s)	$x_t$ (m/s)	$\langle h \rangle$ (m)	Sample ID	Bulk mean grain size ( $\mu$ )
No HCl treatment					
1	0.03	2157	7.65	LM25_069	235.13
2	0.03	2157	7.50	LM25_102	229.99
3	0.03	1750	6.55	LM29_10	231.25
4	0.03	1750	6.88	LM29_26	244.03
5	0.02	2274	6.76	LM30_130	198.43
6	0.02	2274	6.64	LM30_136	194.62
7	0.02	3567	8.87	LM32_087	192.48
8	0.03	2393	7.36	LM33_73	209.34
9	0.03	2393	8.02	LM33_80	229.54
HCl treatment					
1	0.03	2157	7.79	LM25_069	240.11
2	0.03	2157	7.54	LM25_102	231.43
3	0.03	1750	6.41	LM29_10	225.59
4	0.03	1750	6.59	LM29_26	232.67
5	0.02	2274	6.69	LM30_130	196.17
6	0.02	2274	6.76	LM30_136	198.44
7	0.02	3567	8.89	LM32_087	192.92
8	0.03	2393	7.67	LM33_73	218.70
9	0.03	2393	7.70	LM33_80	219.57

Figure A-4: Comparison of representative washover samples with and without HCl treatment from all cores. There is little variability in predicted  $\langle h_t \rangle$  values between treated and untreated samples.

## A.1 Calculating $\langle h_b \rangle$

A storm's flow depth over the barrier ( $\langle h_b \rangle$ ) can be calculated (Woodruff et al., 2008):

$$\langle h_b \rangle = \left( \frac{x_L^2 w_s^2}{g} \right)^{1/3}, \quad (1.1)$$

where,  $x_L$  = the distance at which inundating currents transport a suspended particle a horizontal distance into the lagoon,  $w_s$  = particle settling velocity, and  $g$  = acceleration due to gravity.  $w_s$  was calculated using a recently derived universal equation for sediment fall velocities (Ferguson and Church, 2004):

$$w_s = \frac{RgD^2}{C_1\nu + (0.75C_2RgD^3)^{0.5}}, \quad (1.2)$$

where  $R$  = the submerged specific gravity (1.65 for quartz),  $g$  = the acceleration due to gravity,  $D$  = grain diameter,  $C_1$  = constant with value of 18 for grains of varied shape,  $\nu$  = the kinematic viscosity of the fluid ( $9.2 \times 10^{-7} \text{ m}^2\text{s}^{-1}$ ), and  $C_2$  = constant with value of 1 for grains of varied shape. For each discrete storm bed, the bulk mean grain size ( $(\phi 16 + \phi 50 + \phi 84)/3$ ) was used to determine  $w_s$ , followed by  $\langle h_b \rangle$ .

## A.2 Error Analysis

Shell material was avoided during grain size measurements. However, in order to quantify potential error from carbonate material in the calculation of  $\langle h_b \rangle$ , representative samples from washover sands were taken from each core. One was treated with HCl to dissolve all shell material, while the other was left untreated. Both samples were then analyzed for grain size, and potential errors for predicted  $\langle h_b \rangle$  values for each sample were calculated based on the grain size differences.

These errors appear to be negligible, and there is no evidence that shell material is abundant enough to shift the bulk mean grain size towards the coarser fraction (Figure A-4).

### **A.3 Total Hurricane Counts**

We classify hurricanes as intense using the predicted  $\langle h_b \rangle$  value from Hurricane Allen as a baseline. If the total number of storms is used for each probability calculation regardless of the predicted  $\langle h_b \rangle$  value, the probabilities change slightly. Ten total hurricane events are recorded from 4,235–1,582 yr B.P. (0.38% landfall probability) in core 30, eleven from 2,382–1,433 yr B.P. (1.16% landfall probability) in core 25, sixteen are recorded from 3,558–940 yr B.P. (0.61% landfall probability) in core 33, and a total of twelve from 5,377–2,072 yr B.P. (0.36% landfall probability) in core 32 (Fig. 4-2). The average landfall probability of these values is  $\sim .63\%$  (with a standard deviation value of  $\pm .37\%$ )

### **A.4 Radiocarbon Reservoir Effect**

Along the Texas coast, a recent study has quantified radiocarbon reservoirs associated with organisms utilizing  $\text{CO}_2$ , which has not been in contact with the atmosphere for long periods of time (Milliken et al., 2008a). This study concluded that the reservoir increases from west to east in Texas, and ranges from  $\sim 400$ -700 yrs. No reservoir data currently exists for LM. However, given the extremely limited exchange between LM, fluvial systems, and the Gulf of Mexico, this effect is likely to be negligible. Therefore, the standard  $\sim 400$ -year global average reservoir is used (Marine04-Hughen et al., 2004).

### **A.5 Geologic History**

Subsidence has decreased in more recent time, and our data suggest negligible average long-term subsidence rates ( $\sim .5$  mm/yr). Shortly after LM formed, tidal currents were probably important for sediment transport as SPI had more numerous tidal inlets.

Due to post-glacial climate changes in southwest Texas, the discharge of the Rio Grande River has been significantly reduced naturally, resulting in decreased sedimentation rates in LM and adjacent areas. During historic time, river discharge and suspended sediment loads have been further reduced by over 80% and 90%, respectively, due to damming and irrigation practices (Morton and Pieper, 1975a; Morton, 1979). Throughout much of the Holocene, the Rio Grande Delta prograded seaward despite rapidly rising sea-level (Banfield and Anderson, 2004).